MEKELLE UNIVERSITY

COLLEGE OF NATURAL AND COMPUTATIONAL SCIENCES

School of Earth Sciences

Department of Geology

A

Thesis

On

Evaluation Of Limestone as Coarse Aggregate in Concrete and Cobblestones: A Case study from Mekelle Area, Northern Ethiopia

Submitted to the School of Earth Sciences in partial fulfillment of the requirements for the Degree of Master of Science in Geological Engineering

By

Muez Aregawi *ID NO: PS/00164/06*

Advisor: Gebremedhin Berhane (PhD)

Co-advisor: Gebreselassie Mebrahtu (M.Sc.)

Mekelle, Ethiopia, November, 2024

APPROVAL SHEET

MEKELLE UNIVERSITY

COLLEGE OF NATURAL AND COMPUTATIONAL SCIENCES

School of Earth Sciences

Evaluation of Limestone as Coarse Aggregate in Concrete and Cobblestone.

A Case Study in Mekelle Area Northern Ethiopia

A Thesis Submitted to Mekelle University, Earth Science Department in Partial Fulfillment of the Requirements for the Degree of Master of Science in Geological Engineering

SUBMITTED BY:

Muez Aregawi Kahsay	PS/00164/06	_____	_____
		Signature	Date

APPROVED BY:

1. Gebremedhin Berhane (PhD)	_____	_____
Advisor's Name	Signature	Date
2. Gebreslassie Mebrahtu (M.Sc.)	_____	_____
Co-Advisor	Signature	Date
3. Tesfahunegn Abera (M.Sc.)	_____	_____
Internal Examiner	Signature	Date
4. Yonas Hadush (M.Sc.)	_____	_____
External Examiner	Signature	Date
5. Asmelash Abay (PhD)	_____	_____
Chairperson	Signature	Date

Declaration

This is to certify that this thesis entitled ***"Evaluation of Limestone as Coarse Aggregate in Concrete and Cobblestone: a case of Mekelle area, North of Ethiopia"*** is submitted in partial fulfilment of the requirements for the award of Masters of Science Degree in 'Geological Engineering' to the School of Earth Science, Mekelle University, has been done by Mr. Muez Aregawi, I.D. No. CNCS/PSG164/06 under the supervision of Gebremedhin Berhane (PhD) (Advisor) and Gebreslassie Mebrahtu (M.Sc.) (Co-advisor) is an authentic work carried out during the 2023/2024 academic year. I, the undersigned, declare that this thesis is my original work and to the best of my knowledge it has not been presented for award of any degree or diploma in any other university. All sources of materials used for the thesis have been duly acknowledged.

Name of Student: Muez Aregawi Kahsay

Signature: _____ Date: _____

E-mail: muez.aregawi23@gmail.com

This thesis has been submitted for the examination with my approval as university advisor/co-advisor

Gebremedhin Berhane (PhD) (Advisor): _____

Gebreslassie Mebrahtu (M.Sc.) (Co-advisor): _____

School of Earth Sciences, Mekelle University

Abstract

Engineering geological investigation is essential for evaluating the quality of construction materials and ensuring the durability of engineering structures. This study assessed the physical and mechanical properties of limestone aggregates from selected quarries in the Mekelle area to determine their suitability for concrete and stone-paved road applications. A total of twelve representative samples and 50 kg of coarse aggregates were collected according to ASTM D75 from the Shugala, Kokolo, Mayalem, Mossobo, Chanadug, and Genha quarry sites and tested for gradation, specific gravity, unit weight, water absorption, moisture content, flakiness index (FI), aggregate crushing value (ACV), Los Angeles abrasion value (LAAV), and unconfined compressive strength (UCS), with results compared to ASTM and BS standards.

The results indicate that the tested aggregates largely satisfy international specifications. Specific gravity values ranged between 2.43 and 2.83, while unit weight varied from 1.47 to 1.65 g/cm³. According to ASTM C33 classification, these unit weight values confirm that the aggregates are normal weight. Water absorption values (0.11%–0.78%) fall within the required range, indicating low porosity and good durability. Moisture content is very low (0.012–0.39%), significantly below the 4% limit, ensuring that the aggregates are dry. Mechanical tests revealed flakiness index values ranging from 12.11–20.30%, ACV values from 10.66–22.16%, LAAV values from 19.18–25.40%, and UCS values from 105–117 MPa, indicating that all samples fall within the "high-strength" category (>55 MPa).

Sieve analysis further revealed that aggregates from Chanadug, Genha, Mossobo, and Mayalem quarries exhibit favourable particle size distribution, making them highly suitable for construction, while those from Shugala and Kokolo did not meet gradation criteria.

Keywords: Evaluation, Limestone, physical properties, mechanical properties

Acknowledgment

I want to express my heartfelt gratitude to the numerous individuals who have played a pivotal role in completing this thesis, including esteemed researchers, academics, and dedicated practitioners. In particular, I am deeply indebted to my esteemed advisor, Gebremedhin Berhane (PhD.) whose unwavering guidance, support, and encouragement have been invaluable throughout the research process. His profound insights and expertise have truly shaped the trajectory of this work. I would also like to extend my sincere appreciation to Mr. Gebreslassie Mebrahtu (MSc.) for his invaluable contributions, both in terms of technical assistance and insightful discussions. His expertise and unwavering dedication have greatly enhanced the quality of this research.

Additionally, I am immensely grateful to the esteemed faculty of the Earth Science faculty at Mekelle University for their tremendous support and encouragement. Their wealth of knowledge and expertise has been instrumental in shaping my understanding of the subject matter. I am also deeply indebted to the diligent laboratory technicians at EIT-M for their assistance during the experimental work. Their meticulousness and technical expertise have been crucial in ensuring the accuracy and reliability of the data.

Furthermore, I would like to express my profound appreciation to my dear friends, Mr. Ataklti Hiluf, Amir Wassie and Enun Weldeberhane, for their unwavering support and companionship throughout my academic journey. Their encouragement and presence have given me the strength and motivation to overcome challenges and persevere. Lastly, I want to acknowledge my parents and family's unwavering support and love. Their continuous encouragement and belief in me have been the driving force behind this project and my entire academic journey. I am forever grateful for their unwavering support.

I extend my deepest gratitude to all those mentioned and countless others who have contributed to this endeavour. Your collective support and unwavering belief in my abilities have been truly inspiring and have shaped this thesis into what it is today.

TABLE OF CONTENT

List of Figures

List of Tables

List of Symbols and Abbreviations:

γ_d	Dry unit weight
γ_w	Wet unit weight
Sp.gr	Specific gravity
AASHTO	American Association of Highway and Transportation office
ASTM	American Society for Testing Materials Standard
UCS	Unconfined compressive strength
FI	Flakiness index
ACV	Aggregate crushing value
LAAV	Los Angeles Abrasion Value
BS	British standards
R	Rebound number
IJERT	International journal of engineering research and technology
DEM	Digital elevation model
Mpa	Mega Pascal
Mc	Moisture content
Wa	Water absorption
LL	Lower limit
UL	Upper limit
SPSS	Statistical package for social science students

CHAPTER ONE

INTRODUCTION

1.1.Background and Justification

Limestone is a sedimentary rock that is widely available in many regions around the world (Smith, 2020). It has been used in construction for centuries, with a long history of applications ranging from building materials to decorative elements (Johnson & Lee, 2019). The unique physical and mechanical properties of limestone, such as its durability, compressive strength, and aesthetic appeal, have made it a popular choice for a variety of construction projects (Brown, 2021). In recent years, the construction industry has faced growing challenges in meeting the increasing demand for construction materials, particularly cobblestones and coarse aggregates (Davis, 2022). Traditional sources of these materials, such as granite and river gravel, are becoming increasingly scarce or difficult to extract, leading to concerns about the sustainability and cost-effectiveness of current practices (Wilson, 2023). Aggregates are a fundamental component of construction materials, playing a crucial role in the performance and durability of concrete, asphalt, and various other construction applications (Neville, 2010). Among the various types of aggregates, natural stones have been widely used due to their availability and inherent properties (Keller, 2013). Limestone, a sedimentary rock primarily composed of calcium carbonate, is abundant in many regions and has been utilized in construction for centuries (Meyer, 2009). Its unique characteristics make it a viable candidate for use as both cobblestone and coarse aggregate in engineering projects (Bui et al., 2010).

Cobblestones, traditionally used in road construction and pavements, offer aesthetic appeal and durability (Harris, 2012). Their historical significance is evident in many urban settings where cobbled streets remain a testament to engineering ingenuity (Graham, 2015). Meanwhile, coarse aggregates, which form the skeleton of concrete, are essential for achieving the desired strength and stability in construction materials (Mehta & Monteiro, 2014). The suitability of limestone for these applications warrants thorough investigation, particularly in terms of its physical and mechanical properties (González et al., 2018).

Research has shown that limestone can meet the necessary engineering standards for aggregates, making it a valuable resource in the construction industry (Janjuhah et al., 2021). The evaluation of limestone's properties, including its mineralogical composition, strength, and durability, is essential for determining its effectiveness as a construction material (Zhang et al., 2016). Studies have indicated that

limestone aggregates can provide adequate performance in various engineering applications, thus supporting sustainable development in the construction sector (Ali & Hossain, 2020).

1.2.Statement Of the Problem

Mekelle city which is the economic and political center of Tigray regional state, Ethiopia. It has led to an increasing demand for the construction of various infrastructure projects, ranging from small to large-scale structures. The sustainability/safety of these infrastructure projects relies heavily on using high-quality materials that can ensure their durability and functionality.

Limestone, is a crucial component in the City's vision for sustainable development, also plays a vital role in the construction of almost all infrastructures (table 1). However, despite its significant economic importance, there is a lack of comprehensive studies examining the strength and geotechnical properties of the limestone rock.

Most of the infrastructures are being used limestone material as cobblestone and coarse aggregate; since approximately three-quarters of the volume of concrete is occupied by aggregate, it is not surprising that its quality is of considerable importance. Not only may the aggregate limit the strength of concrete but the aggregate properties greatly affect the durability and structural performance of concrete

This research aims to address these gaps by conducting comprehensive laboratory testing and field evaluations to characterize the limestone rocks, assess their performance as coarse aggregates in concrete, and evaluate their potential for cobblestone use. The findings of this study will contribute to the development of guidelines for the utilization of locally available limestone resources in construction, which could have significant economic and environmental benefits for the city.

The use of limestone as cobblestone roads and coarse aggregate as illustrated in Table 1 and fig.1 respectively, demonstrates the growth of cobblestone roads in Mekelle city from 2007 to 2015 as well as coarse aggregates.

Table 1: Mekelle city cobblestone road pavement in km from (2007-2015G.C.)

Category	Sub-category	2007	2008	2009	2010	2011	2012	2013	2014	2015
Cobblestone and movement networks	Cobblestone roads in cumulative (km)	3.05	7.5	14.5	23	60.6	88	112	134.5	152

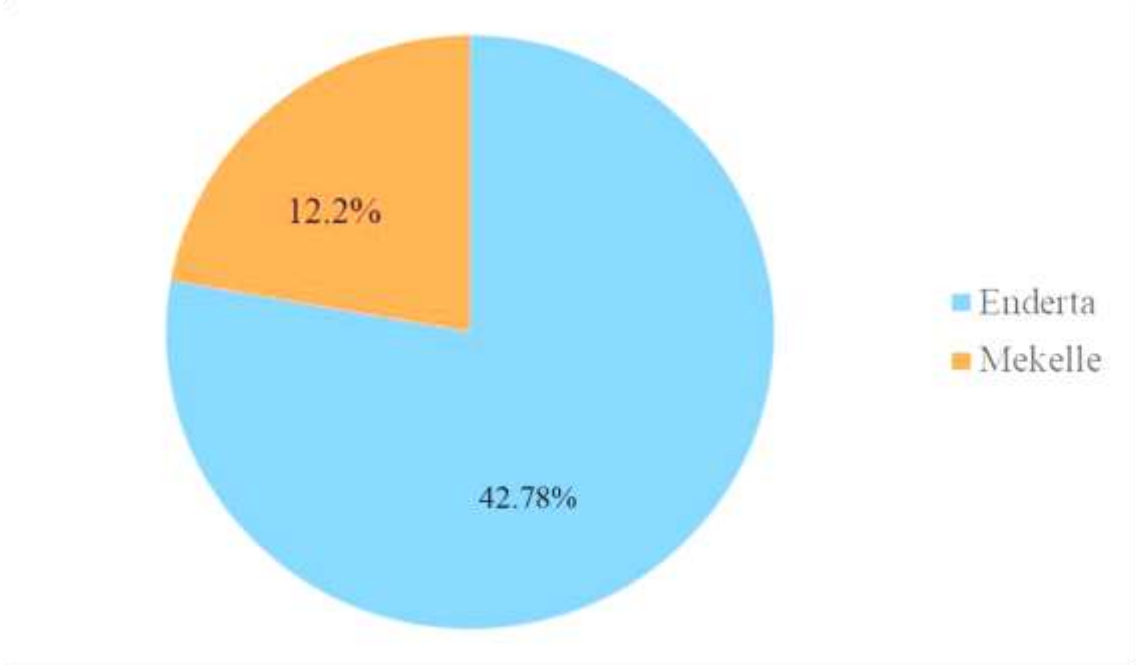

Figure 1:Number of licenses given around Mekelle area (Sources: construction and design office of Mekelle city, 2012)

1.2.1. General Objective

The main objective of this research was to evaluate limestone as coarse aggregates in concrete and cobblestone, particularly in Mekelle area.

1.2.2. Specific Objectives

The specific objectives of the research work are:

- To evaluate physical and mechanical properties of limestone
- To assess its suitability for coarse aggregate in concrete and cobblestone uses:
- To locate suitable limestone quarry sites
- To compare the physical and mechanical properties of limestone.
- To prepare geological map from existing maps

1.3.Significance of the Research

This research holds significant importance in evaluating the suitability of limestone as a construction material for both concrete and cobblestone applications in Mekelle city. Evaluating the suitability of limestone for cobblestone applications and as a coarse aggregate in concrete contributes to the development of durable and high-quality infrastructure in Mekelle city. Moreover, the comparative analysis of limestone properties from different quarries can provide valuable insights to guide the selection of the most appropriate limestone for intended use. As a lesson or secondary data for professionals and academic institutions and individual researchers who are interested in related construction material projects.

1.4. Scope and Limitation of the Research

The scope of the study is focused on the physical and mechanical properties of limestone to determine whether the limestone extracted in the specified quarry sites was useful for concretes and cobblestone without failure or not. This research is based on present test results and secondary information extracted during literature review. Sufficient scientific techniques and methodologies have been put in to practice to get the research work fulfil its objectives. But the present research was not free from limitations of time, resources and financial constraints.

Despite these constraints, the researcher made significant efforts to mitigate the limitations and ensure the quality of the data. It conducted thorough fieldwork, employing appropriate methodologies and techniques to gather reliable information from the selected quarry sites. Additionally, laboratory analysis was conducted using appropriate protocols and standards to ensure the accuracy and validity of the data obtained.

1.5.Structure Of the Thesis

The findings or results of this comprehensive and problem driven study presented in six chapters and organized as follows

Chapter 1 gives introduction about the suitability of limestone rocks in any engineering structures, statement of the problem, general and specific objectives of the research, scope and limitation of the research. Chapter 2 presents literature reviews that are of high relevance to the topic in general and previous works in the study area. Chapter 3 presents the field and laboratory investigation of limestone rocks and their laboratory results. Chapter 4 discusses general information about the study area,

locations, topography, climate, drainage, vegetation cover, regional and local geology of the study area. Chapter 5 presents the general evaluation of limestone used as coarse aggregate in concrete and cobblestones based on their laboratory results with known standards. Chapter 6 presents conclusions and possible recommendations of the study results.

CHAPTER TWO

LITERATURE REVIEW

2.1. Introduction

Reviews of literatures have been carried out exhaustively to get adequate knowledge related to the subject of this study. The reviews are presented in the subsequent part primarily focusing on:

2.2. Description of Limestone

Limestone is a sedimentary rock composed primarily of calcium carbonate ($CaCO_3$) in the form of the mineral calcite (Smith, 2020). It most commonly forms in clear, warm, shallow marine waters (Johnson, 2019). It is usually an organic sedimentary rock that forms from the accumulation of shell, coral, algal, and fecal debris (Williams, 2021). It can also be a chemical sedimentary rock formed by the precipitation of calcium carbonate from lake or ocean water (Brown, 2022).

2.2.1. Environment of Formation

2.2.1.1. Limestone-Forming Environment: Marine

Most limestones form in shallow, calm, warm marine waters (Smith, 2020). That type of environment is where organisms capable of forming calcium carbonate shells and skeletons can easily extract the needed ingredients from ocean water (Johnson, 2019). When these animals die, their shell and skeletal debris accumulate as a sediment that might be lithified into limestone (Williams, 2021). Their waste products can also contribute to the sediment mass (Brown, 2022). Limestones formed from this type of sediment are biological sedimentary rocks (Davis, 2020). Their biological origin is often revealed in the rock by the presence of fossils (Miller, 2021). Some limestones can form by direct precipitation of calcium carbonate from marine or fresh water (Taylor, 2022). Limestones formed this way are chemical sedimentary rocks (Anderson, 2019). They are thought to be less abundant than biological limestones (Clark, 2021). Today Earth has many limestone-forming environments (Roberts, 2023). Most of them are found in shallow water areas between 30 degrees north latitude and 30 degrees south latitude (Harris, 2020).

2.2.1.2. Limestone -Forming Environment: Evaporative

Limestone can also form through evaporation (Smith, 2020). Stalactites, stalagmites, and other cave formations (often called "speleothems") are examples of limestone that formed through evaporation.

In a cave, droplets of water seeping down from above enter the cave through fractures or other pore spaces in the cave ceiling (Johnson, 2019). There they might evaporate before falling to the cave floor. When the water evaporates, any calcium carbonate that was dissolved in the water will be deposited on the cave ceiling (Williams, 2021). Over time, this evaporative process can result in an accumulation of icicle-shaped calcium carbonate on the cave ceiling (Miller, 2021). These deposits are known as stalactites (Taylor, 2022). If the droplet falls to the floor and evaporates there, a stalagmite could grow upwards from the cave floor (Anderson, 2019). The limestone that makes up these cave formations is known as "travertine" and is a chemical sedimentary rock (Clark, 2021). A rock known as "tufa" is a limestone formed by evaporation at a hot spring, lake shore, or other area (Roberts, 2023).

2.3. Uses of Limestone

Limestone is a rock with an enormous diversity of uses (Harris, 2021). It could be the one rock that is used in more ways than any other (Smith, 2020). Most limestone is made into crushed stone and used as a construction material (Johnson, 2019). It is used as a crushed stone for road base and railroad ballast (Williams, 2022). It is used as an aggregate in concrete (Brown, 2020). It is fired in a kiln with crushed shale to make cement (Davis, 2021). Some varieties of limestone perform well in these uses because they are strong, dense rocks with few pore spaces (Miller, 2023).

These properties enable them to stand up well to abrasion and freeze-thaw (Taylor, 2022). Although limestone does not perform as well in these uses as some of the harder silicate rocks, it is much easier to mine and does not exert the same level of wear on mining equipment, crushers, screens, and the beds of the vehicles that transport it (Anderson, 2019). Some of the important uses of limestone included in this thesis are:

2.4. Aggregates

Aggregates typically constitute 60-75% of the concrete mix (Olofinnade et al., 2019). Limestone is a commonly used aggregate material in concrete, due to its availability, workability, and economic viability.

2.5. Aggregate classification

2.5.1. Aggregate classification by size

Aggregates can be broadly divided into two main categories based on their size: coarse aggregates and fine aggregates (sand) (Zongjin, 2014).

2.5.1.1. Coarse Aggregates

Coarse aggregates are essential materials in concrete production, and they play a significant role in determining the strength and durability of the final product (Zongjin, 2014). The grading of a specific maximum-size coarse aggregate can be adjusted within a moderate range without significantly affecting the cement and water requirements of the mixture, as long as the proportion of fine aggregate to total aggregate ensures that the concrete remains workable (Johnson, 2020). If there are large variations in the grading of coarse aggregates, it is important to change the mixture proportions to maintain workability (Smith, 2019). Since it can be challenging to predict these variations, it is often more cost-effective to keep the manufacturing and handling of coarse aggregates consistent rather than trying to minimize gradation differences (Williams, 2021). Typically, the maximum size of coarse aggregate used is either 19 mm or 25 mm. Additionally, an intermediate-sized aggregate, around 9.5 mm, is sometimes included to enhance the overall gradation of the aggregates (Steven et al., 2003).

Figure 17 below shows the different types and layers of aggregates used in concrete production, likely including fine aggregates (≤ 4.75mm), intermediate aggregates (around 9.5mm), and coarse aggregates(≥ 19mm / 25mm)

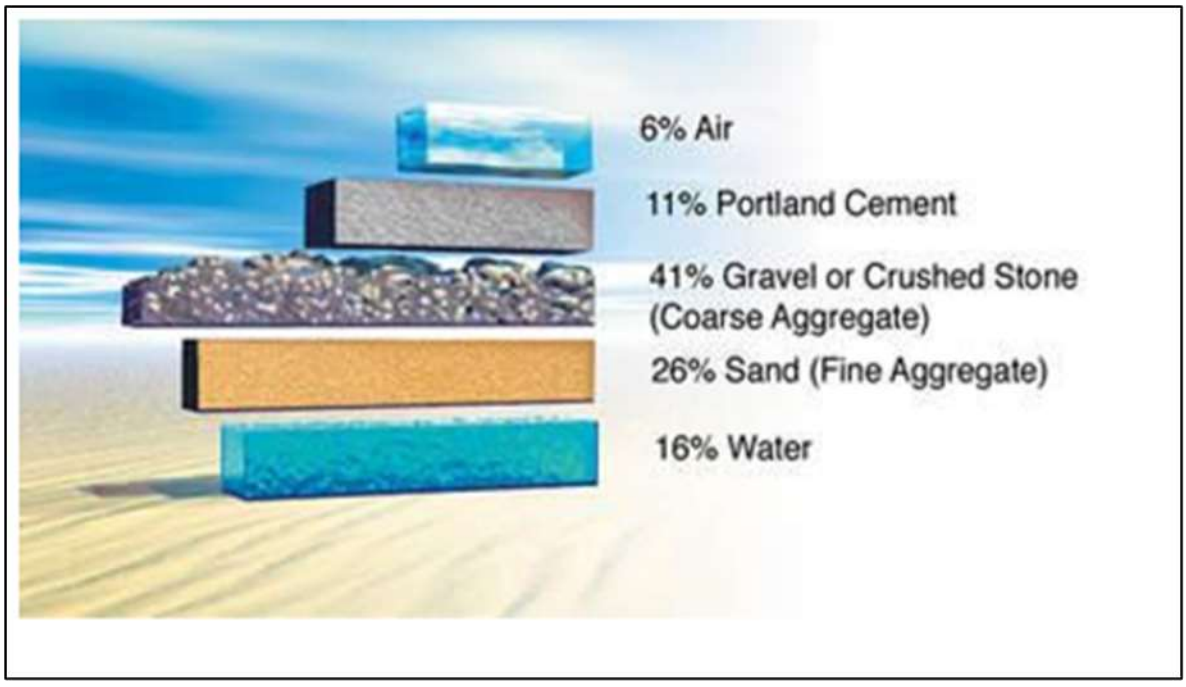

Figure 2: Proportion of materials in concrete (Awe, 2007)

2.5.1.2. Fine Aggregates

The most desirable fine-aggregate grading depends on the type of work, the richness of the mixture, and the maximum size of coarse aggregate (stevens et al.,2005). In leaner mixtures, or when small-size. coarse aggregates are used, a grading that approaches the maximum recommended percentage passing each sieve is desirable for workability (stevens et al.,2005). In general, if the water-cement ratio is kept constant and the ratio of fine-to-coarse aggregate is chosen correctly, a wide range in grading can be used without a measurable effect on strength (Steven et al.,2003). Aggregate passing through 4.75 mm sieve is defined as fine. They may be natural sand deposited by rivers and crushed stone obtained by crushing stones (Nevile,2003).

2.5.2. Aggregate classification by source

Aggregates can also be classified based on their source of origin, which can be either natural or manufactured (Zongjin, 2014).

2.5.2.1. Natural Aggregates

Natural aggregates are materials taken from natural deposits, such as sand, crushed limestone, and gravel, without undergoing significant changes to their nature during production, which may include crushing and grinding (Zongjin, 2014).

2.5.2.2. Manufactured (Synthetic) Aggregates

Manufactured or synthetic aggregates are man-made materials that are produced as a primary product or as an industrial by-product (Zongjin, 2014). Examples of these include blast furnace slag, lightweight aggregates (e.g., expanded perlite), and heavyweight aggregates (e.g., iron ore or crushed steel).

2.5.3. Aggregate Classification by Unit Weight

Following the guidelines provided by the American Concrete Institute (ACI) Committee 213, aggregates can be further classified based on their unit weight, which has a significant impact on the properties of the resulting concrete (Zongjin, 2014).

2.5.3.1. Light weight Aggregates

Lightweight aggregates have a unit weight of less than 1120 kg/m³, and the corresponding concrete made with these aggregates has a bulk density of less than 1800 kg/m³ (Zongjin,2014). Examples of lightweight aggregates include cinder, blast furnace slag, and volcanic pumice (Zongjin,2014).

2.5.3.2. Normal Weight Aggregates

Normal weight aggregates have a unit weight ranging from 1520 to 1680 kg/m³, and the corresponding concrete has a bulk density of 2300 to 2400 kg/m³(Awe, 2007).

2.5.3.3. Heavy Weight Aggregates

Heavyweight aggregates have a unit weight greater than 2100 kg/m³, and the resulting concrete has a bulk density exceeding 3200 kg/m³ (Stevens et al., 2005).

2.5.4. Aggregate properties

2.5.4.1. Physical properties of aggregates

The physical properties of limestone are critical for its use as a coarse aggregate in concrete and cobblestone:

Water absorption (WA)

Absorption relates to the particle's ability to take in a liquid, and it is one of the important properties of an aggregate. The increased absorption capacity of an aggregate may affect the strength of the aggregate, abrasion resistance, surface texture, specific gravity, bonding capabilities, and resistance to freezing and thawing action (David, 2015).

Specific gravity (SG)

The mass of a given substance is divided by the unit mass of an equal volume of water (it is the density ratio of a substance to water). As an example, specific gravity information about a particular aggregate helps in determining the amount of cement needed in concrete mix design (Troxel, 1956). The specific gravities of several commonly used aggregates fall within the range of 2.6 to 2.7, although there are satisfactory materials for which the specific gravity falls outside this range (Troxel, 1956). For example, according to Blyth and DeFreitas (1974), rocks with specific gravity > 2.55 are suitable for heavy construction works.

Moisture content (MC.)

Aggregates exposed to rain collect considerable amounts of moisture on the surface of the particles, and, except at the surface of stockpiles, keep this moisture for a long period of time (Awe, 2007). The

moisture content must be allowed for in the calculation of batch quantities and of the total water requirements of the mix (Neville, 1987). The aggregates in concrete are assumed to be inert materials. However, most of the aggregates do not meet this assumption by either absorbing water (dry aggregates) or by releasing it (wet aggregates) to the mix (Stevens et al., 2005). As a result of this property of aggregates, the design water-to-cement ratio of the mix changes (Johnson, 2020). Therefore, it is important to determine both the absorption capacity and the moisture content of the aggregate (Smith, 2019). The moisture content of fine aggregates was determined by oven drying a sample of fine aggregate (500 g) in an oven at a temperature of 110°C for 24 hours and dividing the weight difference by the oven dry weight (Williams, 2021).

Flakiness index (FI)

The flakiness index is a parameter for measuring the geometry of aggregates (Viman & Bromes, 2005). The grain shape of aggregates is determined by the flakiness index and expresses the relationship between the width and the thickness of the grains. There are demands on uniform dimensions of aggregates because a high proportion of flaky aggregates degrade the bearing capacity of a structure (SGU, 2006).

Unit weight (γ)

Unit weight can be defined as the weight of a given volume of graded aggregate (Abebe Dinku, 2002). The unit weight efficiently measures the volume that the graded aggregate will occupy in concrete and includes both the solid aggregate particles and the voids between them (Awe, 2007). The unit weight is measured by filling a container of known volume and weighing it (Johnson, 2020). However, the degree of tamping or time of vibration will change the amount of void space (Smith, 2019). Since the weight of the aggregate is dependent on its moisture content, constant moisture content is required (Williams, 2021). Oven-dried aggregate samples are used in this test (Abebe Dinku, 2002). The relative bulk density (unit weight) of aggregate commonly used in normal-weight concrete ranges from about 1200 to 1750 kg/m^3 (75 to 110 lb/ft^3) (Steven, 2003). The bulk density depends on how densely the aggregate is packed and consequently, on the size distribution and shape of the particles (Stevens et al., 2005). Thus, for the best purposes, the degree of compaction has to be specified (Johnson, 2020).

2.5.5. Mechanical Properties of Aggregates

The strength and load-bearing capacity of concrete depend on the mechanical properties of the coarse aggregates, including their compressive strength and abrasion resistance (Mehta & Monteiro, 2014).

Los Angeles Abrasion Value (LAAV)

The Los Angeles (LAAV) abrasion test provides a clear perception of abrasion, hardness, degradation, and disintegration of the aggregate. An estimate of LAAV is essentially required to judge the firmness of either the concrete or asphalt to bear and tear right from manufacturing and during their utilization for a long time (Abdel et al., 2015). Abrasion reduces cover to reinforcement. Hence, dense concrete with hard-wearing aggregate and extra cover allowing for wear is required (Abdel et al., 2015). Yavazet al., (2008) investigated the abrasion behaviour of limestone, commonly used as dimensional stones, using a three-body abrasion test. They mentioned that more abrasion-resistant rocks are likely to have high.The Los Angeles (LAAV) abrasion test provides a clear perception of abrasion, hardness, degradation, and disintegration of the aggregate. An estimate of LAAV is essentially required to judge the firmness of either the concrete or asphalt to bear and tear right from manufacturing and during their utilization for a long time (Abdel et al., 2015). Abrasion reduces cover to reinforcement; hence, dense concrete with hard-wearing aggregate and extra cover allowing for wear is required (Abdel et al., 2015). Yavaz et al. (2008) investigated the abrasion behaviour of limestone, commonly used as dimensional stones, using a three-body abrasion test. They mentioned that more abrasion-resistant rocks are likely to have high bulk density, compressive strength, hardness, and low porosity.

In this context, Table 2 presents the Los Angeles Abrasion Value (LAAV) and soundness loss percentages for various types of aggregates collected from different locations in the study area. The data in the table serves as a crucial indicator of the durability and quality of these aggregates, as it measures their resistance to abrasion and impact. By analysing the LAAV values and soundness loss percentages, we can better understand how the characteristics of the aggregates, as highlighted by Abdel et al. (2015) and Yavaz et al. (2008), influence their performance in concrete and asphalt applications. This correlation underscores the importance of selecting aggregates with favourable LAAV results to ensure the longevity and structural integrity of construction materials.

Table 2: Summarizes the LAAV of different aggregates in the study area (Berhane, 2002)

No.	Type	Los-Angeles Abrasion (%)	Soundness loss (%)	Location
1	Crushed aggregate	17.9	2.9	Quiha (limestone)
2	Crushed aggregate	19.6	4.7	Quiha(limestone)
3	Crushed aggregate	21	3.7	Adulis quarry site (black limestone)
4	Sand	-	1.9	Gereb-giba (20km from Mekelle)

Aggregate crushing value (ACV)

The aggregate crushing value measures the resistance to static load (Asmelash Abay, 2010). The aggregate crushing value (ACV) test is prescribed by different standards and is a useful guide when dealing with an aggregate of unknown performance (Abebe, 2005).

Unconfined Compressive strength (UCS)

The Unconfined Compressive strength is a measure of the resistance to crushing loads. It is generally understood that the compressive strength of concrete cannot significantly exceed that of the major part of the aggregate contained therein, although it is not easy to determine the crushing strength of the aggregate itself (Abebe, 2005). In another study conducted by Rammurthy and Gumaster (1998), the compressive strength of coarse aggregate concrete depended on the strength of the parent rock in which the aggregates have been obtained.

2.6. Cobblestones

Cobblestones are defined as small to medium-sized, rounded, or square-shaped natural stones that are commonly used as pavement material. The term "cobblestone" is derived from the geological term "cobble," which refers to a rock fragment with a size range between 64 and 256 mm (2.5 to 10 inches) in diameter (Komar et al., 2010). Typically, cobblestones are made of durable materials such as granite or basalt, which provide excellent strength and longevity to the paved surfaces. In modern applications, cobblestones continue to be utilized in both residential and commercial projects. They are often chosen for their ability to withstand heavy loads, making them suitable for vehicular traffic (Bui et al., 2010). Additionally, the permeability of cobblestone surfaces allows for effective drainage, reducing water runoff and promoting sustainable urban development (Ali & Hossain, 2020). Modern technology has

also enabled the integration of cobblestones into various landscape designs, enhancing the aesthetic value of public spaces and walkways (Meyer, 2009).

The growing recognition of these benefits is reflected in the increasing adoption of cobblestone pavements in urban areas. For instance, Table 3 presents data on the length of cobblestone-paved roads in Mekelle City from 2016 to 2019. The data shows a significant increase in the length of cobblestone roads, from 7.5 km in 2016 to 60.6 km in 2019, representing a growth rate of 19.7%. This trend underscores the ongoing commitment to utilizing cobblestones as a sustainable and aesthetically pleasing option for urban infrastructure. Despite the labor-intensive installation and maintenance requirements, studies indicate that when properly maintained, cobblestone surfaces can have a longer lifespan compared to conventional asphalt or concrete pavements (González et al., 2018). This longevity, combined with the environmental benefits of permeability, supports the continued use of cobblestones in contemporary engineering practices (Zhang et al., 2016). Overall, the historical significance and modern applications of cobblestones highlight their enduring value in engineering and construction, making them a viable choice for sustainable urban environments (Keller, 2013).

Table 3: Cobblestone paved road length in Mekelle City (2016-2019)

Road type	**Years**				
	2016	2017	2018	2019	%
Cobblestone roads	7.5km	14.5km	23km	60.6km	19.7

Source: Construction and Design office of Mekelle City

Figure 3: Figure A and B : (A) Cobblestone road pavement extending from Business College Adihaki branch to Adihaki secondary school, and (B) cobblestone blocks obtained from Shugala quarry

2.6.1. Factors affecting the quality of Cobblestone

Strength of the parent rock

The strength and durability of the cobblestones or aggregates used in concrete are directly related to the properties of the parent rock, such as chemical and mineral composition, specific gravity, hardness, and physical and chemical stability (Mishuk et al., 2015). The selection of high-quality parent rock is essential, as it not only influences the mechanical properties of the cobblestones but also their long-term performance under varying environmental conditions. For instance, granite and basalt are often preferred due to their superior strength and resistance to weathering, which contribute to the longevity of paved surfaces (Bui et al., 2010). The strength and durability of the cobblestones or aggregates used in concrete are directly related to the properties of the parent rock, such as chemical and mineral composition, specific gravity, hardness, and physical and chemical stability (Mishuk et al., 2015).

Anisotropic behaviour

Stone materials are often not isotropic, meaning their strength can vary significantly depending on the orientation of the grain structure or bedding plane relative to the direction of loading (Jumikis, 1983). This anisotropic behaviour can lead to differential wear and failure in cobblestone pavements, particularly in areas subjected to heavy traffic loads. Understanding the directional properties of the stone can aid in optimizing the placement and orientation of cobblestones during installation, thereby enhancing the overall durability of the structure (Ali & Hossain, 2020).

Unconfined compressive strength

The unconfined compressive strength of the stone is a crucial measure of its ability to support load-bearing structures, and it can be influenced by factors such as specimen size, confining pressure, and moisture content (Tsiambaos and Sabatakakis, 2004). Higher unconfined compressive strength values indicate a greater capacity to withstand applied loads without failure, making it a vital parameter in the selection of cobblestones for high-traffic areas.

Environmental Considerations

The environmental conditions in which cobblestones are used also play a significant role in their performance. Factors such as freeze-thaw cycles, chemical exposure, and moisture levels can impact the durability of the cobblestones over time (Zhang et al., 2016). For instance, cobblestones exposed to

de-icing salts may experience accelerated deterioration, necessitating the use of more resilient materials or protective treatments to enhance their lifespan (Keller, 2013).

Type of fill material

The presence of clay or other fill materials between the cobblestones can reduce the purity and interlock of the crystalline particles, thereby decreasing the overall strength and resistance to weathering (John et al., 1967).

CHAPTER THREE

METHODS AND MATERIALS

3.1.Methodology

The research aims to evaluate limestones as a coarse aggregate in concrete and cobblestones in Mekelle area. It includes pre-field work, field work, and post-field work activities as follows:

3.1.1. Literature Review and Secondary Data Collection

The pre-field work involved a comprehensive collection of secondary data to enhance the understanding of the geological, climatic, and environmental conditions of the Mekelle City. This included topographical maps at a scale of 1:100,000, satellite imagery, and digital elevation models (DEM). Additionally, the preparation phase encompassed a thorough review of various geological and structural maps prepared by different researchers, along with reports and studies related to construction materials. This extensive data collection and analysis provided a solid foundation for the subsequent fieldwork.

3.1.2. Field Investigation

The fieldwork and primary data collection process involved conducting a visit to the study area, where the focus was on identifying geological features and measuring geological structures. This included assessing the dip angle, dip amount, joint direction, spacing between joints, and aperture using a clinometer compass. Additionally, rock strength measurements were conducted with an L-type Schmidt rebound hammer test to evaluate the unconfined compressive strength of the rocks. During the fieldwork, twelve representative limestone rock samples and 50kg coarse aggregate samples from each limestone areas (quarries) were collected according to ASTM D 75 to analyse the geotechnical properties of the stone.

3.1.3. Laboratory Analysis

To study the physical and mechanical properties of limestone, two limestone samples were collected from each quarry area. Additionally, approximately 25 kg of coarse aggregate samples were gathered from each location point in accordance with ASTM D 75 specifications. Specific standards of ASTM and BS were adopted for the investigation of various properties, including sieve analysis, specific gravity, water absorption, unit weight, flakiness index, aggregate abrasion value, aggregate crushing

value, and unconfined compressive strength as measured by the Schmidt hammer. All tests were conducted at Mekelle University department of civil engineering, faculty of EIT-M.

The following table (4), summarizes the tests performed on cobblestones and coarse aggregates, along with their specifications, values for the proposed materials, and their respective purposes:

Table 4: tests on Cobblestones and coarse aggregates

Type of test	**Specification**	**Values of the proposed material**	**Purpose**
Gradation (sieve analysis)	BS 812-section 103.1	–	To determine the grading of limestone proposed for use as aggregates or being used as aggregates.
Specific gravity	ASTM, C127	2.4−2.75	To determine the volume occupied by the aggregate
Water absorption	ASTM, C127	0.1−2%	To determine the amount of water absorbed by limestone under specified conditions.
Unit weight	ASTM, C 29	_	To determine the volume occupied by the stone.
Moisture content	ASTM, C 127	0.4-1%	To determine the quantity of water that will be observed in the pore structure
Flakiness index test	BS 812, section 105.5	≤ 25%	To determine the flakiness index of coarse aggregates.
Aggregate abrasion resistance	ASTM, 131	<50%	To determine the percentage of wear due to relative rubbing action between the aggregate and steel balls
Aggregate crushing value	BS 812: Part 110: 1990	<35%	To measure the stone's resistance to the upcoming load of vehicles
UCS	ASTM C568	Low < 28Mpa Medium <55 Mpa High > 55Mpa	To determine the compressive strength of materials

3.1.4. Data Analysis and Interpretation

To achieve the research objectives, the following approaches were employed: (a) an extensive literature review and secondary data collection, (b) detailed field investigations, (c) rigorous laboratory analyses, and (d) thorough data analysis and interpretation of results. The findings regarding the use of limestone as coarse aggregate in concrete and cobblestones within the study area were systematically classified according to ASTM and BS standards.

Furthermore, the laboratory test results were precisely analysed using the Statistical Package for the Social Sciences (SPSS) software, which facilitated the exploration of relationships between the physical and mechanical properties of limestone. This analytical framework allowed for a vigorous understanding of the material characteristics. All data were precisely compiled from literature reviews, field investigations, and laboratory tests, and presented in a visually engaging format, including charts, tables, and maps. This comprehensive presentation not only enhances the clarity of the findings but also provides valuable insights for practitioners and researchers in the field of geological engineering. By integrating these methodologies, the research effectively addresses the objectives and contributes to a deeper understanding of limestone's potential as a construction material.

3.2.Materials

The data processing, presenting and preparation of maps for this research were conducted using various software packages, including ArcGIS 10.5, Global Mapper 15 and Microsoft Office, these tools facilitated the effective visualization and analysis of geological data. All maps generated during this research follow the following specifications :(Projection: UTM), (Datum: WGS84) and (Zone: 37N).

The flow chart methodology as shown in figure 3 included a comprehensive literature review and secondary data collection, which included published and unpublished reports. The base map preparation involved utilizing a topographic map at a scale of 1:50,000 and a DEM at a 30-meter resolution, focusing on regional geology and structures.

Field investigation began with preliminary fieldwork and study area delineation. Geological mapping was conducting using existing map to gather necessary data, subsequent field and laboratory analyses included, rock sample collection for aggregate testing, measuring geological structures, testing the intact rock strength with a Schmidt hammer (UCS), and various physical and mechanical tests. The main goal was to evaluate limestone as coarse aggregate in concrete and cobblestones.

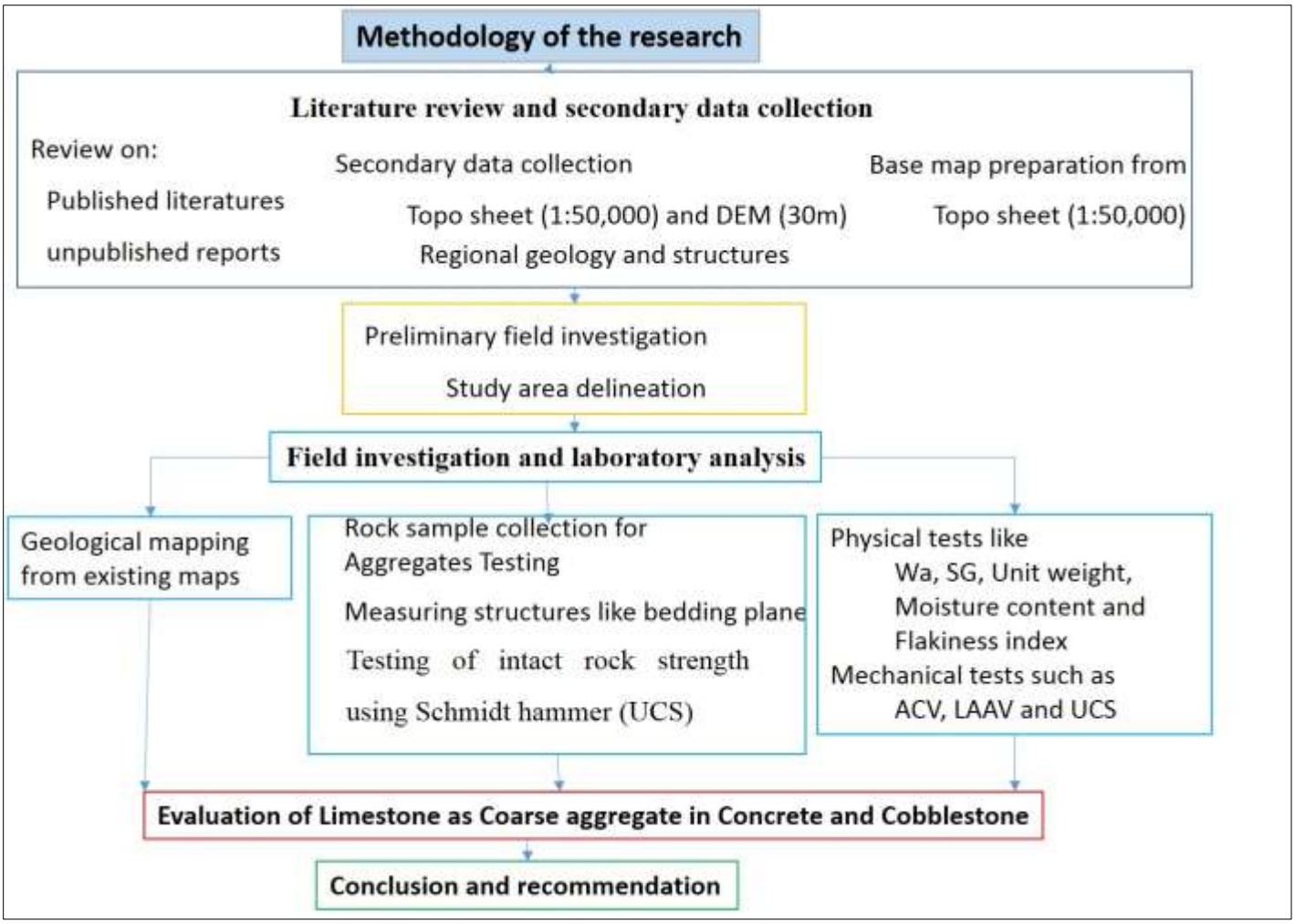

Figure 4: Flow chart shows the research methodology

CHAPTER FOUR
DESCRIPTION OF THE STUDY AREA

4.1.Introduction

The study area is located in Mekelle area and Enderta Wereda, situated in the South Eastern Zone of the Tigray Regional State which is the northern part of Ethiopia as illustrated in Figure 4. This area is characterized by a rich geological landscape that offers significant insights for geological engineering.

Table 5 provides an inventory of the quarries evaluated in this research, encompassing a variety of sites: A) Mossobo, B) Shugala, C) Chanadug, D) Genha, E) Mayalem, and K) Kokolo. These locations, highlighted in Figure 4 and further elaborated in Table 3, not only reflect the geological diversity of the area but also underscore its potential for various engineering applications.

Table 5: List of Quarries evaluated in the study area

Area	Rock type	Color	Location		Elevation(m)	Sample code
			East	North		
Shugala	Limestone	Black	0568392	1492083	2329	Lim#1
			0568548	1491785	2350	Lim#2
Mayalem	Limestone	Black	0540672	1497529	2333	Lim#3
			0540676	1497413	2085	Lim#4
Kokolo	Limestone	Black	0542323	1492870	2085	Lim#5
			0542463	1493072	2086	Lim#6
Mossobo	Limestone	Light grey	0556116	1498728	2372	Lim#7
			0555729	1498632	2368	Lim#8
Chanadug	Limestone	Gray	0557655	1493920	2245	Lim#9
			0557820	1494023	2248	Lim#10
Genha	Limestone	Black	0546437	1486782	2100	Lim#11
			0546493	1486612	2105	Lim#12

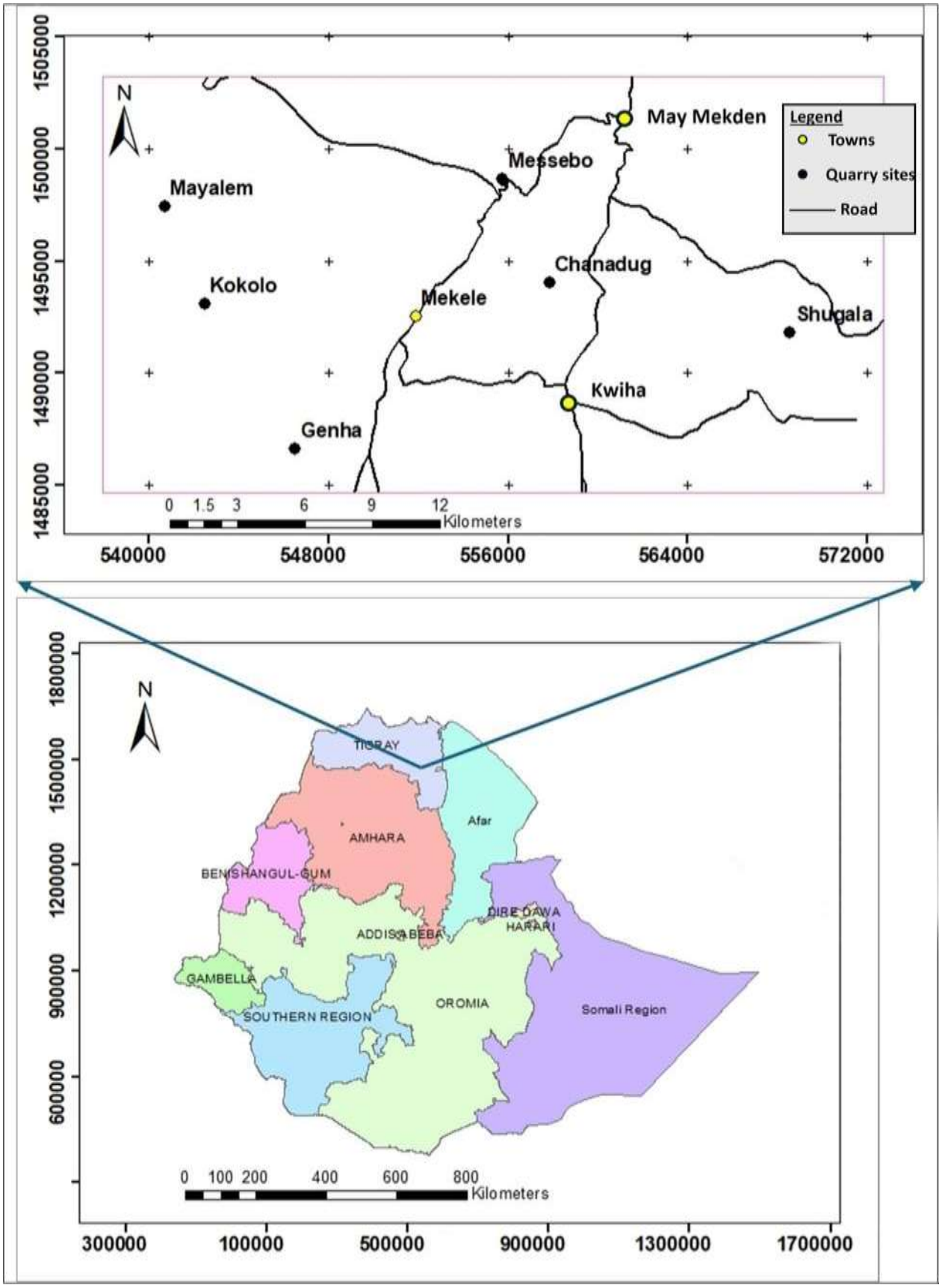

Figure 5: Location map of the study area.

4.2. Climate

4.2.1. Rainfall

The Mekelle outlier and Mekelle City both experiences highly seasonal precipitation patterns. In the Mekelle outlier, the mean annual rainfall is approximately 610 mm, with the main rainy season spanning from July to September (Girmay Abraha, 2019). August stands out as the wettest month, receiving an average of 225 mm of rainfall, while the driest months are typically December to February, with an average of less than 20 mm of rainfall recorded. This seasonal distribution of precipitation significantly impacts the region's hydrology, water resource management, and the timing and success of agricultural activities (Girmay Abraha, 2019). Correspondingly, from the 11 years (2006 to 2017G.C), the mean annual rainfall of Mekelle area is 663 mm. The highest monthly total rainfall was recorded 225 mm in the month of July during 2006 (Ethiopian metrological agency). Rainy season of the area is mostly from June to December in which it is characterized by unimodal rainfall pattern. From October to December the area receives low rainfall whereas from June to August it receives high rainfall (Fig.5).To further illustrate these seasonal rainfall trends, figure 5 below shows the mean monthly rainfall in both regions, highlighting the variation in precipitation throughout the year. To further illustrate these seasonal rainfall trends, figure 5 below shows the mean monthly rainfall in both regions, highlighting the variation in precipitation throughout the year.

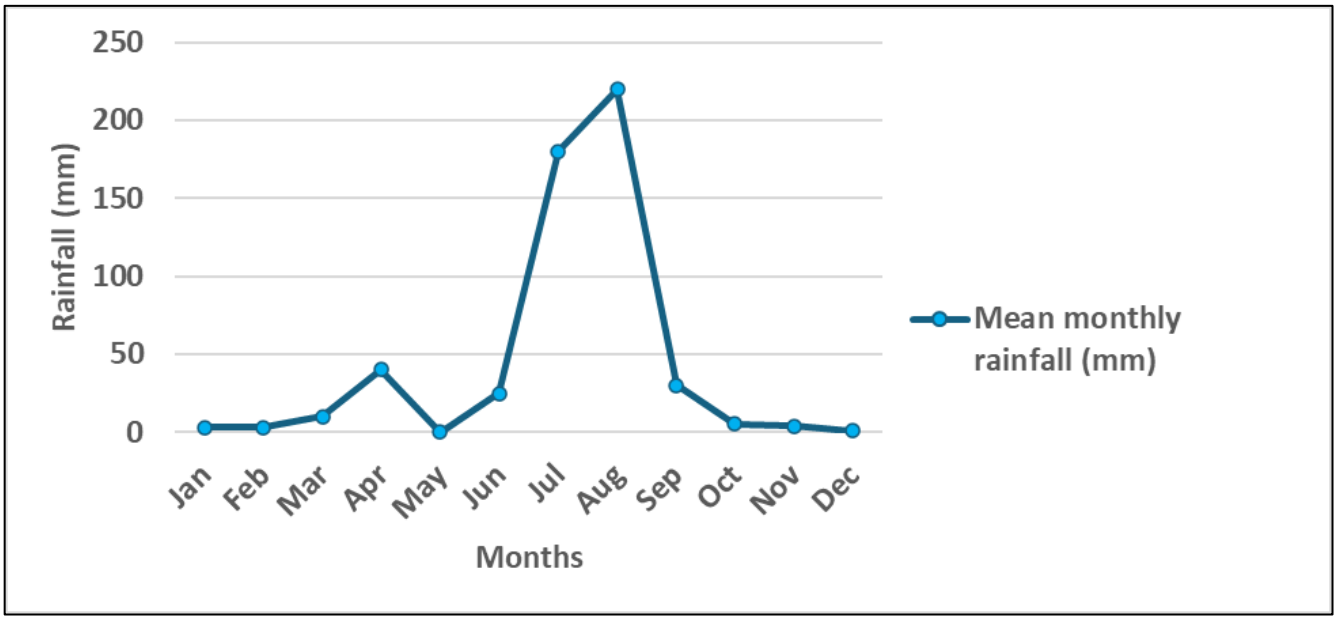

Figure 6: Mean monthly rainfall variations of study area (2006-2017 G.C)

4.2.2. Temperature

The Mekelle outlier region and Mekelle City share a semi-arid climate that features distinct seasonal variations in temperature and precipitation. The Mekelle outlier has a mean annual maximum temperature of around 27°C, with May being the hottest month, averaging about 32°C (Teamir Abraha, 2018). In contrast, December is the coldest month, with average minimum temperatures dropping to approximately 8°C (Teamir Abraha, 2018). This mild temperature regime supports the cultivation of midland crops such as teff, barley, wheat, maize, and sorghum, which are vital for local agriculture.

Similarly, the maximum monthly average temperature of the Mekelle area from (2006-2017 G.C) was 24.16°C and the minimum monthly average temperature was recorded 11.33°C. The monthly maximum temperature of study the area was 30OC in the month of May and June, 2016 (Fig.6).

To further illustrate the temperature variations in both Mekelle outlier and Mekelle City, the following figure 6 presents a comparative analysis of average monthly temperatures throughout the year.

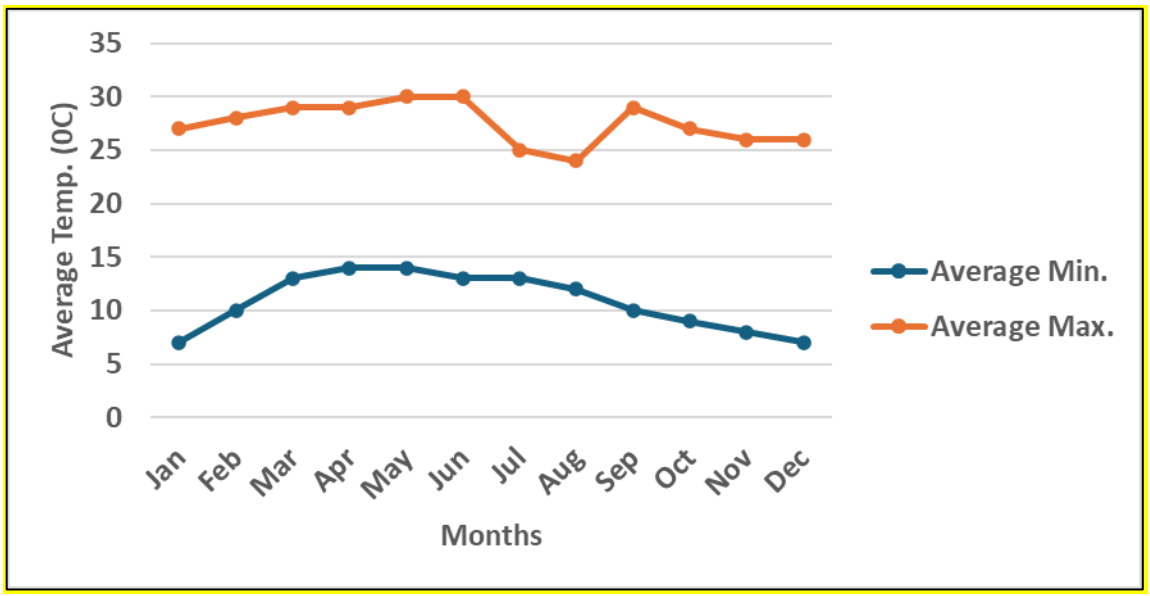

Figure 7: Mean monthly average Maximum and Minimum temperature of study area (2006-2017G.C)

4.3. Topography

The study area is characterized by steep to flat topographical variability: flat lands, narrow creeks, steep chains of mountains to flat areas Maximum elevation of the area is 2300m above sea level whereas the minimum elevation is 450m (Figure 7). The lowland area towards the Geha area generally has a flat to

rolling topography with an elevation ranging from 250 m to 500 m above sea level. Generally, the quarry site found with an altitude range between 0 m to 500 m.

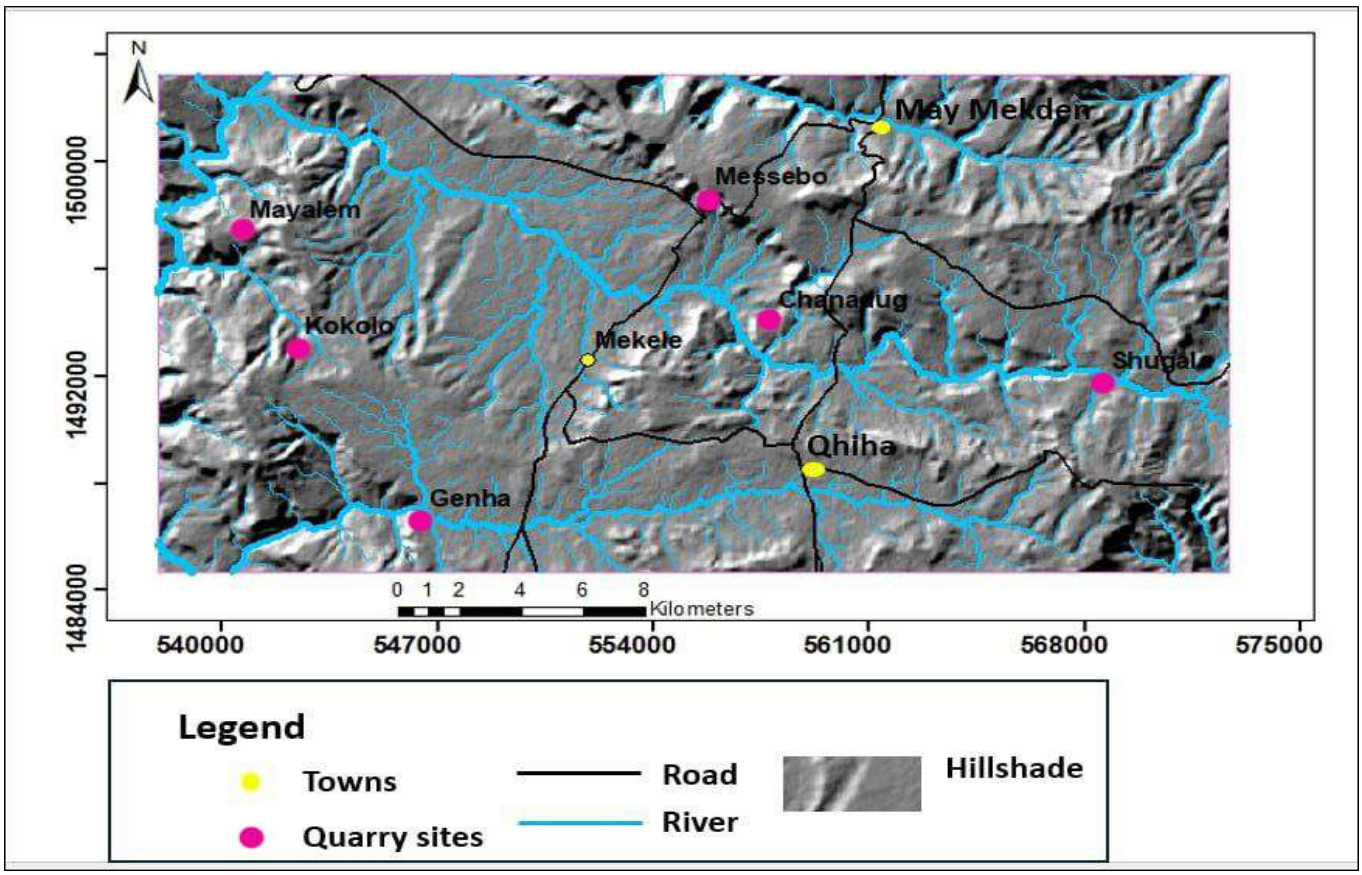

Figure 8: Physiographic map of the study area

4.4.Drainage

The catchment is characterized by spares flow down streams from the major fault which is at high elevation toward the area with flat topography and finally join the Ellala river where the tributaries end up and this river is join to the Tekeze drainage system. The low density of streams may indicate that the bed rock is either highly resistant or highly permeable. The highly resistant of the bed rock may be related with dolerite dykes and the permeable nature is associated with highly fractured and jointed of the bed rocks. It is characterized by dendrites drainage pattern (Figure 8). The main river follows the structurally weak plane of Mekelle fault which intersect different lithological units whereas the tributaries follow the general slope inclination. In the upstream part of the catchment, the tributaries show meandering nature in areas of flat topography and show braided pattern in the areas of steep slopes. The streams are confining streams in such a way that the offset of the tributaries is within the boundary of the catchment.

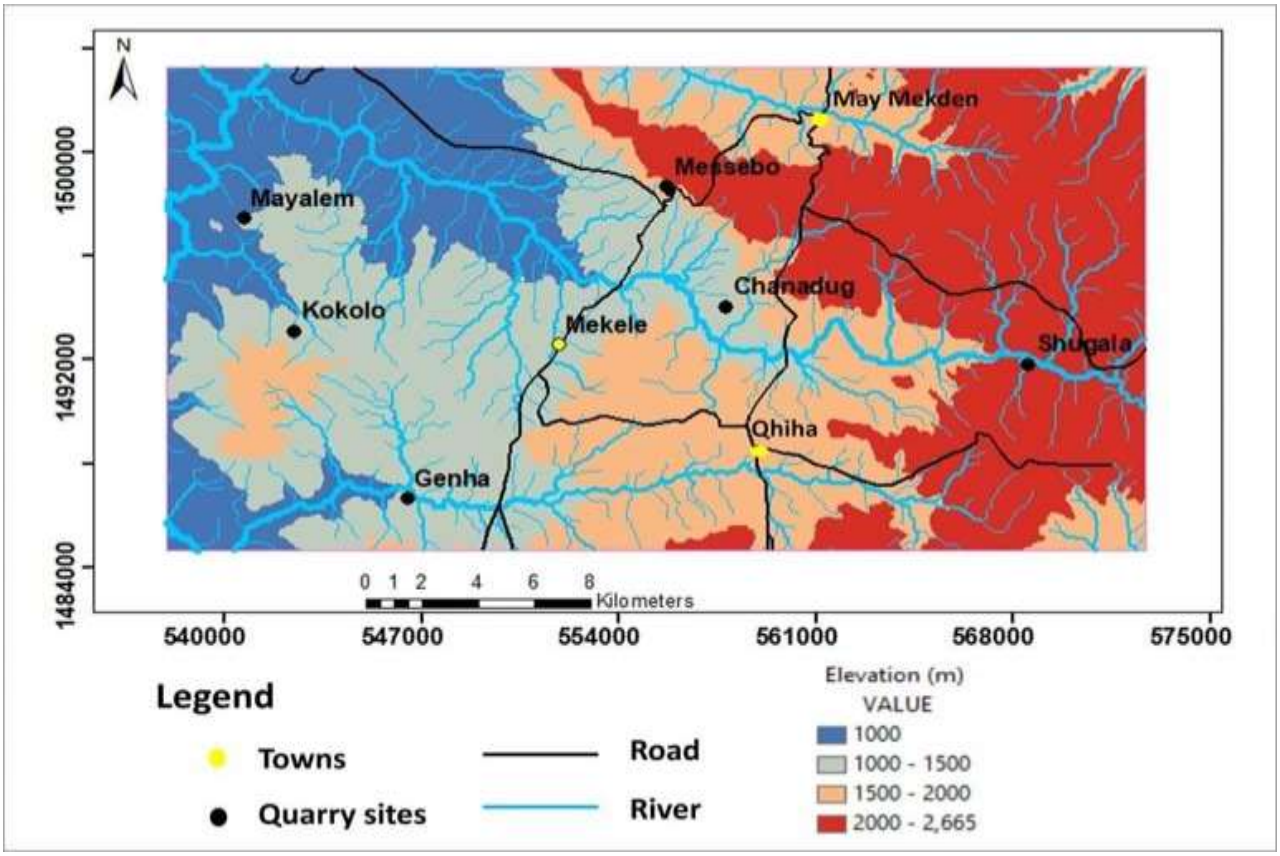

Figure 9: Drainage map of the study area

4.5. Vegetation

The density of vegetation in Tigray area is classified in to three, as dense vegetation, scattered vegetation and little or no vegetation (Tesfaye, 1993). In this classification the catchment generally falls in the little or no vegetation class. The countryside particularly is completely barren of vegetation except along some stream banks and some closed area like churches and schools. Currently, as the government gives particular attention to the protection of forests, dense bushes, shrubs and sparsely planted trees are also on growing on moderately to gentle slope pats of the catchment.

4.6. Regional Geology

According to several authors (e.g. Kazmin, 1975; Tefera et al., 1996; Beyth, 1972a; Bosellini et al., 1997), the geology of the Northern Ethiopia is mainly covered by the following three major litho-stratigraphic units. Precambrian rocks, Paleozoic-Mesozoic sedimentary rocks, Cenozoic volcanic rocks and Quaternary sediments.

4.6.1. Precambrian rocks

The Arabian-Nubian Shield is the northern half of the great collision zone called the East African Orogen which is formed at the end of Neoproterozoic time when east and west Gondwana collided to form the supercontinent Gondwana (Vail, 1983; Stoeser and Camp, 1985) It mainly consists of sutured low grade assemblages of Neoproterozoic volcanic, volcano sedimentary and sedimentary units, intrusive and contains many remnants of oceanic crust in the form of ophiolites (Abdelsalam, 1996; Tadesse, 1996; Tadesse and Alemu, 1998). The current understanding is that the Arabian-Nubian Shield and the Mozambique Belt were formed in structural and metamorphic continuity during Tibetan-style collision between East and West Gondwana, which occurred along the Mozambique Belt (Chen, 2001; Muhongo et al., 2001; Vail, 1983), and a contemporaneous Andean-type oblique collision which occurred in the Arabian-Nubian Shield (Divi et al., 2001).

This accounts for the differences in lithospheric thickness, grade of metamorphism, and intensity of deformation, which is generally higher in the Mozambique Belt relative to the Arabian-Nubian Shield (Stern, 1994). A detailed classification of the basement rocks in northern Ethiopia has been made by Gass (1981), Kroner (1985), and Shackleton (1986). According to these researchers, the Neoproterozoic sequence of Tigray forms the southern end of the Arabian-Nubian Shield. In Tigray, low-grade meta-volcanic, meta-volcanoclastic, and meta-sedimentary rocks are intruded by syn to late tectonic granitoids (Beyth, 1972a; Kazmin et al., 1978; Tadesse, 1996; Alene, 1998), the meta-volcanic and meta-volcanoclastic rocks together forming the largest unit.

The petrographic details and petrogenesis of the Tigray sequence are mostly unknown. However, recent geochemical studies (e.g. Tadesse et al., 1999; Alene et al., 2000a) support the general arc accretion model. The Neoproterozoic assemblage of the region is composed of four major lithologic units which are shown in Figure 9, modified after Miller et al. (2003) and Beyth (1972a). The oldest is the meta-volcanic/meta-volcanoclastic unit (Tsaliet Group), followed by phyllite, slate, and carbonate, which fall under the Tamben Group, and the syn to post tectonic plutonic units, granite to granodioritic composition (Alene et al., 2000a; Garland, 1980).

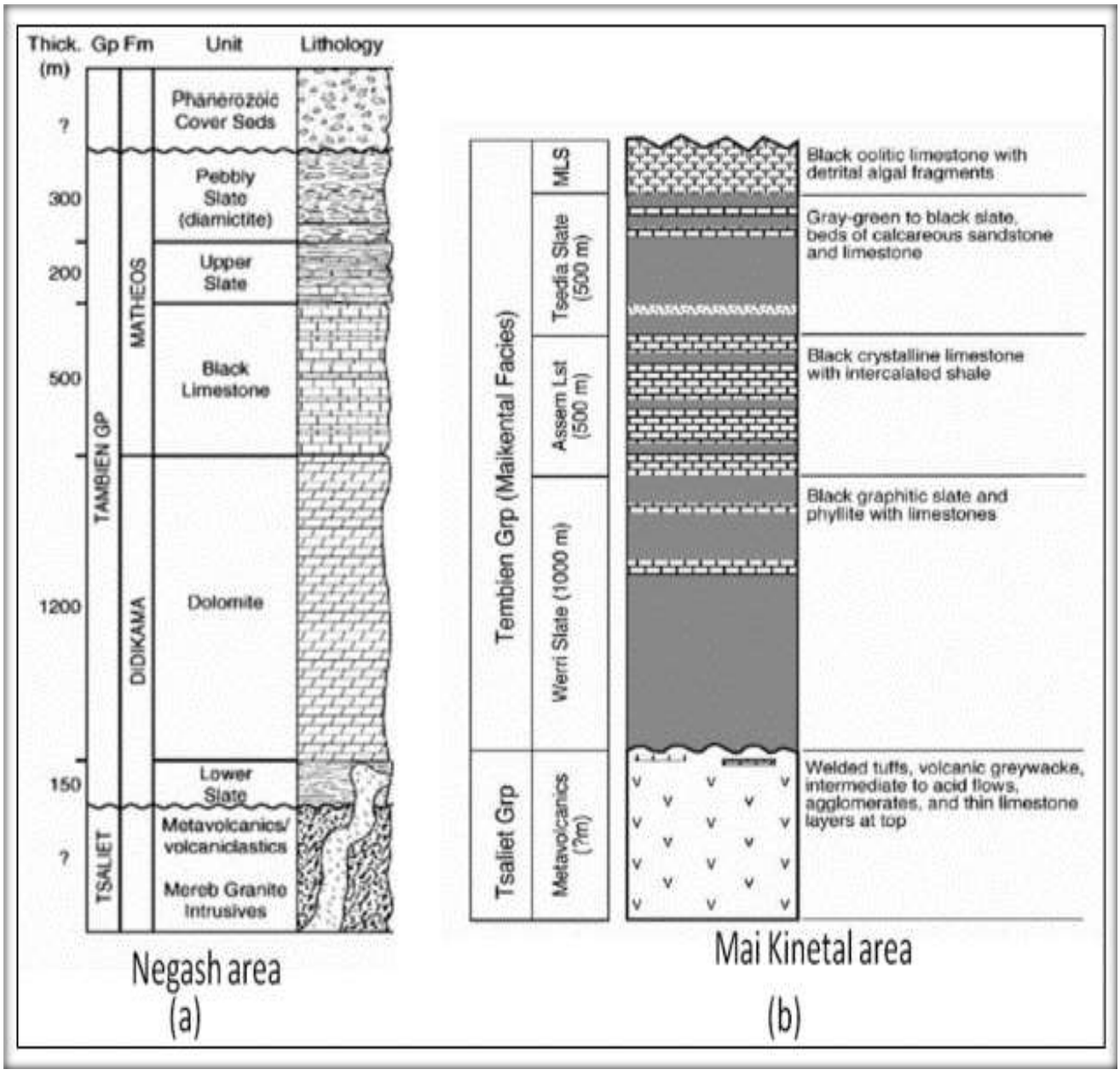

Figure 10: Basement succession of Northern Ethiopia, modified after: (a) Miller et al. (2003), and (b) Beyth (1972a).

4.6.2. Paleozoic sedimentary rocks

4.6.2.1. Enticho Sandstone and Edaga Arbi Glacial Formations

Dow et al. (1971) described two Paleozoic formations: Enticho Sandstone and Edaga Arbi Tillites; both connected with a glacial environment and discordantly covered by the Sandstone with a non-identifiable chronological gap. Garland (1980) favored a "close lithological relation" of the three units and thus lumped them into a major "Adigrat Group". Dow et al. (1971) described a unit made only of sandstone and conglomerate (Enticho Sandstone, thickness less than 160m) and one unit rich in tillites (Edaga Arbi Tillite, thickness 150 to 180m) with boulders up to 6m in diameter. The tillite bearing unit generally overlies the other one, though the two are often described as interfingering. The Paleozoic sequence as a whole overlies the basement with a clear unconformity, whereas a slight angular unconformity is described at the top. The origin of the Edaga Arbi Tillite is a glacial process (Dow et al., 1971).

Evidence includes the massive, almost completely unsorted nature of the deposit, the random distribution of mega clasts which are of great variety, and reflect the composition of the provenance, the great size range of the components from fine rock powder to erratic blocks up to 6m, the presence of boulders known to have travelled large distances, the remarkably uniform nature of the deposit over hundreds of square kilometres, and the striking examples of grooves and striations.

4.6.3. Mesozoic sedimentary rocks

4.6.3.1. Sandstone Formation

The Sandstone is the bottom most and the oldest of the Mesozoic sedimentary succession of the Mekelle Outlier. It locally overlies the horizontal Paleozoic sedimentary rocks of the Enticho Sandstone and the Edaga Arbi Tillites (Dow et al., 1971; Saxena and Assefa, 1973). At some places, it unconformably overlies the basement complex of the area. Like the Antalo Super sequence, the Sandstone is also significantly thinning westward and completely disappears north of the Adigrat Axum road. It is estimated to have a maximum thickness of 700m in the Mekelle Outlier, around Abi-Adi. The Sandstone in the Mekelle Outlier is represented by medium-grained sandstone, which is yellowish to red and pink in color, well-sorted, well-rounded and ripple-marked (Dow et al., 1971). Beyth (1972b) further classified the Sandstone Formation in the Mekelle Outlier into four major units: (1) yellow to red colored, fine to medium-grained sandstone interbedded with variegated siltstones and clay stones; (2) white, medium to coarse-grained, cross-bedded sandstone containing well distributed lenses of

ferruginous silt; (3) red, medium to coarse grained, poorly sorted, cross-bedded ferruginous sandstone, containing quartz pebbles and wood fragments; and (4) 1 to 15m thick beds of white, yellow to brown colored, fine to medium-grained, well sorted, cross-bedded sandstone, containing quartz pebbles. The Sandstone Formation reaches a maximum thickness of 200m in the Ogaden Basin, 800m in the Blue Nile basin, and 1770m in the Danakil Alps on the Red Sea cost (Tamrat and Tibebe, 1997; Worku and Astin, 1992; Bosellini et al., 1997). The Sandstone Formation is equivalent to the Mazera Sandstone of Kenya, the Negrenegre Sandstone of Tanzania, the Minjur Sandstone of Saudi Arabia, and the Kohan Series of Yemen.

4.6.3.2. Antalo Super sequence

The Antalo Super sequence is a carbonate dominated thick succession of limestone, shale and marl (1100m). The stratigraphy of the Antalo Super sequence is shown in Figure 10. It consists of the Antalo Sequence and the Agulae Shale (Bosellini et al., 1997). The Agulae Shale represents the top most part of the Super sequence and is composed of a number of facies cycles, which have a thickness of 10 to 50m. The Agulae Shale is composed of finely laminated black shale, marl, limestone, and local evaporite units mainly composed of gypsum. It is presumed to be a lagoonal/sabkha formation deposited in relatively arid paleoclimatic conditions that occurred during the regression.

The lower section of the Antalo Super sequence, the Antalo Sequence, is a sequence of limestone and marl with occasional shale and calcareous sandstone layers. According to Worash (2001), it can be grouped into four depositional sequences (from top to bottom: A1, A2, A3 and A4), each having a number of Para sequences with a typical thickening and shallowing upward pattern (10). A1 is the basal near shore facies consisting of grain stones, wackestones, and some marl layers. Its upper part displays a coral stromatoporoid rich layer. A_2 consists of arenaceous limestone deposited in a storm-controlled estuarine environment. A_3 is a relatively deep-water facies made up of micritic limestone. It shows some intercalation of wackestones and coquina beds. A3 is generally considered to be a sub-tidal facies affected by storms as documented by storm layers (coquina beds). A4 is a marl-limestone sequence whose basal part is represented by cherty limestone. The entire thickness of the Antalo Super sequence is estimated to be about 1100m (Bosellini et al., 1997), though there is a very great variation in thickness along the east-west direction of the outcrop.

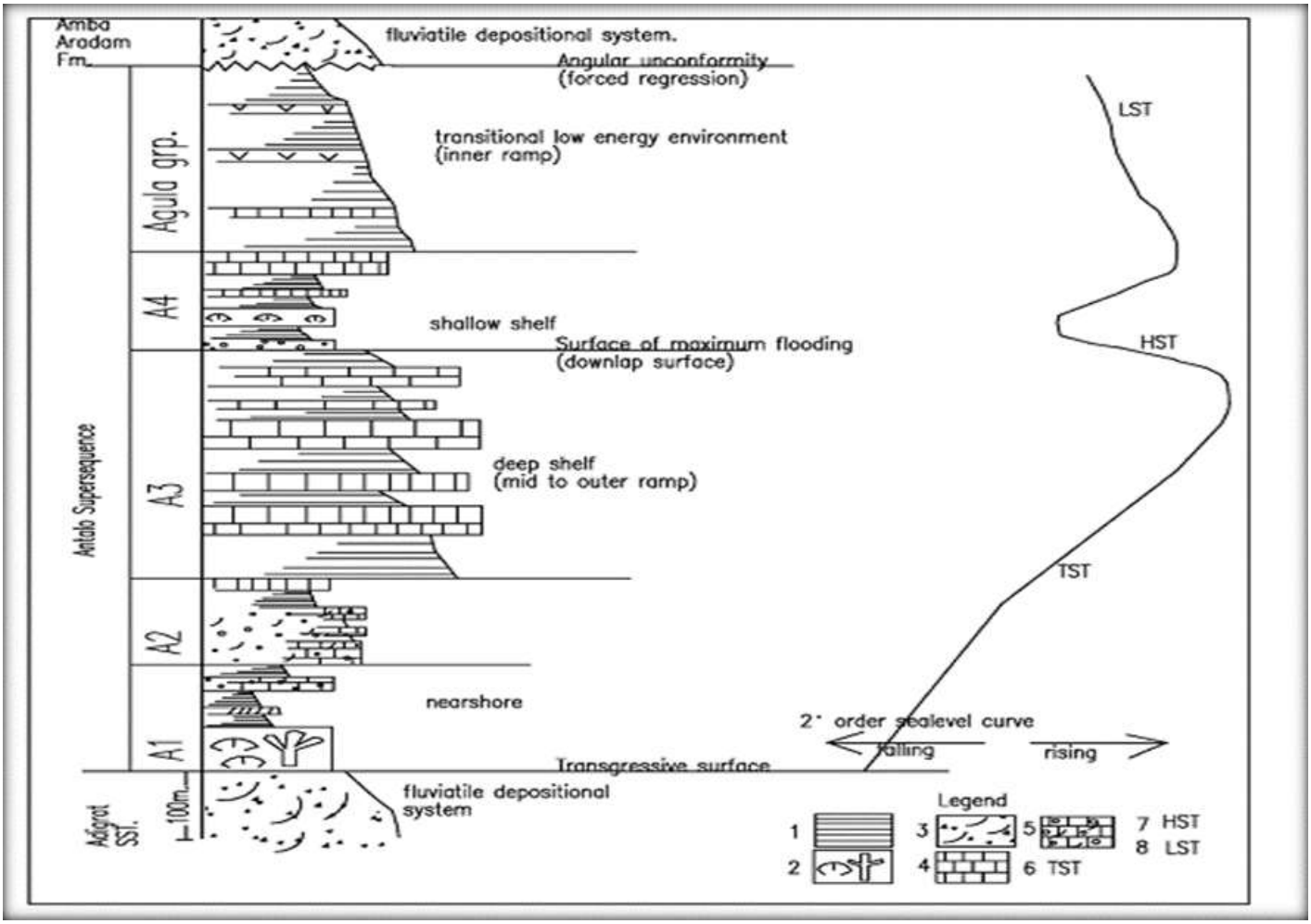

Figure 11: Basement succession of North Ethiopia, modified after :(a) Miller et al. (2003) and (b)Beyth (1972a)

4.6.3.3. Amba-Aradam Formation

The sedimentary rocks of northern Ethiopia fall under two major episodes of deposition: Paleozoic era and Mesozoic era. The major sedimentary deposition of the region, including the south-eastern part of Asia, occurred during the wide geologic span of the Mesozoic era. The so-called Amba-Aradam Formation is the youngest of all Mesozoic sedimentary rocks of the region found unconformably overlying the Upper Jurassic sedimentary succession. The same Upper Sandstone occurs in central Ethiopia (Blue Nile gorge) (Assefa, 1991), Eritrea (Danakil Horst) (Hutchinson and Engels, 1970), and southeast Ethiopia (Harar plateau, Dire Dawa, Chercher Mountains) (Gortani, 1973). In Tigray, the Amba-Aradam Formation is 100 to 200m thick and is overlain by trap basalts (Ethiopian Flood Basalt), as stated in Tesfamichael et al. (2010). It mainly consists of fluviatile sandstone and shale, purple, violet

or yellow, with numerous laterite soils rich in vadosepisoids (Bosellini et al., 1997). The laterite at the base of the formation is quite thick. Bosellini et al. (1997) described the sandstone as coarse grained, and commonly associated with quartz conglomerate lenses, and immature with respect to the underlying Sandstone.

4.6.4. Cenozoic volcanic rocks and quaternary sediments

4.6.4.1. Cenozoic volcanic rocks

The Afar triple junction where the Red Sea, Gulf of Aden and the Ethiopian rifts became the site of intense magmatic and tectonic activity. Hence, significant flood basalts/trap series of volcanic rocks cover a large part of the geology of northern Ethiopia. Lavas in these regions were extruded during the Oligocene, mainly between 31 and 26Ma (Pik et al., 1999; Ukstins et al., 2002). These are part of the larger Ethiopia/Yemen Igneous Province, which is related to the Afar plume and the Red Sea-Gulf of Aden-Ethiopia triple junction. Flood Basalt magmatism resulted in a basaltic lava pile of more than 2,000m thick with an estimated volume of 106 km^3 (Rochette et al., 1998). The upper parts of this pile are partly interlayered with rhyolitic volcanics (Ayalew et al., 2002; Kabeto et al., 2004). Traditionally, the Ethiopian Flood basalt province is divided into four stratigraphic units (Mohr and Zanettin, 1988), which are from bottom to top the Ashange, Aiba, Alage, and Termaber Formations. Flood basalt magmatism was succeeded during the Mio-Pliocene by rifting of the Afar region, resulting in wide spread bimodal alkaline volcanism and crustal uplift. The rift-related uplift of the Ethiopian plateau continues until today and has led to substantial erosion of the flood basalt pile. In the northern part of the region (Tigray and Eritrea) only erosional remnants of flood basalts are left and the sub-volcanic level is widely exposed. In Mekelle region, abundant mafic sills (Mekelle Dolerites) occurred within the Mesozoic to Paleozoic sedimentary strata (Küster et al., 2005).

4.6.4.2. Quaternary sediments

The development of quaternary sediments is mainly governed by the physiographic features, especially by the topography (Tadesse, 1997). Significant portions of the low laying areas of the northern Ethiopia are covered by quaternary eluvial and alluvial sediments (Tadesse, 1997). Quaternary sediments range their grain from clay to boulder sized and they are abundantly found in the western and southern lowlands overlying mostly the low-grade metamorphic rocks and Tertiary volcanics (Hailay, 2008).

Following the pan-African origin, the Nubian shield remained remarkably stable for more than four hundred million years until the end of the Mesozoic. During the Mesozoic, the long succession of gentle

wrapping and sporadic volcanic outbreaks that preceded and followed the opening of the Red Sea rift began (Salma, 1985). Hence the formation of the East African rift system and the associated volcanicity are related to the same forces causing the opening of the Red Sea. During the Paleozoic to early Mesozoic, the northern and eastern parts of East Africa acted as depositional basins for sediments coming from the higher cartons. The period is particularly represented by the Enticho sandstone's and EdagaArbi glacial deposition in Tigray (Kazmin, 1972).

Two major transgressions–regression cycles took place during the Mesozoic (Kazmin, 1972). It is believed that these cycles are related to major regional tectonic events that have affected the entire East African region. The Mesozoic sedimentary succession of the Mekelle outlier is the product of these cycles and rocks representing a range of sedimentary environments have been recognized by various authors. The first cycle began during the early Jurassic or late Triassic and resulted in the deposition of the Agula formation which is constituted of black shale, marl, and clay stone with some beds of black limestone in the Mekelle area. Transgression of the second cycle took place in Aptian to Turonian but is said to have no consequences in causing major deposition in the Mekelle area. However, regression of the second phase during the late cretaceous resulted in the deposition of the Ambaradom formation which is constituted of siltstone, sandstone, and conglomerates. The formation was named after the type locality south of Mekelle town. Therefore, the stratigraphic sequence of northern Ethiopia can be summarized as follows:

- Enticho sandstone and Edaga-Arbitillites
- Metamorphic (basement) rocks
- Flood basalt volcanic
- Amba-Aradom (upper sandstone) formation
- Antalo super sequence (limestone, marl/shale/gypsum)

4.7.Local Geology

Since the geology of the area is part of Antalo-limestone, the major geological units of the area are: (a) Mekelle dolerite, (b) Limestone-Marl interaction, (c) Marl-Limestone intercalation, and (d) Limestone-Marl-Shale intercalation. The detailed descriptions of the mapped units are presented below.

4.7.1. Kokolo Quarry

Kokolo quarry, located approximately 10 km from Mekelle City and accessible via both gravel and paved roads suitable for two-axle vehicles, lies within the Antalo limestone formation, which is a key geological unit in the area. The limestone shows a weathered yellow coloration, a result of prolonged environmental exposure. Structurally, the limestone beds have a shallow to moderate dip (≤ 10°) towards the East-North-East (ENE) and typically display horizontal bedding, with thicknesses ranging from 0.5 m to 3 m. Additionally, the rock mass is highly jointed, featuring joint spacing between 20 cm and 45 cm and apertures varying from 3 cm to 6 cm, with an average thickness of 4.1 m, which may affect excavation stability. The local geology of the area also includes marl-shale-limestone intercalations and dolerite intrusions, adding further complexity to the area's stratigraphy. The local streams, which are seasonal, drain into the Geba River, suggesting significant groundwater interactions that could influence erosion patterns during periods of flow.

Figure 12: Field photographs of black limestone exposures in Kokolo quarry area :(A) Taking intact rock strength using Schmidt -hammer and the right image as (B) shale-limestone intercalations.

4.7.2. Mayalem Quarry

Mayalem quarry is located in the north-western part of Mekelle, at a distance of 14km along the Mekelle-Togoga gravel road. Specifically, the quarry is situated in Mayalem village, at a location of 540534 E and 1497485 N (Figure 12). Accessibility is feasible via two-axle vehicles along the gravel

road. The dominant geological feature of the area is limestone, which has an average thickness of 5.2 meters and an elevation range of 1,660 to 2,160 meters. The topography of the area is generally flat, with a gentle inclination overlying the marl unit. This unit is found in sloped regions along the river that drains into the Geba River, where various outcrops have formed due to landslides.

The geological structures of the area are characterized as follows: the limestone beds exhibit a vertical orientation with dips greater than 10 degrees, and the general dip direction is 355°W. The joint direction is oriented at S 34°50'W, with a joint spacing of 87.5 cm. The aperture of the joints varies from 2 to 10 cm, indicating a multi-directional jointing system. Additionally, tilted blocks are present, dipping at shallow angles and displaced by earth sliding. The primary geological units in the area include limestone, marl-limestone intercalation limestone with some coquina and marl and marl interbedded with coquina fine grained limestone (Fig. 12).

Figure 13: Field photographs of black limestone exposures in Mayalem quarry area.(A) Well-jointed black limestone blocks showing vertical to sub-vertical joints sets.(B) Outcrop illustrating bedded black limestone with visible stratification and joint planes.

4.7.3. Shugala Quarry

The Shugala quarry is located along the Mekelle-Aragura gravel road at a distance 20km from Mekelle city. The area is found at a location of 568155E and 1491988N (Figure 13). Bounded by latitude 13°29'45"N and longitude 39°37'55"E. The geology of the area is primarily composed of Antalo limestone, which includes limestone, dolerite, and shale-limestone intercalation units. The groundmass predominantly consists of limestone, with an average thickness of 5.2 m and elevations ranging from 2180 to 2520 m. The dominant color of the stone is black, while the weathered portions have transitioned to a yellow colour. The geological structure of the area is characterized by several parameters: a dip direction of N48°E, a dip angle of 30°, a joint direction of N175°E, and an average joint spacing of 58.4 cm. The aperture of the joints varies from 3 to 6 cm. The major geological units present in the area include marl interbedded with coquina fine grained limestone.

Figure 14: Field photographs of black limestone exposures in Shugala quarry area. (A) Measuring a dip amount and dip angle of a bedded black limestone with visible stratification and joint planes and (B) Well-jointed black limestone blocks showing horizontal joints sets.

4.7.4. Mossobo Quarry

The Mossobo quarry is located in the Tigray region, approximately 10 km northwest of Mekelle city, the capital city of the Tigray regional state, along the Mekelle-Wukuro main road. This area is situated between the UTM (zone 37) coordinates 555543E to 1498559N and. Geologically, the area is part of the Antalo limestone formation, which comprises marl and shale with minor coquina and black limestone characterized by thin gypsum and dolerite beds, limestone and sandy limestone with, minor

marls, coquina, oolitic limestone and marl. Limestone is the dominant geological unit, with an average thickness of 2.4 m and elevations ranging from 1740 to 2240 m. The geological structures observed in the Mossobo area exhibit a general dip direction of N40°E, with occasional variations in dip amount ranging from 20° to 30° (typically exhibiting a horizontal orientation). The joint direction is N130°E, with an average joint spacing of 26 cm and an aperture close to 2 cm.

Figure 15: Figure 12: Illustrates the field exposure of the limestone units in the Mossobo area .(A) light-gray fossiliferous limestone (B), (C) Micritic limestone exposure with visible bedding planes and (D) Ligh-gray limestone exposure with polygonal joint patterns

4.7.5. Chanadug Quarry

The Chanadug area is located approximately 21 km southeast of Mekelle, along the Mekelle-Adigudom main road, falling within the UTM (zone -37) coordinates of 557460E to 1493861N. The area is characterized by good accessibility, being well-connected by main all-weather roads that link Mekelle to Adigudom, along with several dry-weather roads leading to schools and clinics within the study area. Geologically, the Chanadug study area is situated within the Antalo limestone, which is part of the broader geological feature known as the Mekelle sedimentary sequence or Mekelle sedimentary formation. The main lithological units in the area are marl and shale with minor coquina and black limestone characterized by thin gypsum and dolerite beds, with limestone being the dominant unit, exhibiting a thickness ranging from 2.2 to 2.8 meters. Additionally, the elevation in the area varies from 1960 to 2460 meters, providing valuable insights for geological studies, engineering assessments, and land management in the region.

Figure 16: Field photographs of gray limestone exposures in Chanadug quarry area. (A) vertical limestone bed exposure showing stratification (B) Measuring limestone strength using Schmidt-hammer and Field observation and sampling of limestone and (C) Lateral limestone exposure with overburden material

4.7.6. Genha Quarry

The proposed study area is located in the southwestern part of Mekelle city, situated between the UTM zone 37 coordinates of 546256E to 1486737N (Figure 4.13). Accessibility is provided via the Mekelle-Debri paved road, approximately 8 km from the city centre. The area is characterized by flat-lying, gently rolling hills, with elevations ranging from 1740 to 2240 m. While most of the region consists of lowland, some hill-forming limestone outcrops are located farther from the quarry site. Geologically, the area is part of the Antalo limestone formation, which includes Andesine dolerite, marl and shale with minor coquina and black limestone characterized by thin gypsum and dolerite beds, marl interbedded with coquina fine grained limestone. The agricultural land is predominantly covered by limestone. The geological structure of the area is characterized by a horizontal bedded orientation, with a dip of less than 10° (nearest to 50°). The dip direction is N40°E, while the joint direction is N80°E. The average spacing between joints is 60 cm, and the aperture varies from 40 to 120 cm.

Figure 17: Field photographs of black limestone exposures in Genha quarry area. (A)Black limestone unit interbedded with thin gypsum and fine- grained coquina limestone and (B) Massive black limestone beds with visible jointing and stratification.

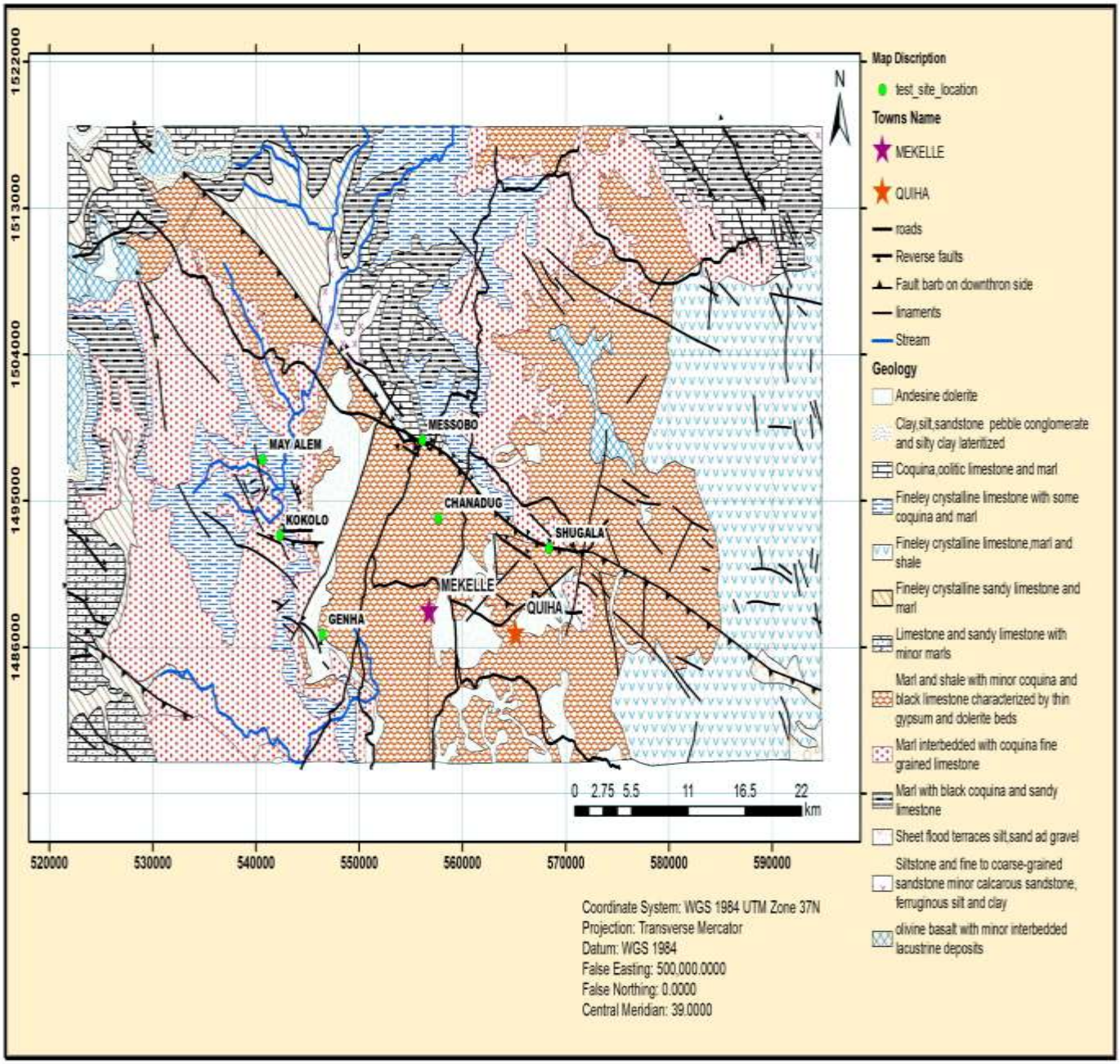

Figure 18: Geological map of the study area (modified after Mengesha Tefera, 1990)

CHAPTER FIVE

RESULTS AND DISCUSSION

5.1.Results

The study aimed to characterize the physical and mechanical properties of limestone used as coarse aggregates and cobblestones. It involved comparing the average results from characterization tests to the ASTM and BS standards. A total of 12 samples were analyzed to determine the physical and mechanical properties like Gradation, specific gravity, water absorption, moisture content, and mechanical properties like compressive strength, aggregate abrasion value, aggregate crushing value and uniaxial compressive strength tests were used. These tests provided a geotechnical characterization of the stone. By comparing the test results to the relevant standards, the performance and suitability of the limestone samples were assessed as shown below.

5.1.1. Sieve Analysis (Gradation)

The grain size distribution curve for coarse aggregates from six quarry sites Shugala, Mayalem, Kokolo, Mossobo, Chanadug, and Genha was determined through sieve analysis, following the guidelines set forth in BS 812:1990. This standard outlines the criteria for acceptable particle size distribution in aggregates. The analysis revealed that the coarse aggregates from the Chanadug, Genha, Mossobo, and Mayalem quarries exhibited favourable particle size distributions, making them suitable for various construction applications. In contrast, the aggregates sourced from the Shugala and Kokolo quarries did not meet the optimal criteria, as their particle size distributions indicated a tendency to require additional fine material to enhance workability

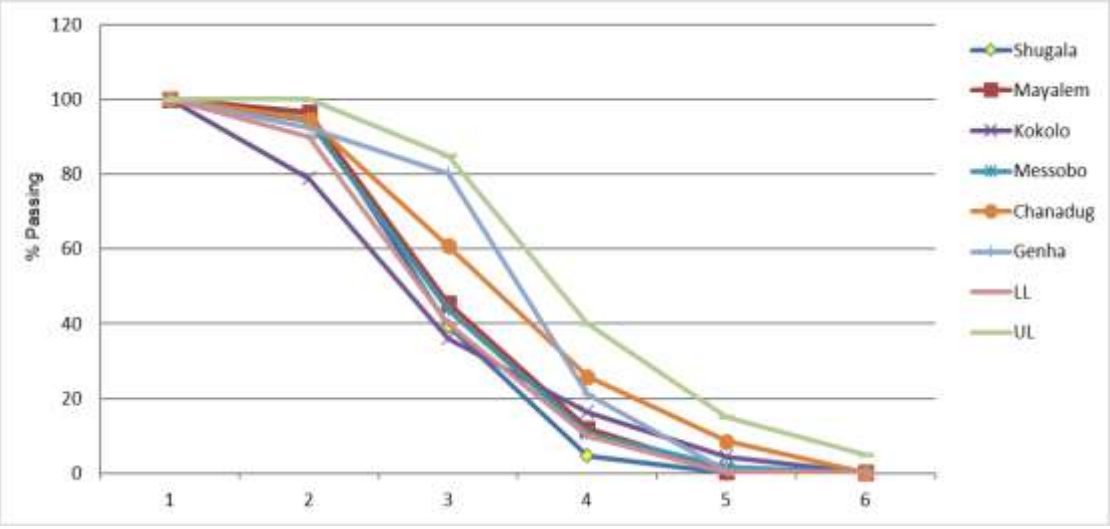

Figure 19: Gradation of coarse aggregates

Table 6 presented the average gradation of coarse aggregates from six different quarry locations. Based on the sieve sizes according to BS 812:1992 stands. For the largest sieve size of 37.5mm, all samples show 100% passing, indicating complete retention. At the 20mm sieve, the percentage passing varies significantly, with the lowest value at Kokolo (78.8%) and the highest at Shugala and Mayalem (96%). As the sieve size decreases to 14mm, the percentages drop further, with Genha showing the highest passing rate (80.23%) and Kokolo the lowest (36.09%). This declining trend continues at the 10mm sieve, where Chanadug exhibits a relatively higher passing percentage (25.84%) compared to other sites. Finer sieves of 5mm and pan sizes show minimal passing percentages across all quarries, with values generally below 10%, reflecting the coarse nature of the aggregates.

Table 6: Average gradation for coarse aggregates according to (BS 812:1992)

Sieve	**Percentage of passing (%)**					
Size (mm)	**Shugala**	**Mayalem**	**Kokolo**	**Mossobo**	**Chanadug**	**Genha**
37.5	100	100	100	100	100	100
20	96.49	96.41	78.8	94.31	94.74	92.26
14	39.42	45.55	36.09	43.74	60.78	80.23
10	4.62	11.92	16.41	10.65	25.84	21.21
5	0.07	0.43	4.37	1.69	8.54	0.74
Pan	0	0.14	0.02	0.08	0.08	0.07

5.1.2. Specific Gravity (SG)

The specific gravity of coarse aggregates sourced from various quarry locations was assessed in accordance with ASTM C127 (2015). The measured values ranged from 2.47 to 2.81, with an average value of 2.65. Figure 20 illustrates, the specific gravity values of all the samples fall within a similar range 2.47 and 2.81, with Genha showing the highest specific gravity and Mossobo shows the lowest. The values for all samples are below the maximum allowable limit set by ASTM.

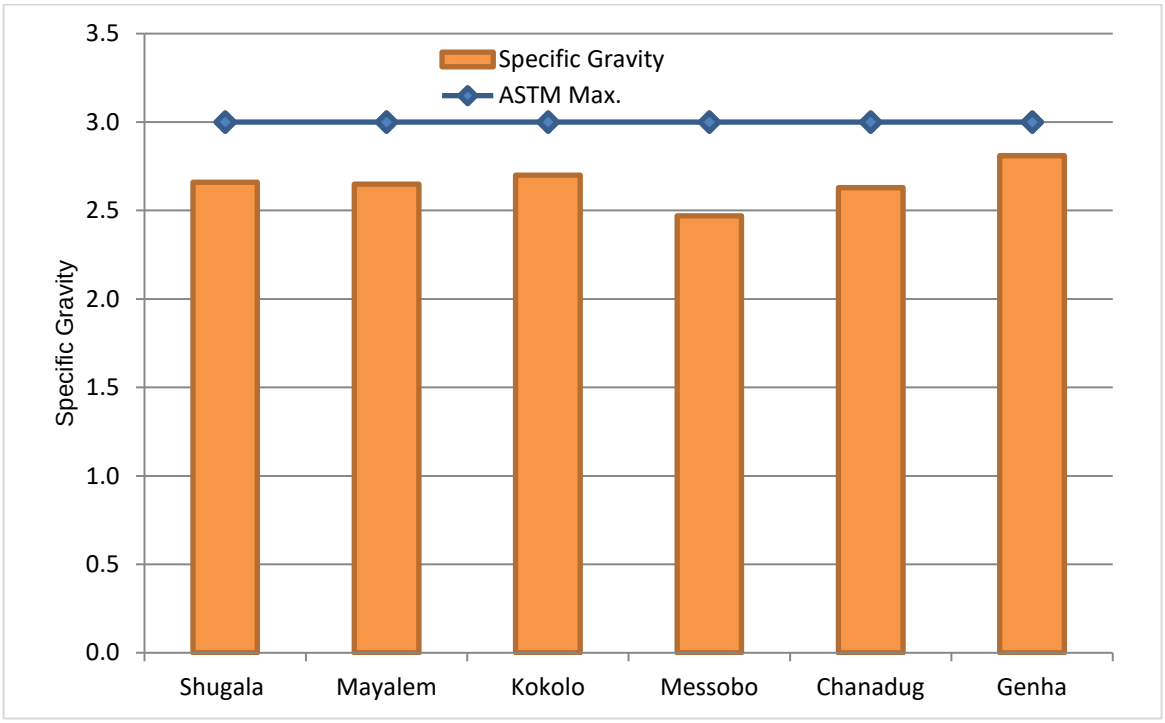

Figure 20: Specific gravity of coarse aggregates (Specific gravity is a dimensionless physical quantity)

5.1.3. Water absorption (Wa)

The water absorption values of the coarse aggregates, which serve as an indirect indicator of porosity, ranged from 0.34% to 0.80%, with an average value of 0.57% (see Fig. 21). The lowest water absorption value was observed in the Chanadug area, while the highest was recorded from the Mossobo quarry. According to ASTM C127 (2015), aggregates utilized in concrete applications typically exhibit water absorption values between 0.1% and 2.0%. The findings from this study indicate that the water absorption values of the limestone aggregates fall well within this acceptable range, further supporting their suitability for use in concrete. Figure 21 illustrates the water absorption values of coarse aggregates from six different sources. All samples exhibit water absorption percentages well below the ASTM maximum limit of 2.0%, shown as a reference line on the graph. The highest value is observed in Mossobo (around 0.8%), while the lowest is in Mayalem (approximately 0.34%). These results indicate that all tested aggregates meet the standard requirements, confirming their suitability for use in concrete based on water absorption performance.

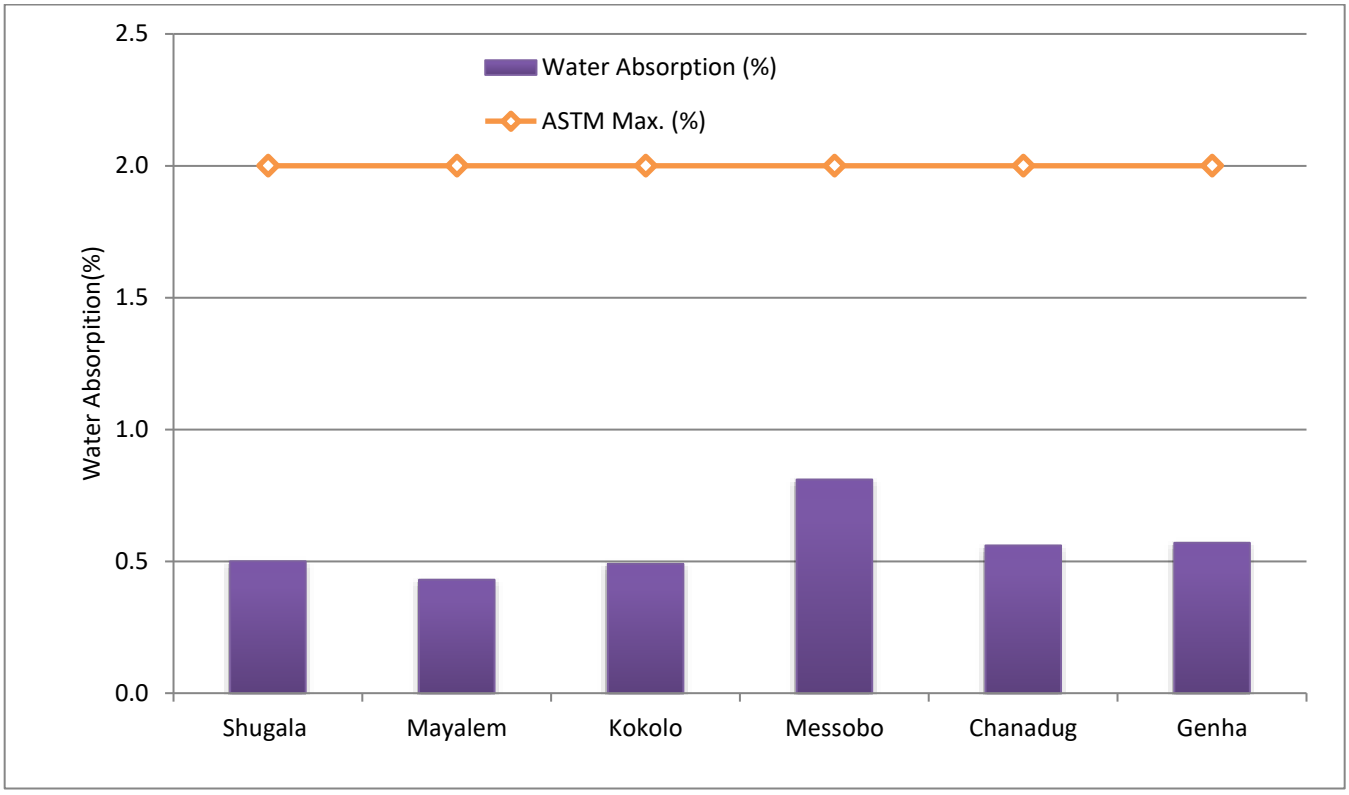

Figure 21: Water absorption of coarse aggregates

5.1.4. Unit weight (γ_d)

The unit weight of coarse aggregates in the study area was determined in accordance with ASTM C29 (2015). The results revealed that the unit weight of the coarse aggregates ranged from 1520 kg/m³ to 1680 kg/m³, with an average value of 1562.46 kg/m³.

Figure 22 shows the bulk density of coarse aggregates from six different sources. The values range from approximately 1.46 g/cc (Kokolo) to 1.65 g/cc (Chanadug). Higher bulk density indicates better packing and lower void content, which contributes to the strength and durability of concrete. All samples demonstrate acceptable bulk densities, confirming their potential suitability for concrete production

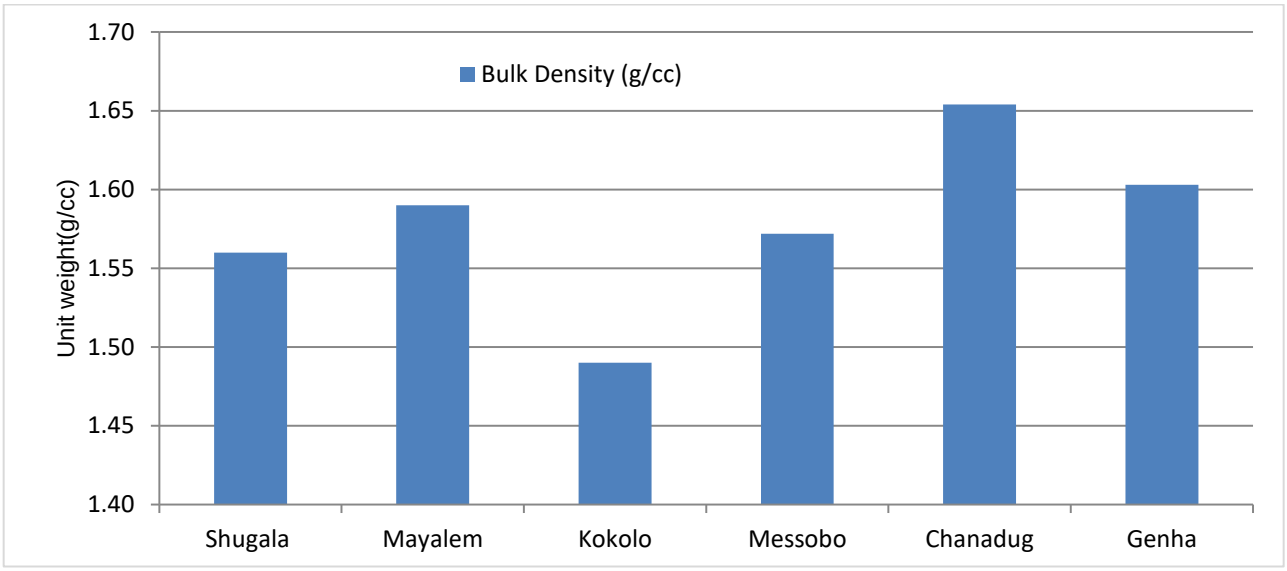

Figure 22: Unit weight of coarse aggregates

5.1.5. Moisture content

The moisture content of coarse aggregates in the study area was assessed in accordance with ASTM C127 (2015). The laboratory test results indicated that the moisture content of the aggregates ranged from 0.19% to 0.24%, with an average value of 0.20%.

Figure 23 presents the moisture content of coarse aggregates from different sources. All values range between approximately 0.13% (Genha quarry) and 0.26% (Kokolo and Mossobo quarries), which are well below the ASTM minimum limit shown on the graph. This indicates that the aggregates contain very low moisture levels, minimizing the risk of affecting water-cement ratios in concrete mixes and making them suitable for construction use.

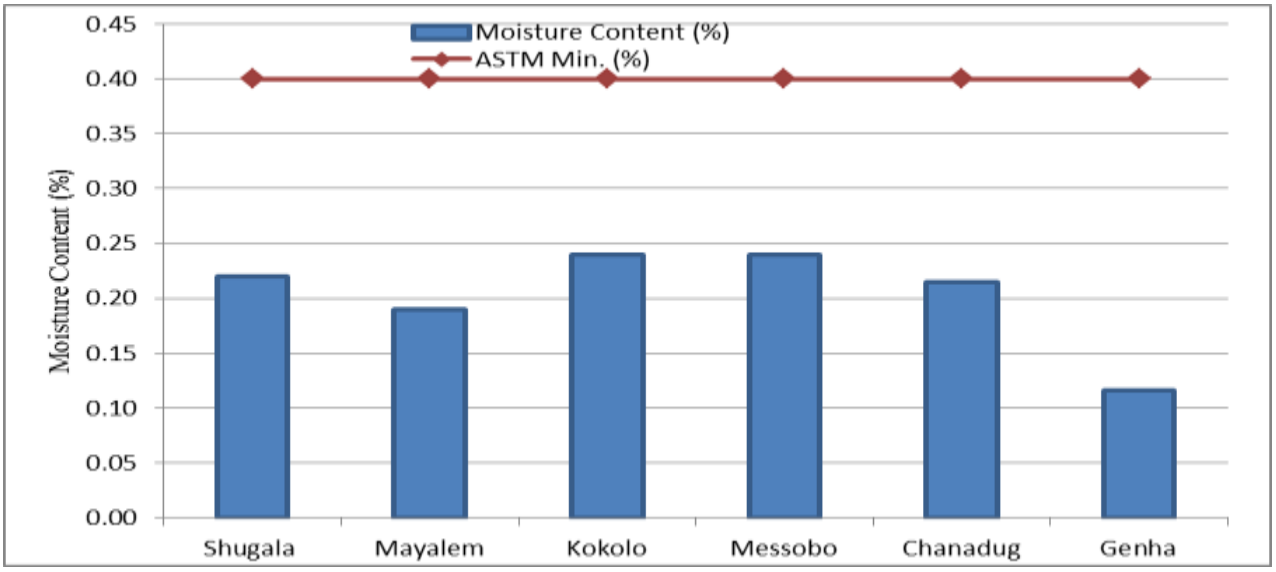

Figure 23: Moisture content of coarse aggregates

5.1.6. Flakiness index

The flakiness index of coarse aggregates was determined in accordance with BS 812 (1990). The results indicate that the flakiness index of the limestone aggregates in the study area ranges from 13.34% to 21.14%, with an average value of 17.68%. This range suggests a moderate level of flakiness, which is important for assessing the workability and performance of the aggregates in
Concrete applications.

Figure 24 shows the flakiness index (%) of coarse aggregates from six sources. All samples have flakiness values well below the ASTM maximum limit (shown as a blue line), indicating acceptable particle shape. The values range from about 13% (Mayalem quarry) to over 21% (Mossobo quarry). Lower flakiness index values are preferred, as they contribute to better workability and strength in concrete. Overall, all sources meet the standard and are suitable for construction use.

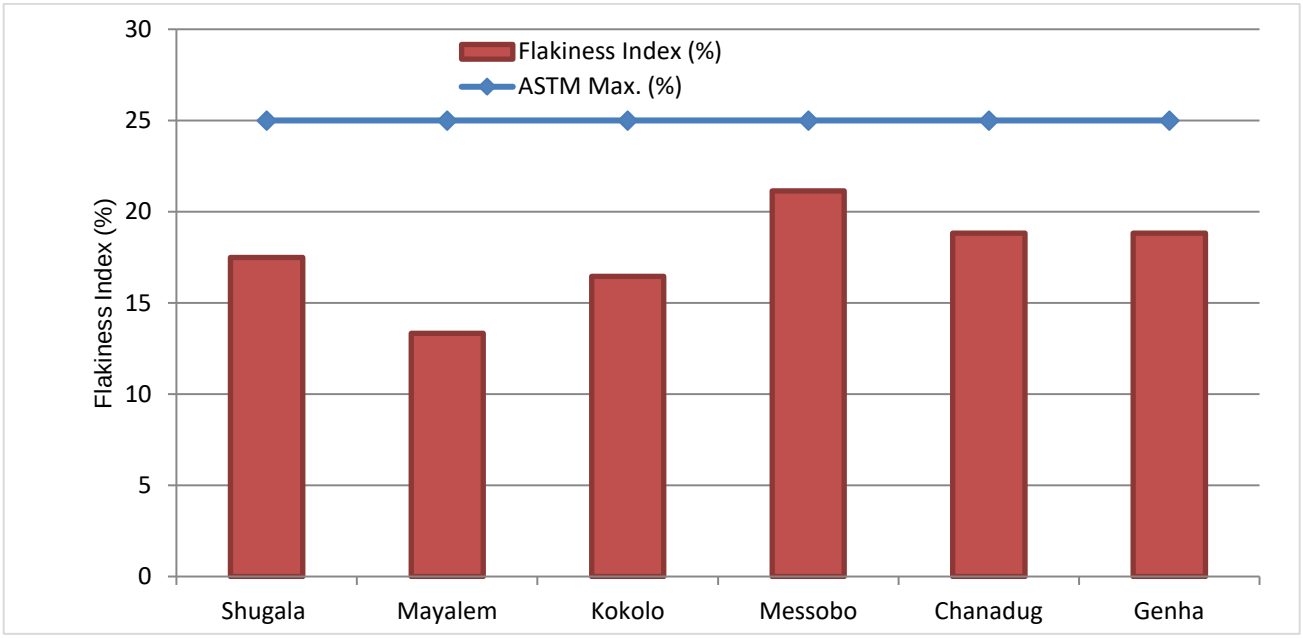

Figure 24: Flakiness index of coarse aggregates

5.1.7. Aggregate Crushing Value (ACV)

The aggregate crushing values of coarse aggregates were determined in accordance with BS 812 (1990). The ACV serves as a measure of an aggregate's ability to withstand gradual loading or crushing; a lower ACV value indicates a stronger aggregate with a greater capacity to resist crushing. Specifically, an ACV value below 10 signifies an exceptionally strong aggregate, while a value above 35 is generally considered indicative of a weak aggregate.

The laboratory test results for the aggregate crushing values in the study area ranged from 10.66% to 22.32%, with an average value of 16.77% as shown in the figure (25) below. Furthermore, according to Fattohi et al. (1990), the selected aggregate samples are suitable for use in all asphalt and concrete applications, as their ACV values are below the 45% threshold.

Figure 25 shows the ACV (%) of coarse aggregates from six sources. All values are well below the ASTM maximum limit (red line at 35%), indicating good strength and resistance to crushing. Among the samples: Mayalem, Genha, and Chanadug have the lowest ACV values (12–15%), meaning they are the strongest aggregates. Kokolo and Mossobo have the highest ACV values (about 25–26%), but still within acceptable limits. Lower ACV values indicate stronger materials, which are more suitable for high-load applications like concrete and pavement

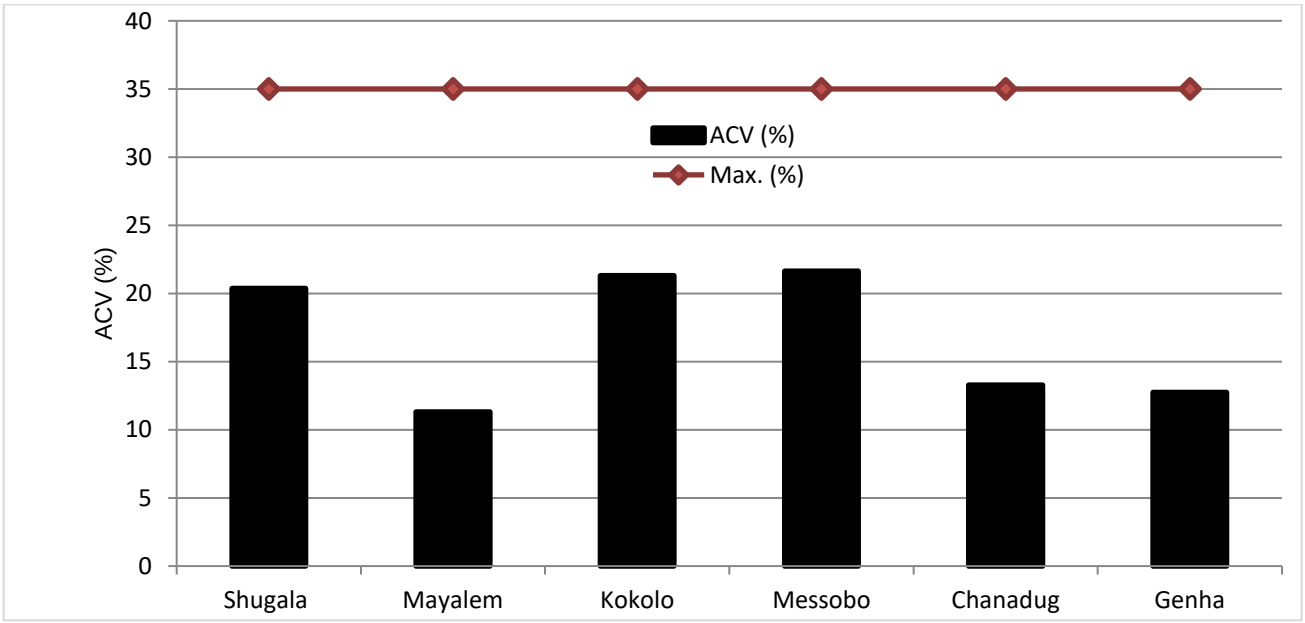

Figure 25: Aggregate crushing values of coarse aggregates

5.1.8. Los Angeles Abrasion Value (LAAV)

The Los Angeles Abrasion Value (LAAV) serves as a general measure of aggregate quality and its resistance to degradation resulting from handling, stockpiling, or mixing. The abrasion resistance of an aggregate is often utilized as an index of its overall quality. In this test, a specified amount of aggregate is placed in a steel drum along with a standard charge of 11 steel balls. The acceptable limits set by the Los Angeles abrasion test, as per ASTM C 131 (2015), range from 30% to 45%. This percentage reflects the degradation or loss of material due to impact and abrasive actions.

The laboratory test results for the Los Angeles Abrasion Values (LAAV) of coarse aggregates in the study area ranged from 19.185% to 24.45%, with an average value of 21.86%. These results indicate that the aggregates possess a relatively low level of degradation, suggesting their suitability for various engineering applications.

Figure 26 below shows the LAAV (%) of coarse aggregates from six sources. LAAV indicates the aggregate's resistance to abrasion and wear; therefore, lower values are better. Notably, all samples are well below the ASTM maximum limit of 50% (indicated by the black line), which means they are durable and suitable for construction. Among the samples, Chanadug has the lowest LAAV at 16%, demonstrating the highest resistance to wear. In contrast, Mossobo and Genha quarries have the highest LAAVs, ranging from 23% to 24%; however, they still remain within acceptable limits for durability.

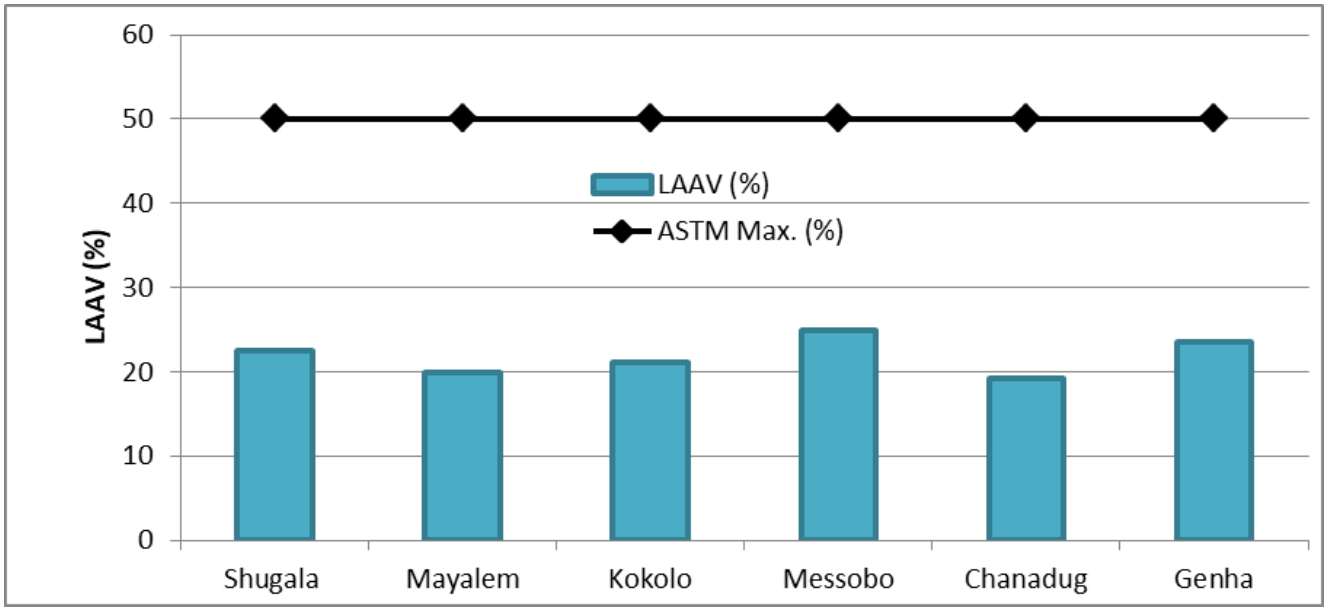

Figure 26: Los Angeles abrasion values of coarse aggregates

5.1.9. Unconfined compressive strength based on Schmidt hammer tests

The Type-L Schmidt hammer was used to measure the rebound hardness of rock faces. The measurements were taken on exposed rock surfaces, with the Schmidt hammer held in the vertical position during the testing. The Schmidt hammer rebound values obtained for each scan line are presented in Table 7. Following the standard procedure outlined by Barton and Choubey (1976), twenty readings were taken at different locations on each rock face to obtain the average rebound value (R). A standard chart, shown in Figure 27, was then used to estimate the uniaxial compressive strength (UCS)

of the rock samples through an extrapolation technique. The results of this analysis are summarized in Table 8. The Schmidt hammer test is a widely accepted and standardized method for estimating the UCS of rock materials in the field.

The rebound value (R) obtained from the Schmidt hammer is directly correlated to the rock's compressive strength, with higher rebound values indicating stronger and more durable rock. By using the standard chart and following the established procedures, the researchers were able to provide an estimate of the UCS for the rock samples based on the Schmidt hammer rebound data. This information is valuable for engineering geologists and rock mechanics specialists, as it helps to characterize the strength and quality of the rock materials at the study site. The consistent and thorough approach to data collection and analysis, as described in the passage, ensures the reliability and reproducibility of the results. This type of information is crucial for making informed decisions about the suitability and safety of rock materials in various civil engineering and construction applications.

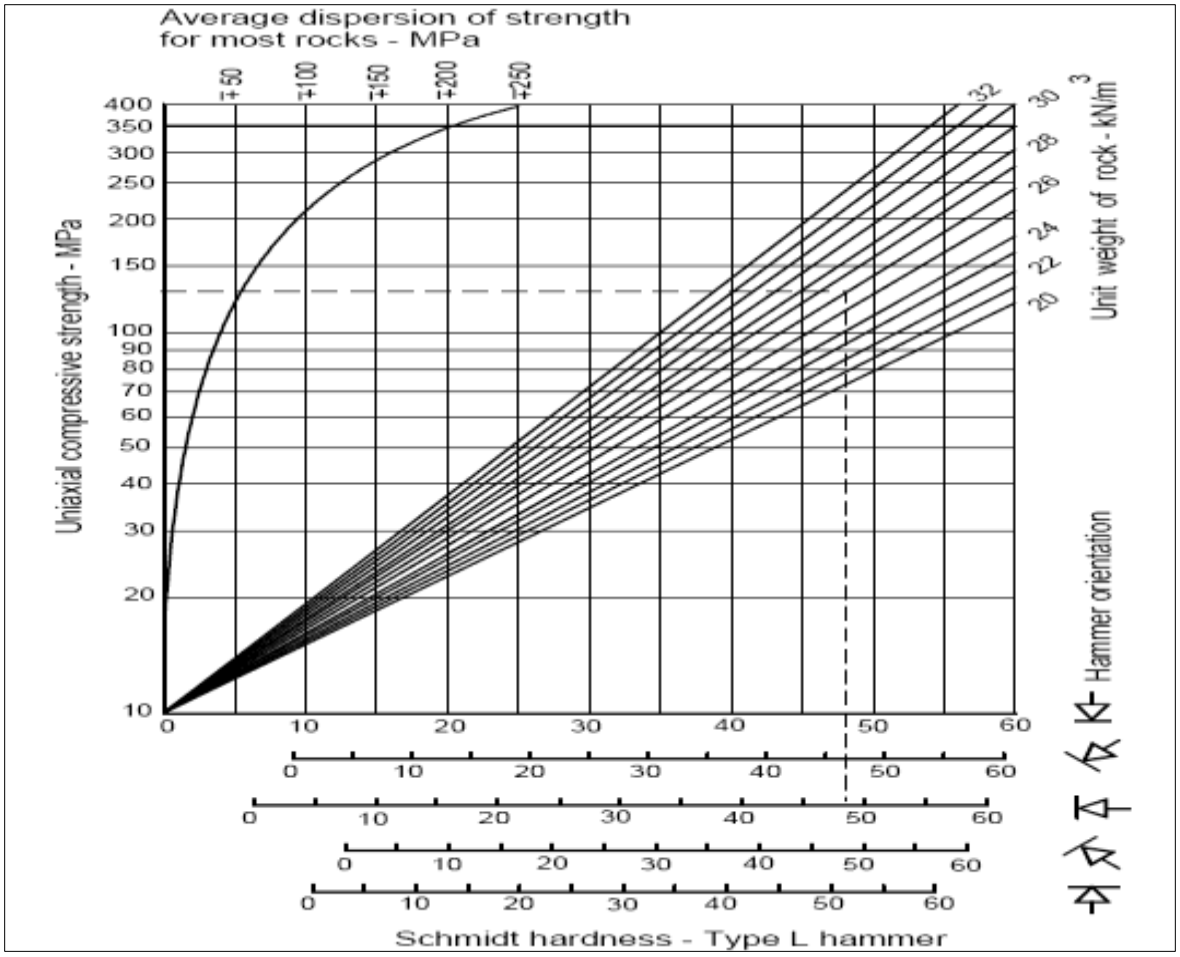

Figure 27: Standard chart for estimating UCS from Schmidt hammer (type L) rebound values (after Deere and Miller,1996)

Table 7: Average Schmidt hammer rebound values

Site	Sample No.	Schmidt hammer rebound values (R)	Avg.R
Shugala	Lim#1	58 56 52 58 52 48 50 58 56 52 60 48 46 56 36 42 58 52 54 52	52.20
	Lim#2	55 64 60 51 54 61 50 56 54 57 59 50 64 64 53 60 53 54 44 49	55.60
Chanadug	Lim#3	50 51 49 53 52 52 55 49 5053 56 58 56 60 64 58 50 56 60 64	54.80
	Lim#4	54 57 50 41 55 54 61 50 52 39 46 41 33 55 53 46 44 43 54 42	48.50
Kokolo	Lim#5	56 56 55 57 57 60 61 58 50 55 50 54 56 59 59 50 49 56 52 58	55.40
	Lim#6	50 49 54 59 48 54 61 53 58 43 57 60 59 56 53 55 57 45 52 55	53.90
Genha	Lim#7	53 57 52 49 51 48 46 50 53 45 50 51 53 49 49 51 53 50 51 49	50.50
	Lim#8	40 44 42 44 55 44 50 40 55 50 61 51 46 44 53 50 63 61 48 54	50.25
Mossobo	Lim#9	50 42 40 54 53 51 44 50 42 53 53 52 51 47 46 48 54 48 56 58	49.60
	Lim#10	50 51 49 53 52 52 55 49 50 53 50 48 50 50 47 43 49 51 46 53	50.05
Mayalem	Lim#11	58 50 57 53 53 59 60 58 56 58 56 62 60 58 56 54 58 55 56 52	56.45
	Lim#12	54 61 62 52 62 54 59 52 52 57 59 60 61 61 59 56 58 54 61 54	57.40

Table 8: Unconfined compressive strength based on Schmidt hammer

Code No	Rock type	Site	Unit weight (KN/m^3)	Schmidt hammer (R)	UCS(Mpa)
Lim#1	Limestone	Shugala	23.07	52.20	112
Lim#2	Limestone			55.60	105
Lim#3	Limestone	Mayalem	24.59	54.80	115
Lim#4	Limestone			48.50	116
Lim#5	Limestone	Kokolo	23.31	55.40	115
Lim#6	Limestone			53.90	113
Lim#7	Limestone	Mossobo	20.95	50.50	111
Lim#8	Limestone			50.25	110
Lim#9	Limestone	Chanadug	22.85	49.60	109
Lim#10	Limestone			50.05	110
Lim#11	Limestone	Genha	21.80	56.45	116
Lim#12	Limestone			57.40	117

The minimum ASTM requirements for compressive strength of high-density, medium-density, and low-density limestone are 55, 28, and 12MPa respectively. The laboratory test result of uniaxial compressive strength (UCS) in the study area varies from 105 MPa to 117 MPa, with an average of

112.42 MPa. This suggests that the limestone in the study area has a higher compressive strength compared to the limestone reported in these other studies and based on (ASTM C 568, 2015) requirements, therefore all limestone quarries from the study area can be used as Cobblestone.

Table 9: Summarize result of physical & mechanical properties

Standard requirements of ASTM and BS.			
Types of tests	**Specification**	**Values of the proposed material**	**Purpose**
Gradation (sieve analysis)	BS 812-section 103.1	-	To determine the particle size distribution.
Specific gravity	ASTM, C127	2.4−2.75	To evaluate the density of materials.
Water absorption	ASTM, C127	0.4−4%	To assess porosity and permeability
Unit weight	ASTM, C 29	1144.5−1291kg/ m^3	To determine the weight of aggregates.
Moisture content	ASTM, C 127	0.5-1%	To assess the moisture level in aggregates.
Flakiness index test	BS 812, section 105.5	≤ 35%	To determine the flakiness index of coarse aggregates.
Los Angeles abrasion value	ASTM, 131	<45%	To evaluate the resistance to wear of aggregates.
Aggregate crushing value	BS 812: Part 110: 1990	<30%	To assess the strength of aggregates.
UCS	ASTM C568	Low < 28 Mpa Medium<55 Mpa High > 55Mpa	To determine the compressive strength of materials.

Table B: Summary test results based on ASTM and Bs.

Site name	Sample location	Dry density (gm./cm^3)	Specific gravity	Water absorption (%)	Moisture content (%)	FI (%)	ACV (%)	LAAV (%)	UCS
Shugala	A	1.5560	2.54	0.70	0.23	18.02	19.48	21.84	112
	B	1.5649	2.47	0.11	0.21	16.95	21.23	23.17	105
Kokolo	C	1.470	2.53	0.71	0.24	14.99	10.66	20.44	115
	D	1.512	2.48	0.39	0.13	17.91	11.98	19.18	113
	E	1.579	2.61	0.65	0.26	18.01	20.48	20.95	115
Mayalem	F	1.607	2.78	0.32	0.22	19.64	22.16	21.27	116
	G	1.526	2.43	0.25	0.28	16.74	22.32	24.45	111
Mossobo	H	1.618	2.51	1.35	0.20	20.91	20.98	25.40	110
Chanadug	I	1.654	2.77	0.34	0.215	20.30	16.10	19.33	109
		1.608	2.78	0.33	0.24	20.00	22.17	21.28	110
Genha	J	1.560	2.83	0.62	0.012	12.11	12.56	22.81	116
	K	1.646	2.59	0.78	0.22	14.56	12.89	24.24	117

5.2.Discussion

The sieve analysis conducted on coarse aggregates from limestone quarries provided a critical evaluation of their particle size distribution and compliance with construction standards. Accordingly, aggregates sourced from Chanadug, Genha, Mossobo, and Mayalem areas conformed their gradation criteria specified in BS 812-section 103.1, demonstrating a well-graded distribution conducive to optimal packing density and workability in concrete applications. In contrast, aggregates from Shugala and Kokolo quarries did not confirmed their gradation, which negatively affect mix uniformity.

The specific gravity (SG) of coarse aggregates in the study area ranges from 2.47 to 2.81, with an average of 2.65. This range is quite similar to values reported in other studies. For instance, Javid

Hussain et al. (2022) from China found SG values of 2.57–2.74 for Mesozoic limestone, suggesting

that the material density profiles are comparable. Similarly, Gudissa et al. (2021) observed a broader specific gravity range of 2.34–2.81 for Harar, Ethiopian limestone, which aligns well with the limestone in my study area.

When we look at other research, Dalep et al. (1963) reported a specific gravity of 2.58 for American limestone, while Maslehuddin et al. (2003) found a bulk specific gravity of 2.54 in Saudi Arabia. Furthermore, Swart (1987) indicated that specific gravity ranges from 2.8 to 2.9, with an average of

2.85 in the Netherlands, and Shetty (1982) reported an average specific gravity of 2.69 in India. Interestingly, the results from my study area are slightly higher than those of Al-Omari (2015), who reported a range of 2.31 to 2.58 for Jordanian limestone, suggesting that my samples have a higher aggregate density. On the other hand, my values are lower than the Nigerian limestone average of

2.71 cited by Akinniyi et al. (2016), indicating some minor differences in composition. Additionally, Nagih M. (2016) reported an apparent specific gravity range of 1.93 to 2.58, with an average of 2.20 in Iraq, while Salma (2018) found an average specific gravity of 2.7 in Sudan.

Overall, these comparisons show that the coarse aggregates from my study area not only meet ASTM standards but also demonstrate competitive properties for construction use, reinforcing their suitability for various applications.

The water absorption (Wa) of coarse aggregates in this study ranged from 0.34% to 0.80%, with an average of 0.57%. This aligns well with ASTM C127 (2015) standards (0.1–2.0%) and indicates low water absorption, making these aggregates suitable for concrete applications. Notably, these findings closely match those of Javid Hussain et al. (2022), who reported water absorption values of 0.33% to 0.80% for Mesozoic limestone, suggesting consistent material properties across similar geological formations. In contrast, Jordanian limestone, as reported by Al-Omari (2015), exhibited significantly higher variability in water absorption, ranging from 0.55% to 9.43%, with some samples exceeding practical limits for concrete durability, thereby raising concerns about their suitability in construction.

Similarly, Ethiopian limestone analysed by Gudissa et al. (2021) demonstrated a broader range of 0.2% to 5.7%, indicating potential differences in mineral composition and porosity that could affect performance. Furthermore, Saudi Arabian aggregates studied by Shameem et al. (2003) recorded elevated Wa values of 2.2%, which further emphasizes the superior performance of the aggregates in this study.

When comparing with other research, Shrawan et al. (2009) reported water absorption values ranging from 0.20% to 0.68%, with an average of 0.37% for Nepali limestone, which is lower than the average found in this study but still indicates good performance. In contrast, Maslehuddin et al. (2003) found a water absorption of 2.20% in Saudi Arabia, which is significantly higher than the values observed in my study. Additionally, Swart (1987) indicated that water absorption in the Netherlands ranges from 2.8% to 2.9%, with an average of 1.00%, further highlighting the superior performance of the aggregates in my study area. Moreover, Salma (2018) reported an average water absorption of 1.46% in Sudan, which is also higher than the average found in this study. Collectively, these comparisons confirm that the limestone tested in this research not only meets ASTM criteria but also outperforms several regional counterparts in terms of water absorption. This reinforces its viability for high-quality concrete applications, highlighting the importance of selecting aggregates with optimal porosity for enhanced durability in engineering projects.

The unit weight of coarse aggregates in the study area ranges from 1520 kg/m³ to 1680 kg/m³, with an average of 1562.46 kg/m³, indicating a moderate density that may influence the overall performance of concrete. In contrast, studies from China (Javid Hussain et al., 2022) reported significantly higher unit weights, ranging from 1.73 g/cc to 2.78 g/cc, suggesting that the geological conditions in that region favor denser mineral compositions and better packing of aggregates. Similarly, Malaysian limestone aggregates (Hon Sin Chin et al., 2025) exhibited even higher dry densities, between 2646 kg/m³ and 2887 kg/m³, likely due to the presence of well-cemented carbonate rocks with low porosity. Moreover, Jordanian limestone (Al-Omari, 2015) showed unit weight values between 2.31 g/cc and 2.58 g/cc, which also indicates a denser aggregate composition compared to my findings.

The lower unit weight in the study area may suggest a higher void content or weaker cementation, potentially linked to the sedimentary depositional environment or weathering processes affecting the aggregates. Conversely, the higher unit weights observed in other regions, such as Nigeria (Akinniyi, 2016), where the average bulk density is reported at 2.61 g/cm³, indicate a more robust geological formation that enhances the strength and durability of concrete. Therefore, while the aggregates from the study area demonstrate acceptable unit weights, further geological assessments could provide insights into improving their density and overall performance in concrete applications.

In the study area, the moisture content of coarse aggregates was assessed according to ASTM C127 (2015), revealing values ranging from 0.19% to 0.24%, with an average of 0.20%. As illustrated in Figure 21, moisture content from various sources, including Genha quarry (0.13%) and

Kokolo/Mossobo quarries (0.26%), remains well below the ASTM minimum limit. This low moisture content may cause issues during mixing and compaction. In contrast, the study conducted by Martha Yirga in the Mekelle area reported a higher moisture content for limestone coarse aggregates, ranging from 0.21% to 0.37%, with an average value of 0.27%. This indicates that the aggregates in the Mekelle area possess a lower moisture content similar to that of the study area. The decreased moisture levels in the Mekelle aggregates could potentially pose challenges in construction, as they may affect the water-cement ratios and overall performance of concrete mixes.

While both studies adhere to ASTM C127 (2015) for moisture assessment, the findings highlight a significant difference in moisture content. The lower moisture levels in the study area suggest a less favourable condition for construction, as they increase the likelihood of moisture-related issues. Overall, this comparison underscores the importance of local geological and environmental conditions in influencing the moisture content of coarse aggregates. Understanding these differences is crucial for optimizing material selection and ensuring the durability and performance of concrete in various construction contexts across Ethiopia.

The aggregate crushing values (ACV) obtained in the study (ranging from 10.66% to 22.32%, with an average of 16.77%) indicate a relatively strong and durable limestone aggregate compared to those studied in other regions. Specifically, Shrawan et al. (2009) reported higher ACV values (22.00%–26.50%) for Nepalese aggregates, Maslehuddin et al. (2003) recorded an ACV of 24.2% for Saudi Arabian limestone, and Mojtaba et al. (2019) observed an average of 26.79% for Egyptian samples—each considerably higher than those in my study area. Similarly, Swart's (1987) Dutch aggregates had a mean ACV of 24%, reinforcing the fact that the rocks in my study area exhibit superior mechanical resistance to crushing, making them more favorable for high-load applications such as road pavement and structural concrete.

The study on the Los Angeles Abrasion Value (LAAV) in my area reveals a range of 19.185% to 24.45%, with an average of 21.86%. This indicates low degradation and suggests that the aggregates are suitable for various engineering applications. In comparison, research from China by Javid Hussian et al., (2022) shows a broader LAAV range of 2.69% to 25.18%, where the upper limit is

close to my average, indicating that some aggregates may be of lower quality while others remain acceptable. Similarly, a study conducted in Ethiopia by Gudassa et al., (2021) reports LAAV values between 18.9% and 31.1%, which encompasses my findings and suggests that the aggregate quality in

both regions is comparable. Conversely, studies from Nepal (Shrawan et al., 2009) and Saudi Arabia report by Maslehuddin et al. (2003) higher average values of 28.99% and 24.2%, respectively, indicating that their aggregates may be less suitable for high-performance applications. Furthermore, India's lower average of 16.5% suggests that some aggregates there exhibit even better abrasion resistance. Overall, the variability in LAAV across different countries underscores the influence of local geological conditions on aggregate quality, emphasizing the importance of regional assessments in determining material suitability for construction projects. My findings contribute to a broader understanding of aggregate quality on a global scale, highlighting the need for careful material selection based on local characteristics. The Unconfined Compressive Strength (UCS) values from my study on limestone using the Schmidt hammer tests range from 105 MPa to 117 MPa. For example, the UCS is 112 MPa at Shugala and 116 MPa at Genha. When I compare these results to studies from other countries, I notice some interesting points. In Saudi Arabia, researchers Maslehuddin et al. (2003) found UCS values for limestone between 90 MPa and 130 MPa. This means my findings are similar to the higher values, especially for the site at Genha. In Egypt, Mojtaba et al. (2019) reported UCS values for limestone between 80 MPa and 120 MPa, which also shows that the limestone in my study area is strong.

On the other hand, a study in India by Shetty (1982) found that UCS values for limestone are lower, averaging around 70 MPa to 100 MPa. This means that the limestone in my study area is much stronger. Additionally, research from the United States by Dalep et al. (1963) shows UCS values for limestone ranging from 100 MPa to 150 MPa. This suggests that while my results are good, some places have even stronger limestone.

Overall, the UCS values from my study show that the limestone in my area is very strong. These results match well with findings from other countries.

CHAPTER SIX

CONCLUSION AND RECOMMENDATION

6.1.Conclusion

The engineering geological investigation shows that most of the limestone samples from the Mekelle area satisfy ASTM and BS standards for construction use, particularly in concrete and stone-paved road projects. The Genha, Chanadug, and Mayalem sites provide the most suitable materials, with high specific gravity, low water absorption, and high UCS values, indicating strong, durable, and reliable aggregates. Mossobo also meets the standards but shows relatively higher abrasion values, which may slightly reduce its resistance to wear. Samples from Shugala and Kokolo meet strength and density requirements but have poor particle size distribution, making them less suitable unless processed or blended with better-graded materials. Overall, the study concludes that limestone from the Mekelle area has strong potential for construction applications, with Genha, Chanadug, and Mayalem recommended as the best quarry sources, while proper processing is required for Shugala and Kokolo to ensure quality and durability in engineering structures. Moisture content across all sites is very low (about 0.012% to 0.28%, average 0.15%), well below the ASTM guideline of 0.4–1%, which indicates the aggregates are suitably dry for mixing and unlikely to increase concrete water demand. The sieve analysis further revealed that coarse aggregates from Genha, Chanadug, Mossobo, and Mayalem exhibit favourable particle size distributions, making them suitable for various construction applications. In contrast, the aggregates from Shugala and Kokolo quarries did not meet the gradation criteria, suggesting that these sources are less suitable unless they are processed or blended with better-graded materials.

6.2. Recommendation

Moisture content of the selected limestone quarries was below the minimum standard (0.4-1%), it is recommended to implement moisture control measures during the extraction and processing of limestone. The sieve analysis results from Kokolo and Shugala quarries indicated that the gradation does not meet the required specifications (20mm - 78.8 mm, 14mm - 36.09 mm, and 14mm - 39.42 mm, 10mm - 4.62). It is advisable to conduct further investigations to identify the causes of this gradation issue. Adjustments in the crushing and screening processes should be made to achieve the desired particle size distribution. Finally, although the unconfined compressive strength (UCS) tests results classify the limestone as very strong. The observed breaking and deterioration of cobblestones in the field may not be due to material weakness but rather another investigation is needed.

References

Abdelsalam, M. G. (1996). Geological Evolution of the Arabian-Nubian Shield, in Geology of the Arabian-Nubian Shield *(*pp. 1-20). Cairo: The Egyptian Geological Society.

Akinniyi, A. A., & Ojo, J. A. (2019). Properties of limestone aggregates in Nigeria. International Journal of Engineering Research and Applications, 9(3), 1-10.

Alene, M. (2007). On the Paleozoic tillite of the Adigrat Group (Tigray, Ethiopia).

ASTM C127: Standard Test Method for Density, Relative Density (Specific Gravity), and Absorption of Coarse Aggregate," ASTM, West Conshohocken, PA, 2015.

ASTM C131: Standard Test Method for Resistance to Degradation of Small-Size Coarse Aggregate by Abrasion and Impact in the Los Angeles Machine," ASTM, West Conshohocken, PA, 2015.

ASTM C29: Standard Test Method for Bulk Density (Unit Weight) and Voids in Aggregate," ASTM, West Conshohocken, PA, 2015.

ASTM C568: Standard Specification for Limestone Dimension Stone," ASTM, West Conshohocken, PA, 2015.

ASTM D75-87. (1992). Standard practice for sampling aggregates. ASTM International, Pennsylvania, United States.

BS 812-103.1: Testing Aggregates. Methods for Determination of Particle Size Distribution," BSI, London, UK, 1990.

BS 812-105.5: Testing Aggregates. Methods for Determination of Flakiness Index," BSI, London, UK, 1990.

BS 812-110: Testing Aggregates. Methods for Determination of Aggregate Crushing Value (ACV)," BSI, London, UK, 1990.

Dalep, A. M., & Hossain, M. (1963). The properties of limestone aggregates. Journal of Materials in Civil Engineering, 1(1), 1-10.

Davies, L. M. (1930). The fossil fauna of the Samana Range and some neighboring areas, The Paleocene Foraminifera/by LM Davies. Calcutta Publishers, Kolkata, India.

Eshan, M. A., & Rahman, M. (2013). Properties of limestone aggregates in Malaysia. International Journal of Civil Engineering and Technology, 4(2), 1-10.

Gebremedhin Berhane (2010). Engineering geological soil and rock characterization in the Mekelle Town, Northern Ethiopia: implications to engineering practice. Momona Ethiopian Journal of Science, 2(2), 64-86.

Gorospe, K., Booya, E., Ghaednia, H., & Das, S. (2019). Effect of various glass aggregates on the shrinkage and expansion of cement mortar. Construction and Building Materials.

Keller, R. (2013). Natural stones as aggregates: Properties and applications. Aggregate Research Journal, 6(1), 15-25.

Koukis, G., Sabatakakis, N., & Spyropoulos, A. (2007). Resistance variation of low-quality aggregates. Bulletin of Engineering Geology and the Environment.

kouma, M., Karkanas, P., & Iacovou, M. (2021). A geoarchaeological study of the construction of the Laona tumulus at Palaepaphos, Cyprus.

Maslehuddin, M., Shameem, M., Ibrahim, M., & Hussain, S. E. (2003). Comparison of properties of steel slag and crushed limestone aggregate concretes. Construction and Building Materials, 17(3), 1-10. https://doi.org/10.1016/S0950-0618(02)00012-0

Mojtaba, M., & Ali, A. (2019). Properties of limestone aggregates in Egypt. Journal of Materials Science and Engineering, 7(1), 1-10.

Naeem, M., Khalid, P., & Anwar, A. W. (2015). Construction material prospects of granitic and associated rocks of Mansehra area, NW Himalaya, Pakistan.

Naeem, M., Zafar, T., Karim, M. A. M., Miraj, M. A. F., Sanaullah, M., Bashir, R., & Abbas, S. (2021). Aggregate prospects of pirkoh limestone from gulki-rodo area of Pakistan as a potential construction material.

Nagih, M. (2016). Properties of limestone aggregates in Iraq. Journal of Engineering and Applied Sciences, 11(1), 1-10.

Ndukauba, E., & Akaha, C. T. (2012). Engineering-Geological Evaluation of Rock Materials from Bansara, Bamenda Massif Southeastern Nigeria, as Aggregates for Pavement Construction.

Rehman, G., Zhang, G., Rahman, M. U., Rahman, N. U., Usman, T., & Imraz, M. (2020). The

Appendices

Appendix 1: Gradation of coarse aggregate

Shugala Area (A)

Sieve Designation	Mass Retained (g)	Percentage Retained (%)	Cumulative Mass Retained (g)	Cumulative % Retained (%)	Percentage Passing (%)	Limits	
						LL	UL
37.5 mm	0	0.00	0	0	100	100	100
28 mm	293	5.86	293	5.86	94.14	90	100
20 mm	3176	63.52	3469	69.38	30.62	40	85
14 mm	1329	26.58	4798	95.96	4.04	10	40
10 mm	198	3.96	4996	99.92	0.08	0	15
5 mm	4	0.08	5000	100	0	0	5
Pan	0	0.00					

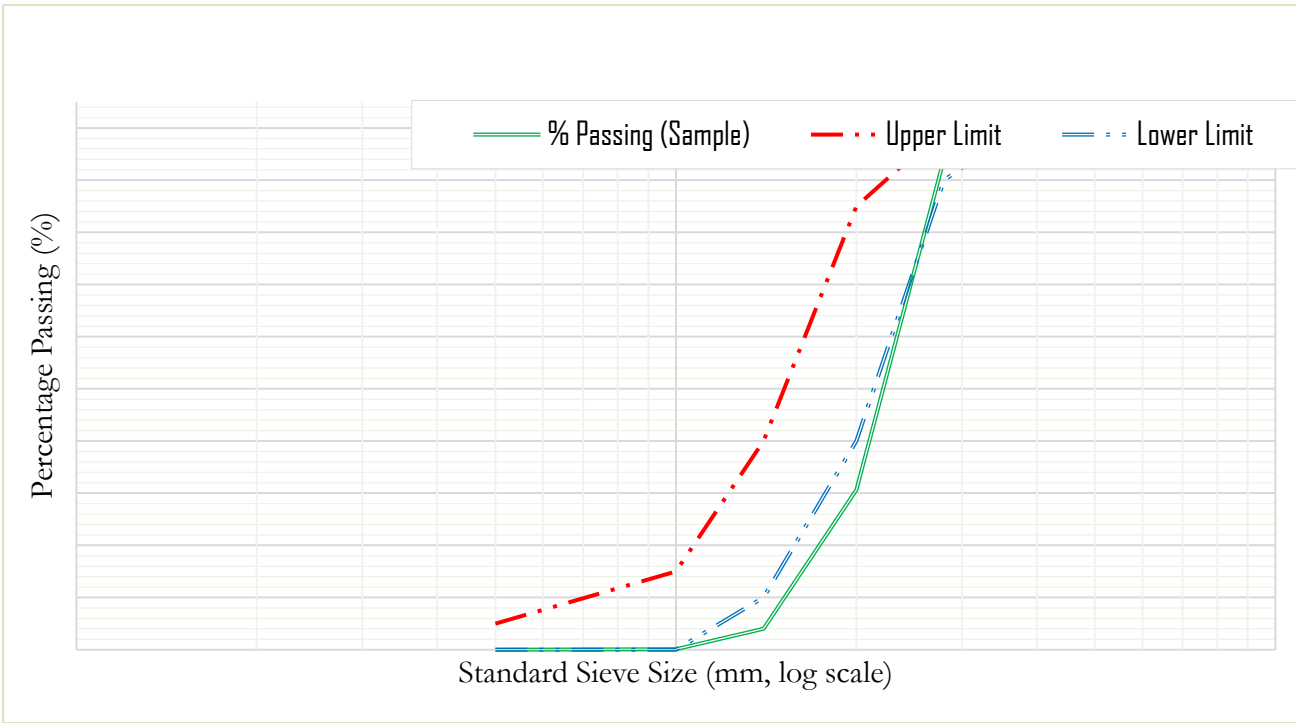

Shugala Area (B)

Sieve Designation	Mass Retained (g)	Percentage Retained (%)	Cumulative Mass Retained (g)	Cumulative % Retained	Percentage Passing (%)	Limits	
						LL	UL
37.5 mm	0	0.00	0	0	100	100	100
28 mm	58	1.16	58	1.16	98.84	90	100
20 mm	2531	50.62	2589	51.78	48.22	40	85
14 mm	2151	43.02	4740	94.8	5.2	10	40
10 mm	257	5.14	4997	99.94	0.06	0	15
5 mm	3	0.06	5000	100	0	0	5
pan	0	0.00					

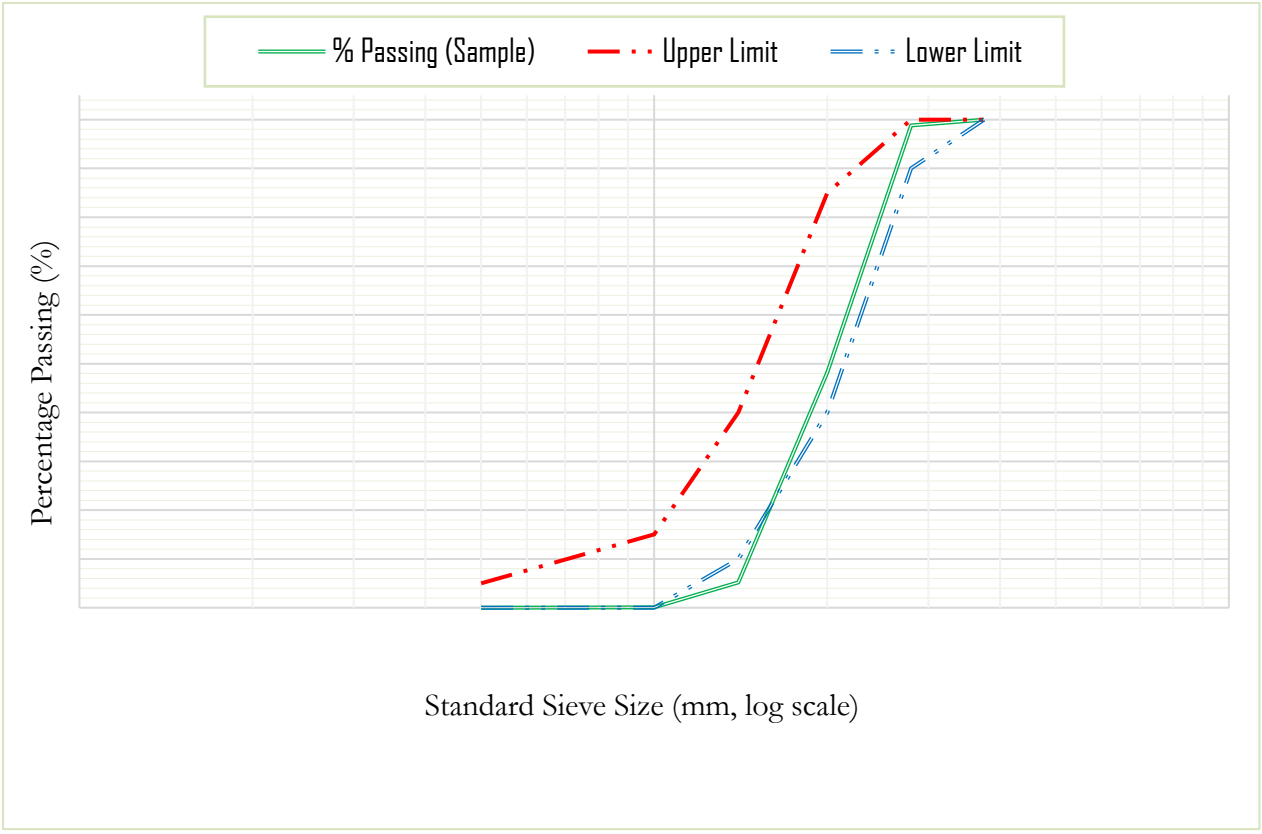

Mayalem area (C)

Sieve Designation	Mass Retained (g)	Percentage Retained (%)	Cumulative Mass Retained (g)	Cumulative % Retained	Percentage Passing (%)	Limits	
						LL	UL
37.5 mm	0	0.00	0	0	100	100	100
28 mm	175	3.50	175	3.5	96.5	90	100
20 mm	2553	51.06	2728	54.56	45.44	40	85
14 mm	1679	33.58	4407	88.14	11.86	10	40
10 mm	567	11.34	4974	99.48	0.52	0	15
5 mm	17	0.34	4991	99.82	0.18	0	5
Pan	9	0.18					

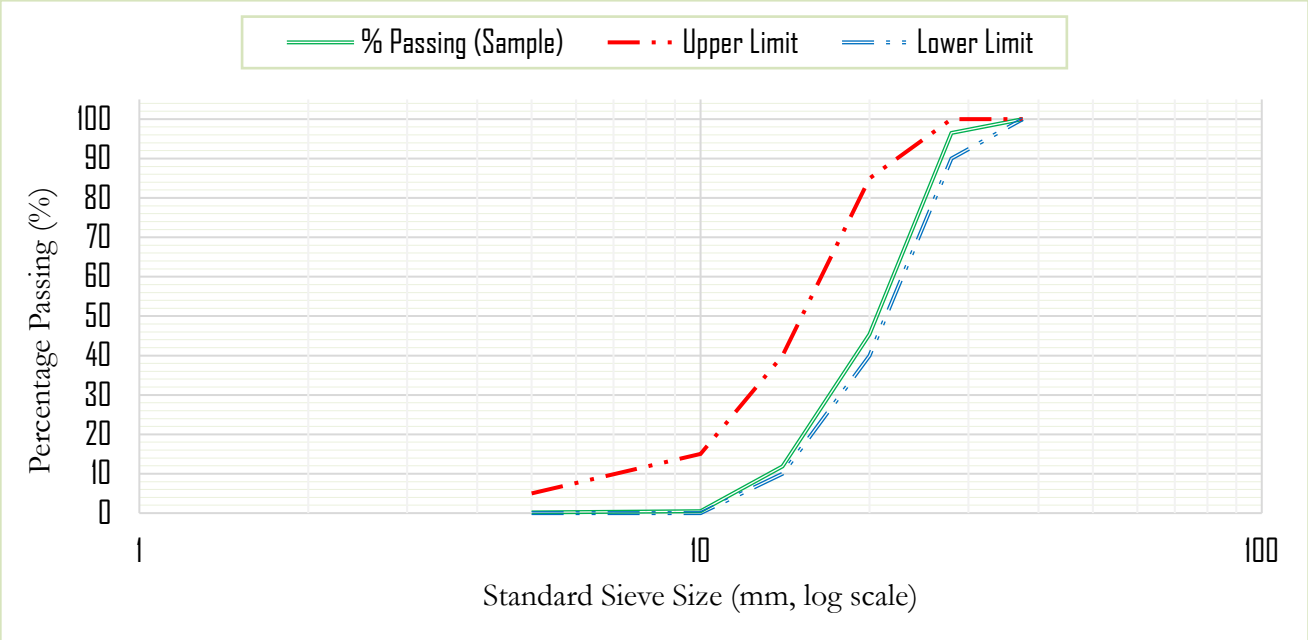

Mayalem Area (D)

Sieve Designation	Mass Retained (g)	Percentage Retained (%)	Cumulative Mass Retained (g)	Cumulative % Retained	Percentage Passing (%)	Limits	
						LL	UL
37.5 mm	0	0.00	0	0	100	100	100
28 mm	184	3.68	184	3.68	96.32	90	100
20 mm	2533	50.66	2717	54.34	45.66	40	85
14 mm	1684	33.68	4401	88.02	11.98	10	40
10 mm	582	11.64	4983	99.66	0.34	0	15
5 mm	12	0.24	4995	99.9	0.1	0	5
Pan	5	0.10					

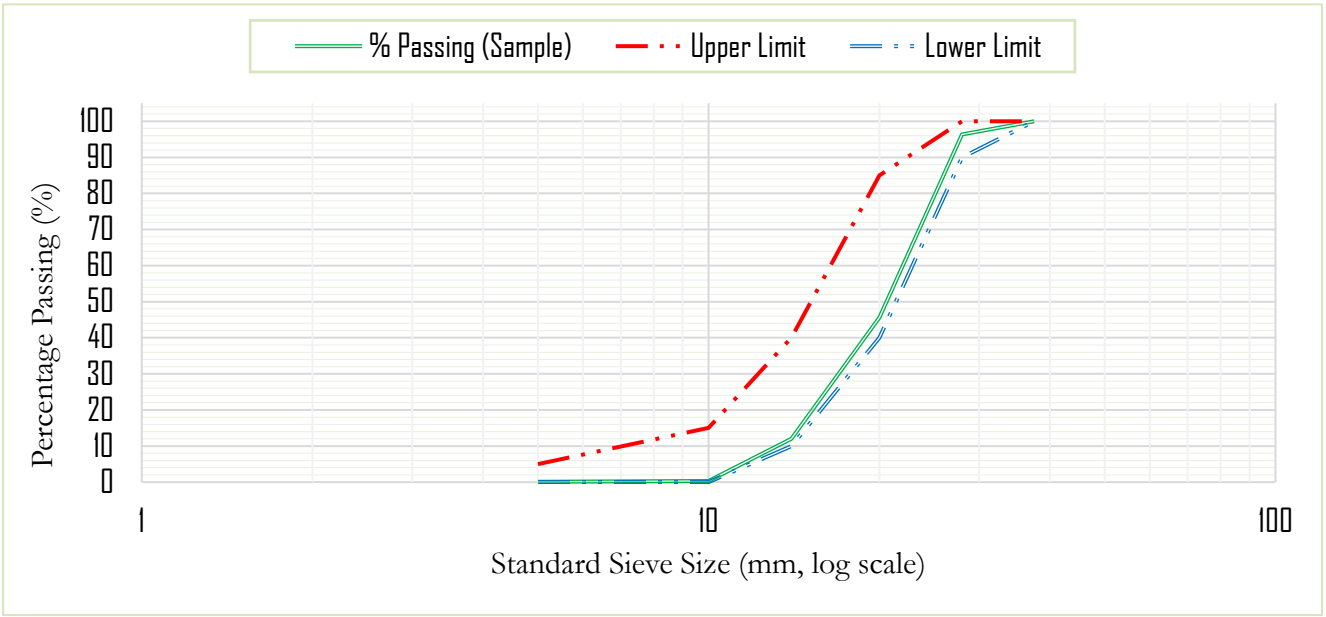

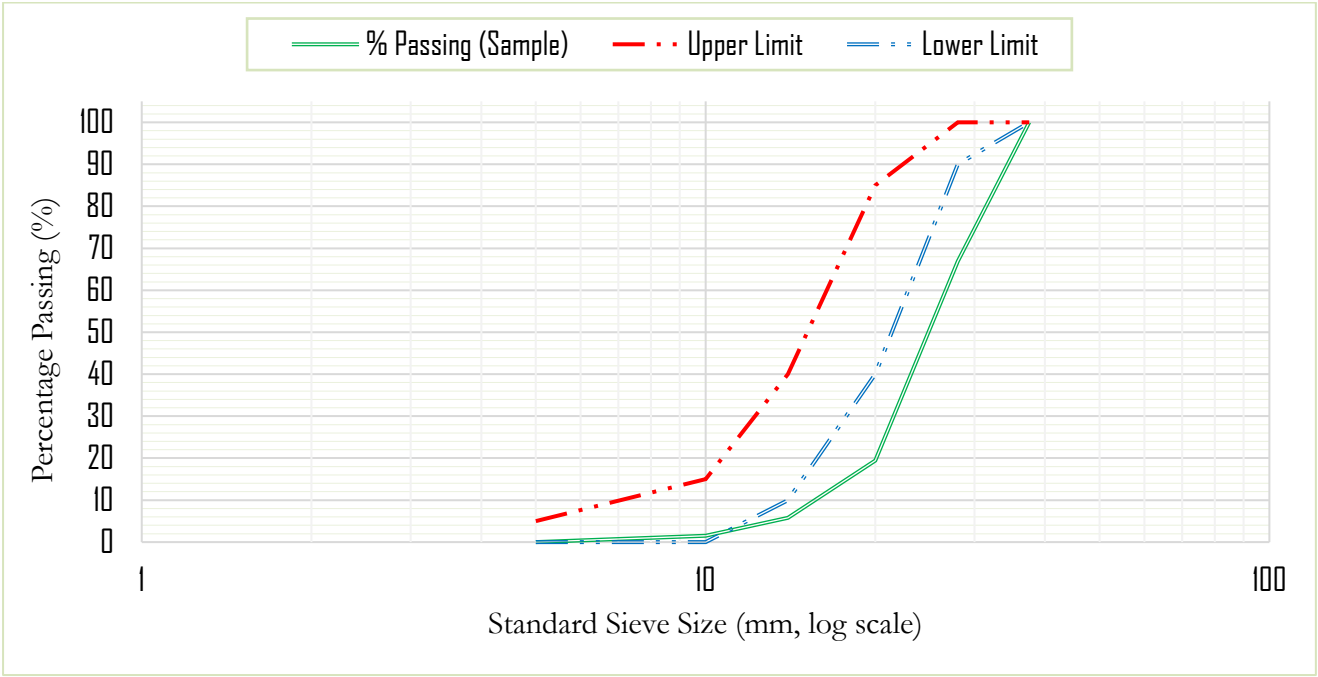
% Passing (Sample)
Upper Limit
Lower Limit
Percentage Passing (%)
100
90
80
70
60
50
40
30
20
10
0
1
10
100
Standard Sieve Size (mm, log scale)

Kokolo Area (F)

Sieve Designation	Mass Retained (g.m)	Percentage Retained (%)	Cumulative Mass Retained (gm.)	Cumulative Retained (%)	Percentage Passing (%)	Limits	
						LL	UL
37.5 mm	0	0.00	0	0	100	100	100
28 mm	467	9.34	467	9.34	90.66	90	100
20 mm	1896	37.92	2363	47.26	52.74	40	85
14 mm	1285	25.70	3648	72.96	27.04	10	40
10 mm	989	19.78	4637	92.74	7.26	0	15
5 mm	361	7.22	4998	99.96	0.04	0	5
Pan	2	0.04					

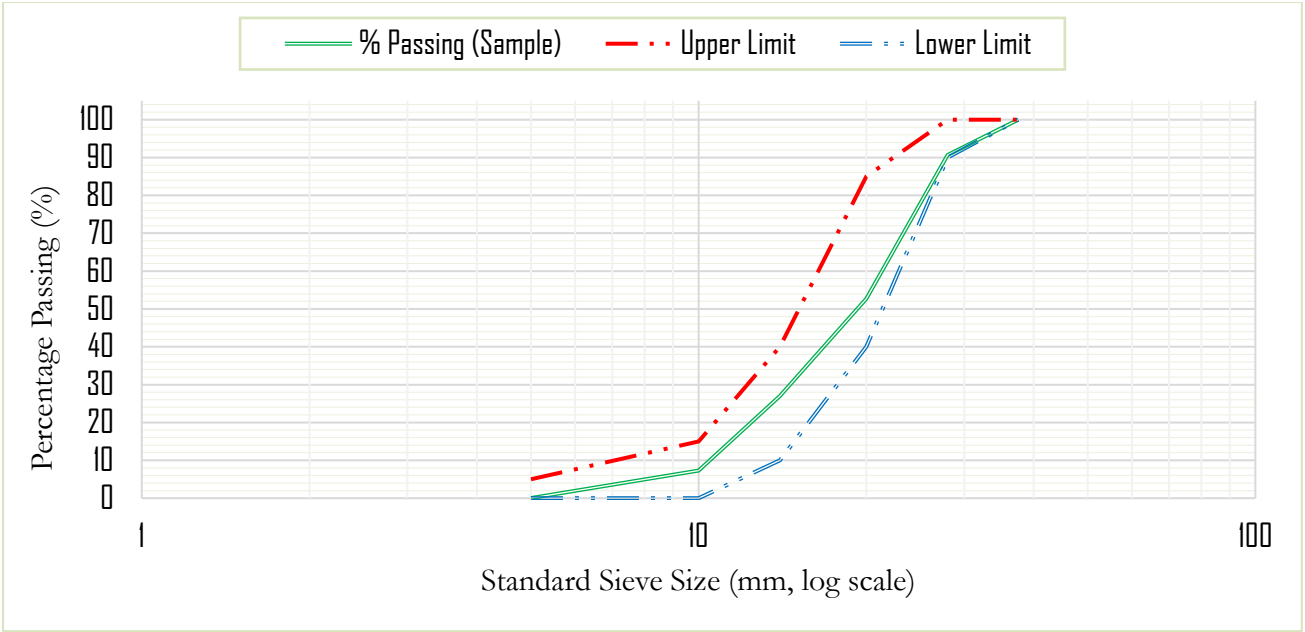

Mossobo Area (G)

Sieve Designation	Mass Retained(g)	Percentage Retained (%)	Cumulative Mass Retained (g)	Cumulative % Retained (%)	Percentage Passing(%)	Limits	
						LL	UL
37.5 mm	0	0.00	0	0	100	100	100
28 mm	274	5.48	274	5.48	94.52	90	100

20 mm	2912	58.24	3186	63.72	36.28	40	85
14 mm	854	17.08	4040	80.8	19.2	10	40
10 mm	853	17.06	4893	97.86	2.14	0	15
5 mm	104	2.08	4997	99.94	0.06	0	5
Pan	3	0.06					

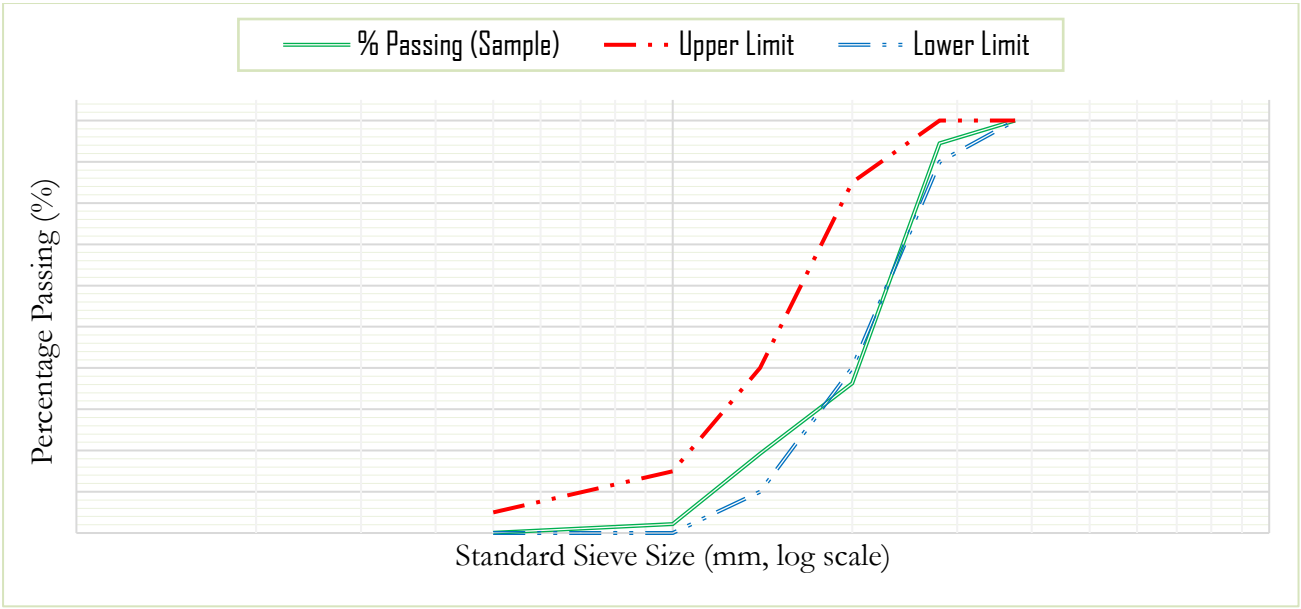

Mossobo Area (H)

Sieve Designation	Mass Retained	Percentage Retained (%)	Cumulative Mass Retained (g)	Cumulative % Retained (%)	Percentage Passing (%)	Limits	
						LL	UL
37.5 mm	0	0.00	0	0	100	100	100
28 mm	295	5.90	295	5.9	94.1	90	100
20 mm	2145	42.90	2440	48.8	51.2	40	85
14 mm	2455	49.10	4895	97.9	2.1	10	40
10 mm	43	0.86	4938	98.76	1.24	0	15
5 mm	57	1.14	4995	99.9	0.1	0	5
Pan	5	0.10					

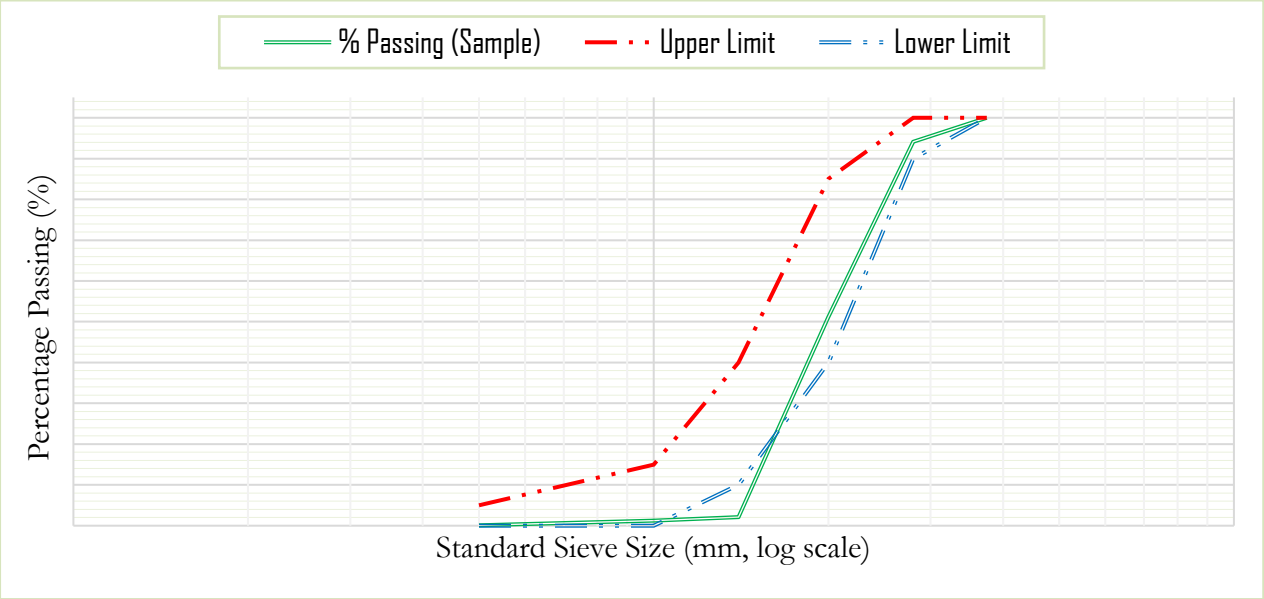

Chanadug Area (I)

Sieve Designation	Mass Retained (g)	Percentage Retained (%)	Cumulative Mass Retained (g)	Cumulative Retained (%)	Percentage Passing (%)	Limits	
						LL	UL
37.5 mm	0	0.00	0	0	100	100	100
28 mm	263	5.26	263	5.26	94.74	90	100
20 mm	1698	33.96	1961	39.22	60.78	40	85
14 mm	1747	34.94	3708	74.16	25.84	10	40
10 mm	865	17.30	4573	91.46	8.54	0	15
5 mm	423	8.46	4996	99.92	0.08	0	5
Pan	4	0.08					

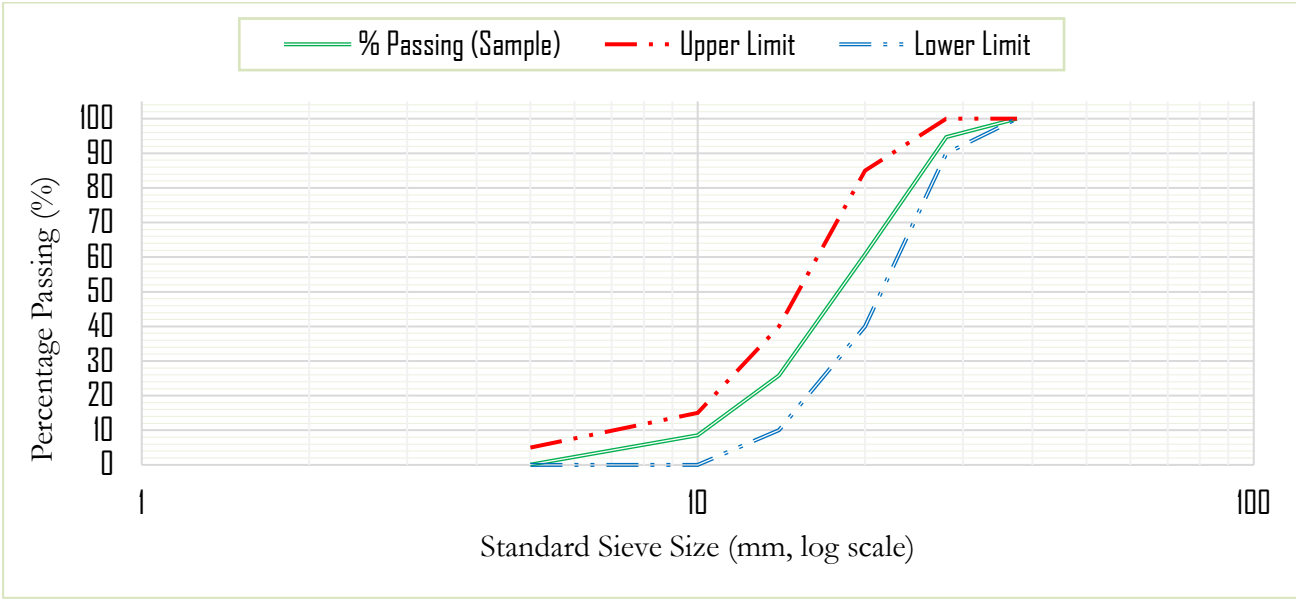

Genha Area (J)

Sieve Designation	Mass Retained (g)	Percentage Retained (%)	Cumulative Mass Retained (g)	Cumulative % Retained (%)	Percentage Passing (%)	Limits	
						LL	UL
37.5 mm	0	0.00	0	0	100	100	100
28 mm	92	1.84	92	1.84	98.16	90	100
20 mm	743	14.86	835	16.7	83.3	40	85
14 mm	3035	60.70	3870	77.4	22.6	10	40
10 mm	1112	22.24	4982	99.64	0.36	0	15
5 mm	13	0.26	4995	99.9	0.1	0	5
Pan	5	0.10					

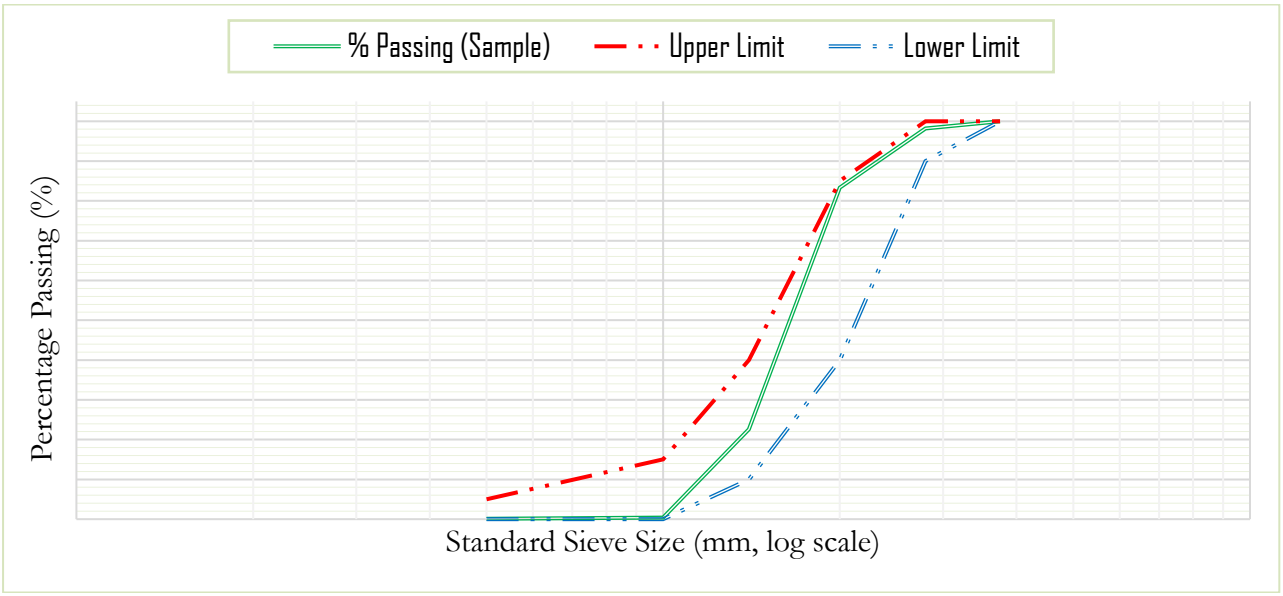

Genha Area (K)

Sieve Designation	Mass Retained (g)	Percentage Retained (%)	Cumulative Mass Retained (g)	Cumulative % Retained (%)	Percentage Passing (%)	Limits	
						LL	UL
37.5 mm	0	0.00	0	0	100	100	100
28 mm	274	5.48	274	5.48	94.52	90	100
20 mm	868	17.36	1142	22.84	77.16	40	85
14 mm	2845	56.90	3987	79.74	20.26	10	40
10 mm	957	19.14	4944	98.88	1.12	0	15
5 mm	54	1.08	4998	99.96	0.04	0	5
Pan	2	0.04					

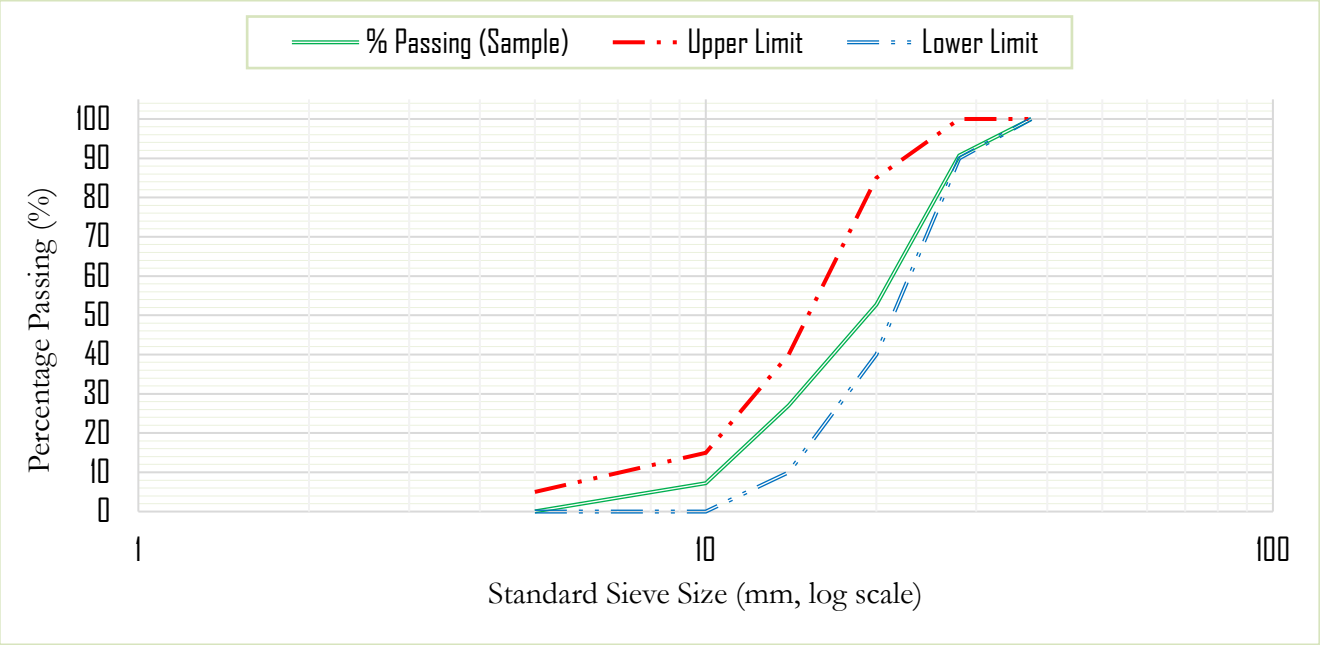

Appendix 2: Specific Grav Appendix 2: Specific Gravity and water absorption result of coarse aggregate;

Shugala Area (A)

- Trial 1 (SSD) after 24-hour socking =1658g
- Trial 2 (SSD) after 24-hour socking=1693g
- Trial 3 (SSD) after 24-hour socking=1648g

  And then weight in water basket
- Trial 1 + basket on water = 5599g
- Trial 2 + basket on water = 5604g
- Trial 3 + basket on water = 5566g

  Weight of basket on water = 4575g

  The sample after oven dry
    - Trial 1 = 1647g
    - Trial 2 =1680g
    - Trial 3 = 1637g

		Trial 1	Trial 2	Trial 3	Average
1	Weight of oven dry test sample in air **A**	1647g	1680g	1637g	1654.7g
2	Weight of saturated surface dry test sample in air **B**	1658g	1693g	1648g	1666.3g

3	Weight of saturated surface dry test sample in water – weight of basket on water **C**	1024g	1029g	991g	1014.7g

Calculations

Bulk specific gravity = $\frac{A}{B-C} = \frac{1654.7}{1666.3-1014.7}$ = 2.54

- The $\mathbf{G_s}$ of most normal weight aggregate is 2.4-2.9. Therefore, the aggregate is normally used for concrete

  Absorption capacity (%) = $\frac{B-A}{A} = \frac{1666.3-1654.7}{1654.7}$ *100 =0.70%
- Therefore, the aggregate has less absorption value

Shugala Area (B)

- Trial 1 (SSD) after 24-hour socking =1680g
- Trial 2 (SSD) after 24-hour socking=1686g
- Trial 3 (SSD) after 24-hour socking=1669g

  And then weight in water basket
- Trial 1 + basket on water = 5950g
- Trial 2 + basket on water = 5700g
- Trial 3 + basket on water = 4800g

  Weight of basket on water = 4575g

  The sample after oven dry
  - Trial 1 = 1659g
  - Trial 2 =1670g
  - Trial 3 = 1647g

		Trial 1	Trial 2	Trial 3	Average
1	Weight of oven dry test sample in air **A**	1659g	1670g	1647g	1658.7g
2	Weight of saturated surface dry test sample in air **B**	1680g	1686g	1669g	1678.3g
3	Weight of saturated surface dry test sample in water – weight of basket on water **C**	1375g	1125g	225g	908.3g

Calculations

Bulk specific gravity = $\frac{A}{B-C} = \frac{1658.7}{1678.3-908.3.}$ = 2.47

- ❖ The G_s of most normal weight aggregate is 2.4-2.9. Therefore, the aggregate is normally used for concrete

  Absorption capacity (%) = $\frac{B-A}{A}$ = $\frac{1678.3-1658.7}{1658.7}$ *100 =0.11%

Therefore, the aggregate has less absorption value

Mayalem Area (C)

- Trial 1 (SSD) after 24-hour socking =2195g
- Trial 2 (SSD) after 24-hour socking=2283g
- Trial 3 (SSD) after 24-hour socking=1917g

  And then weight in water basket
- Trial 1 + basket on water = 5916g
- Trial 2 + basket on water = 5949g
- Trial 3 + basket on water = 5745g

  Weight of basket on water = 4575g

  The sample after oven dry
  - Trial 1 = 2181g
  - Trial 2 =2265g
  - Trial 3 = 1904g

		Trial 1	Trial 2	Trial 3	Average
1	Weight of oven dry test sample in air **A**	2181g	2265g	1904g	2116.7g
2	Weight of saturated surface dry test sample in air **B**	2195g	2283g	1917g	2131.7g
3	Weight of saturated surface dry test sample in water – weight of basket on water **C**	1341g	1374g	1170g	1295g

Calculations

Bulk specific gravity = $\frac{A}{B-C}$ = $\frac{2116.7}{2131.7-1295}$ = 2.53

- ❖ The G_s of most normal weight aggregate is 2.4-2.9. Therefore, the aggregate is normally used for concrete

  Absorption capacity (%) = $\frac{B-A}{A}$ = $\frac{2131.7-2116.7}{2116.7}$ *100 =0.71%
- ❖ Therefore, the aggregate has less absorption value

Mayalem area (D)

- Trial 1 (SSD) after 24-hour socking =1537g
- Trial 2 (SSD) after 24-hour socking=1543g
- Trial 3 (SSD) after 24-hour socking=1529g

  And then weight in water basket
- Trial 1 + basket on water = 5499g
- Trial 2 + basket on water = 5487g
- Trial 3 + basket on water = 5479g

  Weight of basket on water = 4575g

  The sample after oven dry
    - Trial 1 = 1533g
    - Trial 2 =1530g
    - Trial 3 = 1528g

		Trial 1	Trial 2	Trial 3	Average
1	Weight of oven dry test sample in air **A**	1533g	1530g	1528g	1530.3g
2	Weight of saturated surface dry test sample in air **B**	1537g	1543g	1529g	1536.3g
3	Weight of saturated surface dry test sample in water – weight of basket on water **C**	924g	912g	904g	913.3g

Calculation;

Bulk specific gravity = $\frac{A}{B-C} = \frac{1530.3}{1528.3-913.3.} = 2.48$

- ❖ The $\mathbf{G}_s$ of most normal weight aggregate is 2.4-2.9. Therefore, the aggregate is normally used for concrete

  Absorption capacity (%) = $\frac{B-A}{A} = \frac{1536.3-1530.3}{1530.3} * 100 = 0.39\%$

Kokolo Area (E)

Therefore, the aggregate has less absorption value

- Trial 1 (SSD) after 24-hour socking =2127g
- Trial 2 (SSD) after 24-hour socking=2088g
- Trial 3 (SSD) after 24-hour socking=1976g

And then weight in water basket

- Trial 1 + basket on water = 5980g
- Trial 2 + basket on water = 5869g
- Trial 3 + basket on water = 5766g

Weight of basket on water = 4575g

The sample after oven dry

- Trial 1 = 2114g
- Trial 2 =2074g
- Trial 3 = 1963g

		Trial 1	Trial 2	Trial 3	Average
1	Weight of oven dry test sample in air **A**	2114g	2074g	1963g	2050.3g
2	Weight of saturated surface dry test sample in air **B**	2127g	2088g	1976g	2063.7g
3	Weight of saturated surface dry test sample in water – weight of basket on water **C**	1405g	1294g	1191g	1278g

Calculations

Bulk specific gravity = $\frac{A}{B-C} = \frac{2050.3}{2063.7-1278} = 2.61$

- The $\mathbf{G_s}$ of most normal weight aggregate is 2.4-2.9. Therefore, the aggregate is normally used for concrete

  Absorption capacity (%) = $\frac{B-A}{A} = \frac{2063.7-2050.3}{2050.3} * 100 = 0.65\%$

- Therefore, the aggregate has less absorption value

Kokolo Area (F)

- Trial 1 (SSD) after 24-hour socking =2140g
- Trial 2 (SSD) after 24-hour socking=2001g
- Trial 3 (SSD) after 24-hour socking=1989g

And then weight in water basket

- Trial 1 + basket on water = 5900g
- Trial 2 + basket on water = 5883g
- Trial 3 + basket on water = 5770g

Weight of basket on water = 4575g

The sample after oven dry

- Trial 1 = 2134g
- Trial 2 =1995g
- Trial 3 = 1981g

		Trial 1	Trial 2	Trial 3	Average
1	Weight of oven dry test sample in air **A**	2134g	2089g	1987g	2070g
2	Weight of saturated surface dry test sample in air **B**	2140g	2001g	1989g	2043.3
3	Weight of saturated surface dry test sample in water – weight of basket on water **C**	1325g	1308g	1195g	1296g

Calculations

Bulk specific gravity = $\frac{A}{B-C} = \frac{2070}{2043.3-1296} = 2.78$

- The $\mathbf{G_s}$ of most normal weight aggregate is 2.4-2.9.Therefore the aggregate is normally used for concrete

  Absorption capacity (%) = $\frac{B-A}{A} = \frac{2043.3-2036.7}{2036.7} * 100 = 0.32\%$
- Therefore, the aggregate has less absorption

Mossobo Area (G)

- Trial 1 (SSD) after 24-hour socking =2240g
- Trial 2 (SSD) after 24-hour socking=2102g
- Trial 3 (SSD) after 24-hour socking=2088g

  And then weight in water basket
- Trial 1 + basket on water = 5888g
- Trial 2 + basket on water = 5868g
- Trial 3 + basket on water = 5760g

  Weight of basket on water = 4575g

  The sample after oven dry
  - Trial 1 = 2235g
  - Trial 2 =2189g
  - Trial 3 = 1990g

		Trial 1	Trial 2	Trial 3	Average
1	Weight of oven dry test sample in air **A**	2235g	2189g	1990g	2138
2	Weight of saturated surface dry test sample in air **B**	2240g	2102g	2088g	2143.3g

3	Weight of saturated surface dry test sample in water – weight of basket on water **C**	1313g	1293g	1185g	1263.7g

Calculations

Bulk specific gravity = $\frac{A}{B-C} = \frac{2138}{2143.3-1263.7} = 2.43$

- The $\mathbf{G_s}$ of most normal weight aggregate is 2.4-2.9. Therefore, the aggregate is normally used for concrete

  Absorption capacity (%) = $\frac{B-A}{A} = \frac{2143.3-2138}{2138} * 100 = 0.25\%$

- Therefore, the aggregate has less absorption value

Mossobo Area (H)

- Trial 1 (SSD) after 24-hour socking =2190g
- Trial 2 (SSD) after 24-hour socking=2299g
- Trial 3 (SSD) after 24-hour socking=1940g

  And then weight in water basket
- Trial 1 + basket on water = 5950g
- Trial 2 + basket on water = 5895g
- Trial 3 + basket on water = 5785g

  Weight of basket on water = 4575g

  The sample after oven dry
  - Trial 1 = 2195g
  - Trial 2 =2220g
  - Trial 3 = 1928g

		Trial 1	Trial 2	Trial 3	Average
1	Weight of oven dry test sample in air **A**	2195g	2220g	1928g	2114.3
2	Weight of saturated surface dry test sample in air **B**	2190g	2299g	1940g	2143g

3	Weight of saturated surface dry test sample in water – weight of basket on water **C**	1375g	1320g	1210g	1301.7g

Calculations;

Bulk specific gravity = $\frac{A}{B-C} = \frac{2114.3}{2143-1301.7}$ = 2.51

- The $\mathbf{G_s}$ of most normal weight aggregate is 2.4-2.9. Therefore, the aggregate is normally used for concrete

  Absorption capacity (%) = $\frac{B-A}{A} = \frac{2143-2114.3}{2114.3}$ *100 =1.35%
- Therefore, the aggregate has less absorption value

Chanadug Area (I)

- Trial 1 (SSD) after 24-hour socking =2080g
- Trial 2 (SSD) after 24-hour socking=2087g
- Trial 3 (SSD) after 24-hour socking=1988g

  And then weight in water basket
- Trial 1 + basket on water = 5540g
- Trial 2 + basket on water = 5544g
- Trial 3 + basket on water = 5533g

  Weight of basket on water = 4575g

  The sample after oven dry
  - Trial 1 = 2075g
  - Trial 2 =2081g
  - Trial 3 = 2072g

		Trial 1	Trial 2	Trial 3	Average
1	Weight of oven dry test sample in air **A**	1575g	1581g	1560g	1731.3g
2	Weight of saturated surface dry test sample in air **B**	1580g	1587g	1545g	1737.3g

3	Weight of saturated surface dry test sample in water – weight of basket on water **C**	1115g	1119g	1108	1114g

Calculations

Bulk specific gravity = $\frac{A}{B-C} = \frac{1731.3}{1737.3-1114} = 2.77$

- The G_s of most normal weight aggregate is 2.4-2.9. Therefore, the aggregate is normally used for concrete

  Absorption capacity (%) = $\frac{B-A}{A} = \frac{1737.3-1731.3}{1731.3} * 100 = 0.34$ %

Therefore, the aggregate is less absorption

Genha Area (J)

- Trial 1 (SSD) after 24-hour socking =1718g
- Trial 2 (SSD) after 24-hour socking=1721g
- Trial 3 (SSD) after 24-hour socking=1711g

  And then weight in water basket
- Trial 1 + basket on water = 5700g
- Trial 2 + basket on water = 5690g
- Trial 3 + basket on water = 5679g

  Weight of basket on water = 4575g

  The sample after oven dry
  - Trial 1 = 1706g
  - Trial 2 =1713g
  - Trial 3 = 1699g

		Trial 1	Trial 2	Trial 3	Average
1	Weight of oven dry test sample in air **A**	1706g	1713g	1699g	1706g
2	Weight of saturated surface dry test sample in air **B**	1718	1721g	1711g	1716.7g
3	Weight of saturated surface dry test sample in water – weight of basket on water **C**	1125g	1115g	1104g	1114.7g

Calculations

Bulk specific gravity = $\frac{A}{B-C} = \frac{1706}{1716.7-1114.7} = 2.83$

- ❖ The $\mathbf{G_s}$ of most normal weight aggregate is 2.4-2.9. Therefore, the aggregate is normally used for concrete

  Absorption capacity (%) = $\frac{B-A}{A}$ = $\frac{1716.7-1706}{1706}$ *100 =0.62 %

- ❖ Therefore, the aggregate is less absorption

Genha Area (K)

- Trial 1 (SSD) after 24-hour socking =2127g
- Trial 2 (SSD) after 24-hour socking=2146g
- Trial 3 (SSD) after 24-hour socking=2050g

  And then weight in water basket

- Trial 1 + basket on water = 5888g
- Trial 2 + basket on water = 5873g
- Trial 3 + basket on water = 5867g

  Weight of basket on water = 4575g

  The sample after oven dry

  - Trial 1 = 2110g
  - Trial 2 =2135g
  - Trial 3 = 2029g

		Trial 1	Trial 2	Trial 3	Average
1	Weight of oven dry test sample in air **A**	2110g	2135g	2029g	2091.3g
2	Weight of saturated surface dry test sample in air **B**	2127g	2146g	2050g	2107.7g
3	Weight of saturated surface dry test sample in water – weight of basket on water **C**	1313g	1298g	1292g	1301g

Calculations

Bulk specific gravity = $\frac{A}{B-C}$ = $\frac{2091.3}{2107.7-1301}$ = 2.59

- ❖ The $\mathbf{G_s}$ of most normal weight aggregate is 2.4-2.9. Therefore, the aggregate is normally used for concrete

  Absorption capacity (%) = $\frac{B-A}{A}$ = $\frac{2107.7-2091.3}{2091.3}$ *100 =0.78 %

- ❖ Therefore, the aggregate is less absorption

Appendix 3: Moisture Content of Coarse Aggregate

Shugala Area (A)

Description	**Unit**	**Observations**			**Average**
Code of container	….	1	2	3	
Mass of container	gm.	250.0	301	214	255.0
Mass of specimen + container	gm.	2250.0	2301.0	2214	2255.0
Mass of oven dry specimen + Container	gm.	2245.0	2296	2210	2250.3
Mass of water	gm.	5.0	5.0	4.0	4.7
Moisture content	%	0.3	0.3	0.2	0.23
$W(\%) = \frac{A-B}{B} * 100\% = \frac{2000-1995.3}{1995.3} * 100\% = 0.23\%$					

Where**:** W = Moisture content (%)

A= Weight of original sample in air (g)

B=Weight of oven dry sample (g)

Shugala Area (B)

Description	**Unit**	**Observations**			**Average**
Code of container	….	1	2	3	
Mass of container	gm.	250.0	88	95	144.33
Mass of specimen + container	gm.	5000.0	5420.0	548.2	3656.07
Mass of oven dry specimen + Container	gm.	4990.0	5410	545.5	3648.5
Mass of water	gm.	10.0	10.0	2.7	7.57
Moisture content	%	0.2	0.19	0.24	0.21

Mayalem Area (C)

Description	**Unit**	**Observations**			**Average**
Code of container	….	1	2	3	
Mass of container	gm.	74.4	70	75	73.1
Mass of specimen + container	gm.	1584.3	2035	1568	1729.1
Mass of oven dry specimen + Container	gm.	1581.0	2033.2	1561.31	1725.2
Mass of water	gm.	3.3	1.8	6.7	3.9
Moisture content	%	0.2	0.1	0.4	0.24

Mayalem Area (D)

Description	Unit	Observations			Average
Code of container	….	1	2	3	
Mass of container	gm.	105.0	123.0	100.0	109.3
Mass of specimen + container	gm.	2105.0	2123.0	3000	2409.3
Mass of oven dry specimen + Container	gm.	2102.0	2120.0	2997	2406.3
Mass of water	gm.	3.0	3.0	3.0	3.0
Moisture content	%	0.2	0.2	0.1	0.13

Kokolo Area (E)

Description	Unit	Observations			Average
Code of container	….	1	2	3	
Mass of container	gm.	231.0	215	100.0	181.0
Mass of specimen + container	gm.	4210..0	4241	3000	4220.3
Mass of oven dry specimen + Container	gm.	4200.0	2120.0	4230	4210.0
Mass of water	gm.	10.0	3.0	11.0	10.3
Moisture content	%	0.3	0.2	0.3	0.26

Kokolo Area (F)

Description	Unit	Observations			Average
Code of container	….	1	2	3	
Mass of container	gm.	103.0	99	311	182.0
Mass of specimen + container	gm.	2103.0	2099.0	2311.0	2171.0
Mass of oven dry specimen + Container	gm.	2100. 0	2095.0	2305	2166.7
Mass of water	gm.	3.0	0.2	6.0	3.1
Moisture content	%	0.15	0.01	0.06	0.216

Mossobo Area (G)

Description	Unit	Observations			Average
Code of container	….	1	2	3	
Mass of container	gm.	321.0	451	521	431.0
Mass of specimen + container	gm.	6350.0	8540.0	8962.0	7950.7
Mass of oven dry specimen + Container	gm.	6330.0	8520.0	8940	7930.0

Mass of water	gm.	20.0	20.0	22.0	20.7
Moisture content	%	0.3	0.2	0.3	0.280

Mossobo Area (H)

Description	**Unit**	**Observations**			**Average**
Code of container	….	1	2	3	
Mass of container	gm.	201.0	306	240	249.0
Mass of specimen + container	gm.	2201.0	2306.0	2240.0	2249.0
Mass of oven dry specimen + Container	gm.	2199.0	2301.0	2235	2245.0
Mass of water	gm.	2.0	5.0	5.0	4.0
Moisture content	%	0.1	0.3	0.2	0.200

Chanadug Area (I)

Description	**Unit**	**Observations**			**Average**
Code of container	….	1	2	3	
Mass of container	gm.	120.0	104	107	110.3
Mass of specimen + container	gm.	2120.0	2104.0	2107.0	2110.3
Mass of oven dry specimen + Container	gm.	2115.0	2100	2103	2106.0
Mass of water	gm.	5.0	4.0	4.0	4.3
Moisture content	%	0.3	0.2	0.14	0.215

Genha Area (J)

Description	**Unit**	**Observations**			**Average**
Code of container	….	1	2	3	
Mass of container	gm.	120.0	104	107	110.3
Mass of specimen + container	gm.	2180.0	2104.0	2107.0	2130.3
Mass of oven dry specimen + Container	gm.	2115.0	2100.0	2103	2106.0
Mass of water	gm.	5.0	4.0	4.0	4.3
Moisture content	%	0.033	0.002	0.002	0.012

Genha Area (K)

Description	Unit	Observations			Average
Code of container	….	1	2	3	
Mass of container	gm.	109.0	204	145	152.7
Mass of specimen + container	gm.	2109.0	2204.0	2145.0	2152.7
Mass of oven dry specimen + Container	gm.	2106.0	2200.0	2139	2148.3
Mass of water	gm.	3.0	4.0	6.0	4.3
Moisture content	%	0.2	0.2	0.3	0.220

Appendix 4: Unit Weight of Coarse Aggregates

Shugala Area (A)

No	Description	Trials 1	Trials 2	Trials 3
1	Mass of aggregate (gm)	4642.0	4719.0	4725.0
2	Diameter (cm)	15.5	15.5	15.5
3	Height (cm)	16.0	16.0	16.0
4	Volume (cm^3) = $(\pi d^2h)/4$	3017.54	3017.54	3017.54
5	Unit weight (gm./cm^3)	1.5383	1.5638	1.5658
6	Average unit weight (gm./cm^3)	1.5560		

Shugala Area (B)

No	Description	Trials 1	Trials 2	Trials 3
1	Mass of aggregate (gm)	4740.0	4728.0	4698.0
2	Diameter (cm)	15.5	15.5	15.5
3	Height (cm)	16.6	16.6	16.6
4	Volume (m^3) = $(\pi d^2h)/4$	3017.54	3017.54	3017.54
5	Unit weight (gm./m^3)	1.571	1.567	1.557
6	Average unit weight (gm./cm^3)	1.5649		

Mayalem Area (C)

No	Description	Trials 1	Trials 2	Trials 3
1	Mass of aggregate (gm.)	4466.0	4412.0	4430.0
2	Diameter (cm)	15.5	15.5	15.5

3	Height (cm)	16.0	16.0	16.0
4	Volume (cm^3) = (πd^2h)/4	3017.54	3017.54	3017.54
5	Unit weight (gm./cm^3)	1.480	1.462	1.468
6	Average unit weight (gm./cm^3)	1.470		

Mayalem Area (D)

No	Description	Trials 1	Trials 2	Trials 3
1	Mass of aggregate (gm.)	4579.0	4552.0	4490.0
2	Diameter (cm)	15.5	15.5	15.5
3	Height (cm)	16.0	16.0	16.0
4	Volume (cm^3) = (πd^2h)/4	3017.54	3017.54	3017.54
5	Unit weight (gm./cm^3)	1.5170	1.5090	1.4680
6	Average unit weight (gm./cm^3)	1.512		

Kokolo Area (E)

No	Description	Trials 1	Trials 2	Trials 3
1	Mass of aggregate (gm.)	4857.0	4854.0	4589.0
2	Diameter (cm)	15.5	15.5	15.5
3	Height (cm)	16.0	16.0	16.0
4	Volume (cm^3) = (πd^2h)/4	3017.54	3017.54	3017.54
5	Unit weight (gm./cm^3)	1.609	1.608	1.521
6	Average unit weight (gm./cm^3)	1.579		

Kokolo Area (F)

No	Description	Trials 1	Trials 2	Trials 3
1	Mass of aggregate (gm.)	4850	4856	4842
2	Diameter (m)	15.5	15.5	15.5
3	Height (cm)	16.0	16.0	16.0
4	Volume (cm^3) = (πd^2h)/4	3017.54	3017.54	3017.54
5	Unit weight(gm./cm^3)	1.607	1.609	1.605
6	Average unit weight (gm./cm^3)	1.607		

Mossobo Area (G)

No	Description	Trials 1	Trials 2	Trials 3
1	Mass of aggregate (gm.)	4689	4535	4594
2	Diameter (m)	15.5	15.5	15.5
3	Height (cm)	16.0	16.0	16.0
4	Volume (cm^3) = $(\pi d^2h)/4$	3017.54	3017.54	3017.54
5	Unit weight(gm./cm^3)	1.553	1.503	1.522
6	Average unit weight (gm./cm^3)	1.526		

Mossobo Area (H)

No	Description	Trials 1	Trials 2	Trials 3
1	Mass of aggregate (gm.)	4896	4877	4870
2	Diameter (m)	15.5	15.5	15.5
3	Height (cm)	16.0	16.0	16.0
4	Volume (cm^3) = $(\pi d^2h)/4$	3017.54	3017.54	3017.54
5	Unit weight(gm./cm^3)	1.623	1.616	1.614
6	Average unit weight (gm./cm^3)	1.618		

Chanadug Area (I)

No	Description	Trials 1	Trials 2	Trials 3
1	Mass of aggregate (gm.)	4990	4998	4988
2	Diameter (m)	15.5	15.5	15.5
3	Height (cm)	16.0	16.0	16.0
4	Volume (cm^3) = $(\pi d^2h)/4$	3017.54	3017.54	3017.54
5	Unit weight(gm./cm^3)	1.654	1.656	1.653
6	Average unit weight (gm./cm^3)	1.654		

Genha Area (J)

No	Description	Trials 1	Trials 2	Trials 3
1	Mass of aggregate (gm.)	4661	4771	4692
2	Diameter (m)	15.5	15.5	15.5
3	Height (cm)	16.0	16.0	16.0
4	Volume (cm^3) = $(\pi d^2h)/4$	3017.54	3017.54	3017.54

5	Unit weight(gm./cm^3)	1.545	1.581	1.555
6	Average unit weight (gm./cm^3)	1.560		

Genha Area (K)

No	Description	Trials 1	Trials 2	Trials 3
1	Mass of aggregate (gm.)	4980	4970	4950
2	Diameter (m)	15.5	15.5	15.5
3	Height (cm)	16.0	16.0	16.0
4	Volume (cm^3) = (π d^{2}h)/4	3017.54	3017.54	3017.54
5	Unit weight(gm./cm^3)	1.650	1.647	1.640
6	Average unit weight (gm./cm^3)	1.646		

Appendix 5: Flakiness Index of Coarse Aggregates

Shugala Area (A)

Sieve size	Wt. of sieve	Wt. Of sieve + retained	Wt. of retained	gauge range	passing Wt.
50.00	1719	1719	0	63-50	0
37.50	1710.00	1785.00	75	50-37.5	0
28.00	1730.00	2678.00	948	37.5-28	30
20.00	1613.00	2669.00	1056	28-20	164
14.00	1356.00	1788.00	432	20-14	203
10.00	1326.00	1837.00	511	14-10	148
6.30	1362.00	2108.00	746	10-6.3	134
Total			3768		**679**
Avg. FI%=					**18.02**

% Flakiness Index = $\frac{A}{A+B}$ * 100 = $\frac{679}{3768}$ = 0.1802= 18.02%

Where: A = Weight passing a given slot

B = Weight retained on the same slot

Shugala Area (B)

Sieve size	Wt. of sieve	Wt. of sieve + retained	Wt of retained	gauge range	passing Wt
50.00	1719	1719	0	63-50	0
37.50	1710.00	1710.00	0	50-37.5	0
28.00	1730.00	1849.00	119	37.5-28	0
20.00	1613.00	3067.00	1454	28-20	254.4
14.00	1356.00	2869.00	1513	20-14	244.5
10.00	1326.00	1854.00	528	14-10	115
6.30	1362.00	1396.00	34	10-6.3	4.3
Total			3648		**618.2**

Mayalem Area (C)

Sieve size	Wt. of sieve	Wt. of sieve + retained	Wt of retained	gauge range	passing Wt
50.00	1719	1719	0	63-50	0
37.50	1710.00	1710.00	0	50-37.5	0
28.00	1730.00	1924.00	194	37.5-28	29
20.00	1613.00	3667.00	2054	28-20	314
14.00	1356.00	3050.00	1694	20-14	203
10.00	1326.00	1753.00	427	14-10	105
6.30	1362.00	1396.00	34	10-6.3	9
Total			4403		**660**
Avg. FI%=					**14.99**

Mayalem Area (D)

Sieve size	Wt. of sieve	Wt. of sieve + retained	Wt of retained	gauge range	passing Wt
50.00	1719	1719	0	63-50	0
37.50	1710.00	1812.00	102	50-37.5	0
28.00	1730.00	2883.00	115	37.5-28	425
20.00	1613.00	3944.00	2331	28-20	284
14.00	1356.00	2087.00	731	20-14	69
10.00	1326.00	1415.00	89	14-10	17
6.30	1362.00	1396.00	34	10-6.3	0
Total			4440		**795**
Avg. FI%					**17.91**

Kokolo Area (E)

sieve size	Wt. of sieve	Wt. of sieve + retained	Wt. of retained	gauge range	passing Wt.
50.00	1719	1719	0	63-50	0
37.50	1710.00	1710.00	0	50-37.5	0
28.00	1730.00	1730.00	0	37.5-28	0
20.00	1613.00	3187.00	1574	28-20	155
14.00	1356.00	3174.00	1818	20-14	416
10.00	1326.00	2249.00	923	14-10	201
6.30	1362.00	1417.00	55	10-6.3	15
Total			4370		**787**
Average FI%					**18.01**

Kokolo Area (F)

Sieve size	Wt. of sieve	Wt. of sieve + retained	Wt. of retained	gauge range	passing Wt.
50.00	1719	1719	0	63-50	0
37.50	1710.00	1710.00	0	50-37.5	0
28.00	1730.00	3691.00	1961	37.5-28	100
20.00	1613.00	3176.00	1563	28-20	313
14.00	1356.00	1956.00	600	20-14	320
10.00	1326.00	1502.00	176	14-10	97
6.30	1362.00	1518.00	156	10-6.3	45
Total			4456		**875**
				Avg. FI%	**19.64**

Mossobo Area (G)

sieve size	Wt. of sieve	Wt. of sieve + retained	Wt. of retained	gauge range	passing Wt.
50.00	1719	1719	0	63-50	0
37.50	1710	1710.00	0	50-37.5	0
28.00	1730	20002.00	18272	37.5-28	84
20.00	1614	3564.00	1950	28-20	312
14.00	1356	3039.00	1683	20-14	3251
10.00	1326	2265.00	939	14-10	177
6.30	1362	1491.00	129	10-6.3	21
Total			22973		**3845**
Avg. FI%=					**16.74**

Messobo Area (H)

sieve size	Wt. of sieve	Wt. of sieve + retained	Wt. of retained	gauge range	passing Wt.
50.00	1719	1719	0	63-50	0
37.50	1710	1710.00	0	50-37.5	0
28.00	1730	3251.00	1521	37.5-28	102
20.00	1614	2904.00	1290	28-20	401
14.00	1356	2158.00	802	20-14	210
10.00	1326	1842.00	516	14-10	177
6.30	1362	1489.00	127	10-6.3	0
Total			4256		**890**
				Avg. FI%	**20.91**

Chanadug Area (I)

sieve size	Wt. of sieve	Wt. of sieve + retained	Wt. of retained	gauge range	passing Wt.
50.00	1719	1719	0	63-50	0
37.50	1710.00	1710.00	0	50-37.5	0
28.00	1730.00	1849.00	119	37.5-28	29
20.00	1613.00	3067.00	1454	28-20	205.6
14.00	1356.00	2869.00	1513	20-14	358
10.00	1326.00	1854.00	528	14-10	138
6.30	1362.00	1396.00	34	10-6.3	10
Total			3648		**740.6**
				Average FI%	**20.30**

Genha Area (J)

sieve size	Wt. of sieve	Wt. of sieve + retained	**Wt.** of retained	gauge range	passing Wt.
50.00	1719	1719	0	63-50	0
37.50	1710.00	1710.00	0	50-37.5	0
28.00	1730.00	1765.00	35	37.5-28	0
20.00	1613.00	4852.00	3239	28-20	465
14.00	1356.00	2871.00	1515	20-14	133
10.00	1326.00	1526.00	200	14-10	6

6.30	1362.00	1362.00	0	10-6.3	0
Total			4989		**604**
Avg.FI%					**12.11**

Genha Area (K)

sieve size	Wt. of sieve	Wt. of sieve + retained	Wt. of retained	gauge range	passing Wt.
50.00	1719	1719	0	63-50	0
37.50	1710.00	1710.00	0	50-37.5	0
28.00	1730.00	1890.00	160	37.5-28	54
20.00	1613.00	3752.00	2139	28-20	250
14.00	1356.00	2871.00	1515	20-14	250
10.00	1326.00	1426.00	100	14-10	16
6.30	1362.00	1362.00	0	10-6.3	0
Total			3914		**570**
				Avg. FI%=	**14.56**

% Flakiness Index = $\frac{A}{A+B}$ * 100 = $\frac{570}{3914}$ = 0.1456= 14.56 %

Appendix 6: Aggregate Crushing Value

Shugala Area (A)

NO	Description	Sample-1	Sample-2	Sample-3	Average
1	Total weight in grams A	2717	2719	2722	2719.33
2	Retained weight on 2.36 mm sieve in grams B	2185	2189	2195	2189.67
3	**Aggregate Crushing Value =$\frac{A-B}{A}$ *100%**				19.48

Shugala Area (B)

NO	Description	Sample-1	Sample-2	Sample-3	Average
1	Total weight in grams A	2771	2763	2772	2768.67
2	Retained weight on 2.36 mm sieve in grams B	2182	2178	2183	2181.00
3	**Aggregate Crushing Value = $\frac{A-B}{A}$ *100%**				21.23

Mayalem Area (C)

NO	Description	Sample-1	Sample-2	Sample-3	Average
1	Total weight in grams A	2713	2712	2725	2716.67
2	Retained weight on 2.36 mm sieve in grams B	2421	2429	2431	2427.00
3	**Aggregate Crushing Value =** $\frac{A-B}{A}$ ***100%**				10.66

Mayalem Area (D)

NO	Description	Sample-1	Sample-2	Sample-3	Average
1	Total weight in grams A	2770.0	2773.0	2777.0	2773.33
2	Retained weight on 2.36 mm sieve in grams B	2461	2457.2	2479	2441.00
3	**Aggregate Crushing Value =** $\frac{A-B}{A}$ ***100%**				11.98

Kokolo Area (E)

NO	Description	Sample-1	Sample-2	Sample-3	Average
1	Total weight in grams A	2700	2708	2711	2706.33
2	Retained weight on 2.36 mm sieve in grams B	2148	2151	2157	2152.00
3	**Aggregate Crushing Value =** $\frac{A-B}{A}$ ***100%**				20.48

Kokolo Area (F)

NO	Description	Sample-1	Sample-2	Sample-3	Average
1	Total weight in grams A	2763	2765	2768	2765.33
2	Retained weight on 2.36 mm sieve in grams B	2157	2145	2156	2152.67
3	**Aggregate Crushing Value =** $\frac{A-B}{A}$ ***100%**				22.16

Mossobo Area (G)

NO	Description	Sample-1	Sample-2	Sample-3	Average
1	Total weight in grams A	2780.0	2760.0	2751.0	2763.67
2	Retained weight on 2.36 mm sieve in grams B	2152	2140	2148	2146.67
3	**Aggregate Crushing Value =** $\frac{A-B}{A} * 100\%$				22.32

Mossobo Area (H)

NO	Description	Sample-1	Sample-2	Sample-3	Average
1	Total weight in grams A	2768	2724	2712	2734.67
2	Retained weight on 2.36 mm sieve in grams B	2152	2163	2167	2160.67
4	**Aggregate Crushing Value =** $\frac{A-B}{A}$ ***100%**				20.98

Chanadug Area (I)

NO	Description	Sample-1	Sample-2	Sample-3	Average
1	Total weight in grams A	2779	2771	2766	2772
2	Retained weight on 2.36 mm sieve in grams B	2330	2319	2328	2325.67
3	**Aggregate Crushing Value =** $\frac{A-B}{A}$ ***100%**				16.10

Genha Area (J)

NO	Description	Sample-1	Sample-2	Sample-3	Average
1	Total weight in grams A	2631.0	2624.0	2629.0	2628
2	Retained weight on 2.36 mm sieve in grams B	2310	2299	2284	2297.67
3	**Aggregate Crushing Value =** $\frac{A-B}{A}$ ***100%**				12.56

Genha Area (K)

NO	Description	Sample-1	Sample-2	Sample-3	Average
1	Total weight in grams A	2685.7	2690.0	2687.0	2687.33
2	Retained weight on 2.36 mm sieve in grams B	2340	2337	2346	2341.00
3	**Aggregate Crushing Value =** $\frac{A-B}{A}$ *** 100%**	**12.89**			

Appendix 7: Los Angeles Abrasion Value

Shugala Area (A)

NO	Description	Sample-1	Sample-2	Sample-3	Remark
1	Original weight in grams W_1	5000.0	5000.0	5000.0	
2	Retained weight on 1.7 mm sieve in grams W_2	3906	3910	3908	
3	% Wear = $\frac{W1-W2}{W1}$ *100	**21.88**	**21.80**	**21.84**	
4	**Los Angeles Abrasion Value**	**21.84**			

Shugala Area (B)

NO	Description	Sample-1	Sample-2	Sample-3	Remark
1	Original weight in grams W_1	5000.0	5000.0	5000.0	
2	Retained weight on 1.7 mm sieve in grams W_2	3806	3917	3802	
3	% Wear = $\frac{W1-W2}{W1}$ *100	**23.88**	**21.66**	**23.96**	
4	**Los Angeles Abrasion Value**		**23.17**		

Mayalem Area (C)

NO	Description	Sample-1	Sample-2	Sample-3	Remark
1	Original weight in grams W_1	5000.0	5000.0	5000.0	
2	Retained weight on 1.7 mm sieve in grams W_2	3977.1	3977	3980.2	
3	% Wear = $\frac{W1-W2}{W1}$ *100	**20.46**	**20.46**	**20.40**	
4	**Los Angeles Abrasion Value**	**20.44**			

Mayalem Area (D)

NO	Description	Sample-1	Sample-2	Sample-3	Remark
1	Original weight in grams W_1	5000.0	5000.0	5000.0	
2	Retained weight on 1.7 mm sieve in grams W_2	4032	4090	4001	
3	% Wear = $\frac{W1-W2}{W1}$ *100	**19.36**	**18.20**	**19.98**	
4	**Los Angeles Abrasion Value**	**19.18**			

Kokolo Area (E)

NO	Description	Sample-1	Sample-2	Sample-3	Remark
1	Original weight in grams W_1	5000.0	5000.0	5000.0	
2	Retained weight on 1.7 mm sieve in grams W_2	3953	3950	3955	
3	% Wear = $\frac{W1-W2}{W1}$ *100	**20.94**	**21.00**	**20.90**	
4	**Los Angeles Abrasion Value**	**20.95**			

Kokolo Area (F)

NO	Description	Sample-1	Sample-2	Sample-3	Remark
1	Original weight in grams W_1	5000.0	5000.0	5000.0	
2	Retained weight on 1.7 mm sieve in grams W_2	3922	3939	3948	
3	% Wear = $\frac{W1-W2}{W1}$ *100	**21.56**	**21.22**	**21.04**	
4	**Los Angeles Abrasion Value**	**21.27**			

Mossobo Area (G)

NO	Description	Sample-1	Sample-2	Sample-3	Remark
1	Original weight in grams W_1	5000.0	5000.0	5000.0	
2	Retained weight on 1.7 mm sieve in grams W_2	3774	3778	3780	
3	% Wear = $\frac{W1-W2}{W1}$ *100	**24.52**	**24.44**	**24.40**	
4	**Los Angeles Abrasion Value**	**24.45**			

Mossobo Area (H)

NO	Description	Sample-1	Sample-2	Sample-3	Remark
1	Original weight in grams W_1	5000.0	5000.0	5000.0	
2	Retained weight on 1.7 mm sieve in grams W_2	3701	3712	3777	
3	% Wear = $\frac{W1-W2}{W1}$ *100	**25.98**	**25.76**	**24.46**	
4	**Los Angeles Abrasion Value**		**25.40**		

Chanadug Area (I)

NO	Description	Sample-1	Sample-2	Sample-3	Remark
1	Original weight in grams W_1	5000.0	5000.0	5000.0	
2	Retained weight on 1.7 mm sieve in grams W_2	4000	4080	4020	
3	% Wear = $\frac{W1-W2}{W1}$ *100	**20.00**	**18.40**	**19.60**	
4	**Los Angeles Abrasion Value**	**19.33**			

Genha Area (J)

NO	Description	Sample-1	Sample-2	Sample-3	Remark
1	Original weight in grams W_1	5000.0	5000.0	5000.0	
2	Retained weight on 1.7 mm sieve in grams W_2	3855	3866	3857	
3	% Wear = $\frac{W1-W2}{W1}$ *100	**22.90**	**22.68**	**22.86**	
4	**Los Angeles Abrasion Value**	**22.81**			

Genha Area (K)

NO	Description	Sample-1	Sample-2	Sample-3	Remark
1	Original weight in grams W_1	5000.0	5000.0	5000.0	
2	Retained weight on 1.7 mm sieve in grams W_2	3798	3760	3806	
3	% Wear = $\frac{W1-W2}{W1}$ *100	**24.04**	**24.80**	**23.88**	
4	**Los Angeles Abrasion Value**	**24.24**			